UNIVERSITY OF SOUTHAMPTON

HIGH-POWER DIODE-PUMPED FIBRE-LASER

by

Cyril C. RENAUD

This thesis was submitted for the degree of Doctor of Philosophy

FACULTY OF ENGINEERING AND APPLIED SCIENCE
OPTOELECTRONICS RESEARCH CENTRE
DEPARTMENT OF ELECTRONICS AND COMPUTER SCIENCE

JULY 2001

UNIVERSITY OF SOUTHAMPTON

Abstract

FACULTY OF ENGINEERING AND APPLIED SCIENCE
OPTOELECTRONICS RESEARCH CENTRE
DEPARTMENT OF ELECTRONIC AND COMPUTER SCIENCE

Doctor of Philosophy

HIGH-POWER DIODE-PUMPED YTTERBIUM-DOPED FIBRE LASERS

by Cyril C. Renaud

This thesis details the work I have done on double cladding ytterbium-doped fibre lasers. The two main subjects developed were the study of an efficient compact-launching system, and the operation of the double cladding compact fibre as a continuous-wave laser and a Q-switched laser.

I studied two different aspects of the launching system. At first, the optical arrangement to launch the pump light from laser diodes into a multimode fibre was developed. It was designed to make the all fibre laser to fit into a shoebox. Secondly, the use of multimode couplers and multi-fibre-arrangements were studied to separate the pump and the signal in two different guides at the input and output ports.

Concerning the lasing operation of the ytterbium-doped fibre lasers, the continuous wave operation at 1060 nm was investigated to validate the different launching systems. Some fibre designs were developed to generate 976 nm emission from double cladding ytterbium doped fibre laser.

During this work, highly efficient side launching systems were developed. These allowed coupling of more than 70% of the pump light into the doped fibre and gave as good lasing efficiency as end-pumping system. The pump and the signal were also well separated in two different guides at the ends of the device. Efficient lasing at 976 nm (85% slope efficiency) was demonstrated too, by using small inner cladding area and double passed pump. Finally, pulse-energy as high as 7.7 mJ was achieved with a large core cladding pumped ytterbium doped Q-switched fibre laser.

Above all, I would like to thank my supervisor Dr Johan Nilsson for all his help, his patience and his availability.
My thanks also go to Jose-Alfredo Alvarez-Chavez and Shaif-ul-alam for their help and their friendly support during my work.
I am also grateful to all the staff and student of the Optoelectronics Research Centre for the advices they gave me from time to time.
I would like to express my gratitude to the faculty of Engineering and Applied Sciences and the EPSRC for providing me with a scholarship.
Finally I would like to thank all my family and my friends in France for their continuous support.
A very special thank to Caroline, who supported me in the every days life, and for all her understanding of my PhD student "little problems.

SYMBOLS AND ABBREVIATIONS

ASE: Amplified spontaneous emission

h: Planck Constant $h=6.62\times10^{-34}$J.s

V: V number of a fibre (Appendix A) to describe the propagation

W: W number of a fibre (Appendix A) to describe the propagation

U: U number of a fibre (Appendix A) to describe the propagation

v: Gain volume for a fibre laser in m^3

A: Core area of the fibre in m^2

N_i: Population in the energy level i (ion/m^3)

λ: wavelength (m)

l: fibre length (m)

DCF: Double Cladding Fibre

NA(for a fibre): Numerical Aperture

NA(for a beam): As a purpose of comparison we use the term NA for the pump beam convergence towards the fibre, or divergence at the output facet of the pump source.

r: rate of twisting for two fibres twisted together (turn/m)

σ_{ij}: Cross section of emission/absorption from level i to level j (m^2)

I_i: Intensity ($photons/s.m^2$)

τ_{ij}: Time of relaxation from level i to level j.

Γ_i: Overlap integral of the signal/pump with the core/cladding area

INTRODUCTION

High brightness, high power, and if necessary tunable near-infrared sources have applications in many areas such as spectroscopy, laser and amplifier pumping, frequency conversion and medicine. For such sources, rare-earth doped cladding pumped fibre lasers offer an excellent combination of high efficiency and high spatial beam quality. They can retain the small physical size of fibre lasers and can also utilize high-power laser diodes, for power scaling up to the point where they can replace conventional flash lamp and diode pumped solid-state and gas bulk lasers. Nowadays, high power fibre lasers and amplifiers are becoming an important commercial product for several areas such as telecommunication, range finding, or remote sensing [1-2].

Within the family of rare-earth ions, ytterbium (hosted in silica) offers a broad spectral range of emission and essentially quantum limited slope efficiency. Figure 1 shows the absorption and emission cross-sections of ytterbium hosted in silica. As it can be seen, the two main absorption peaks at 915 nm and 975 nm are very close to the two main emission peaks at 975 nm and 1030 nm. This means that it is possible to have a quantum limit of more than 80%, and this will limit the fibre laser slope efficiency. Furthermore, the broad emission spectrum above 1 μm makes ytterbium an attractive source for amplifiers and lasers with a wide tuning range. With core pumping, ytterbium doped fibre has already proved to be an efficient amplifier [1] and laser [2] for emission at 975 nm and from 1010 nm to 1162 nm.

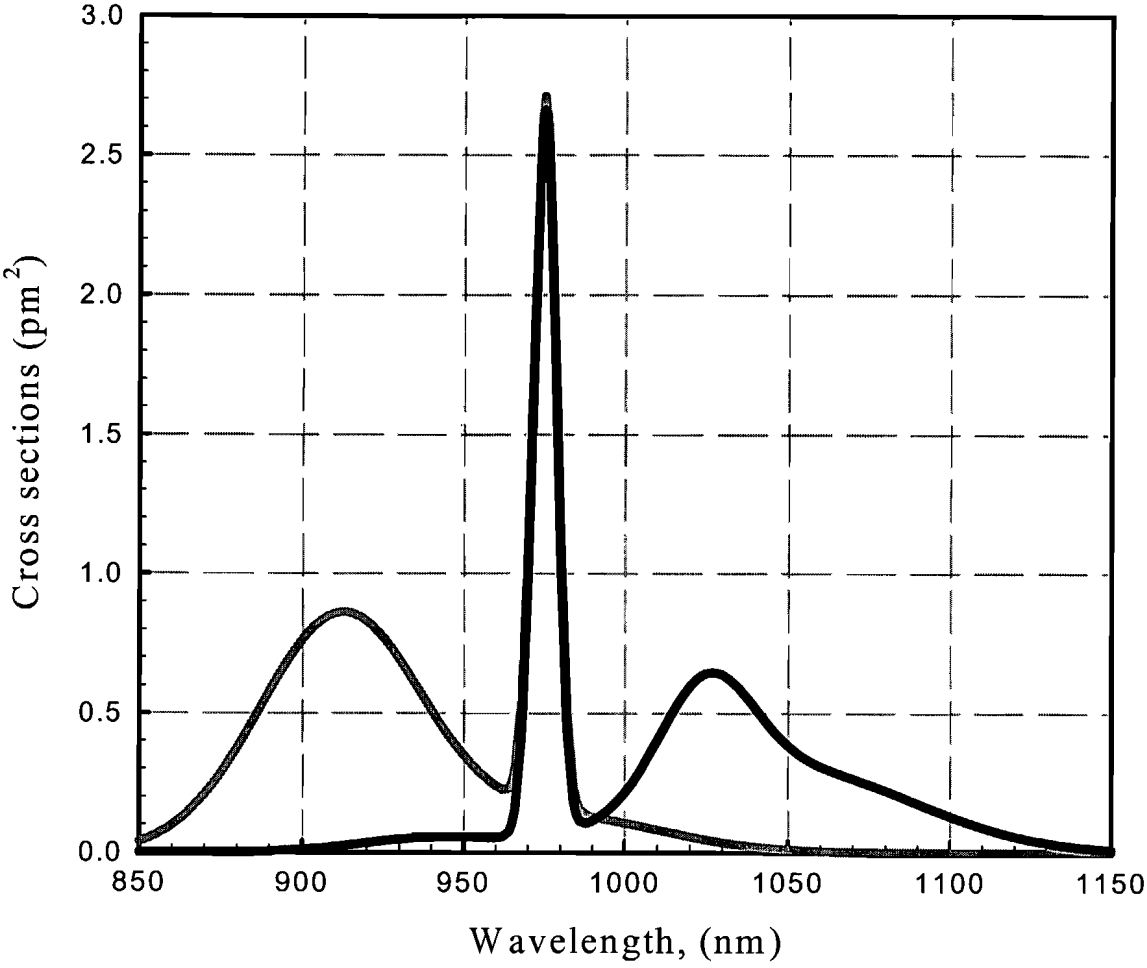

Figure 1: Emission (black) and absorption (grey) cross-sections versus wavelength.

Traditionally, a fibre laser is core-pumped, through a wavelength multiplexing coupler directly into the singlemode doped core. This technique limits the output power that can be achieved with a fibre laser in a compact setup. The main reason for this is the low power available from single mode pump laser diodes. To overcome this limitation, the most typical configuration is double cladding-fibre (DCF). Such a fibre is in fact composed of two optical waveguides. The outer one (the inner cladding) is multimoded for guiding multimoded low-brightness high power pump beams; the inner one is often singlemoded (the core) and contains the laser active dopant. That is the place where the signal propagates. Figure 2 shows how the second guide sits within the first one to enable interaction between the pump and the dopant. The inner cladding can have any shape (circular, rectangular, star, flower...), and the core does not necessarily need to be centred as in figure 2. In fact, it has been proved that non-

circular shape and non-centred core [3] enhanced the performances of DCF. That is mainly because more of the pump light (beams) propagating in a non-circular and/or non-symmetric inner cladding will cross the core; therefore, the absorption will be higher than for a circular centro-symmetric inner cladding, since in this case some of the beams will never cross the core. However, by bending the fibre, one can create a mode mixing which will allow all the beams to cross the core, thus, the circular shape inner cladding with centred core can be as good as the non-circular and/or non-symmetric shapes, as long as the fibre can be suitably bent.

Cladding-pumped fibres can be viewed as a brightness enhancement technique, since one starts from a non-diffraction limited high power beam, and obtains a high power diffraction limited beam.

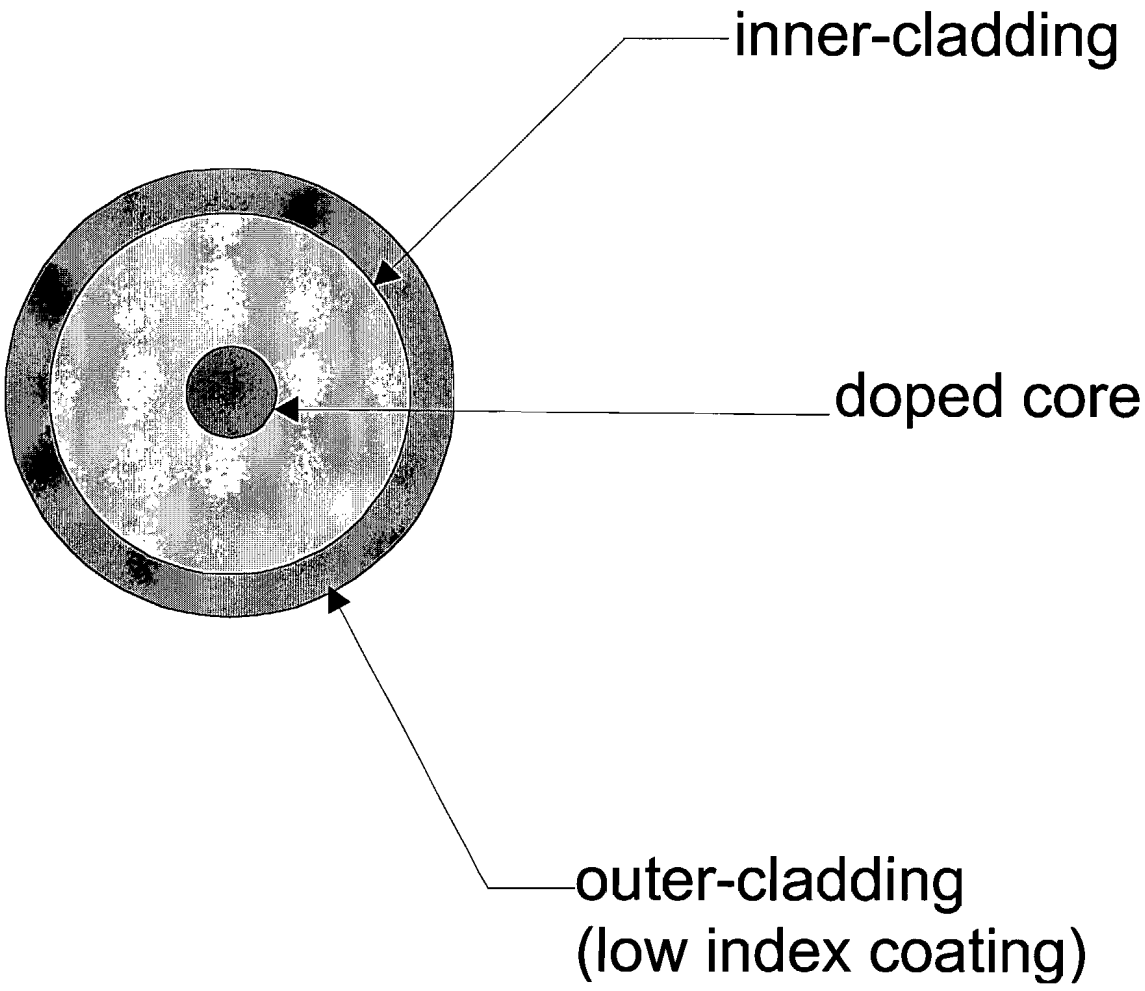

Figure 2: Classic double cladding configuration. The core can have an offset or the inner cladding can have different shapes (rectangular, elliptical, star, flower...)

Using this double cladding configuration, high power devices have already been demonstrated [4-5] for continuous wave (cw) laser emission with output up to 110 W.
The purpose of this thesis was to investigate the level of integration compactness that one can achieve with a DCF laser, and the performance of such a laser in the continuous wave regime (emission around 1.1 μm and at 975 nm) and in the Q-switched regime (around 1.1 μm). The main interest was to generate high-energy pulses and a high power source a 975 nm to pump high power erbium doped fibre amplifiers.
In the first part of this thesis, the work done on the optical system to launch the light from different laser diodes is described (Chapter I). Then Chapter II and III present an investigation of the different ways to separate the pump and signal input and output (like with a wavelength multiplexing coupler for core pumping) with multimode couplers or fibre arrangements.
In the second part of the thesis, details of the results are given for the measured performance of the ytterbium doped fibre laser in continuous wave and Q-switched regime (chapter V and VII). Some theoretical background and simulation results are also presented for both regimes, as a guide to design the fibre used in such lasers (Chapter IV and V). Note that the main purpose of measuring continuous wave performance above 1 μm was to validate the launching and coupling system.
The main achievements of this work were:

-The construction of an efficient side launching and coupling system with at least 70% of the pump power coupled into the doped fibre. This system was comparable to a standard end-pumping scheme. This was mainly performed to create a setup equivalent to wavelength multiplexing couplers for cladding-pumped lasers amplifiers.

-The demonstration of an efficient double cladding ytterbium doped laser emitting at 976 nm (slope efficiency around 85% achieved)

-Realisation of Q-switched fibre lasers with pulse energy up to 7.7 mJ (in one configuration) and 40 nm tuning range (in another configuration).

REFERENCES

[1] R. Paschotta, J. Nilsson, A. C. Tropper, D. C. Hanna, "Ytterbium-Doped Fibre Amplifiers," IEEE J. of Q. Elect., 1997, Vol.33, No.7, pp.1049-1056.

[2] D. C. Hanna, R. M. Percival, I. R. Perry, R. G. Smart, P. J. Suni, J. E. Townsend, A. C. Tropper, "An Ytterbium-doped monomode fibre laser: broadband tunable operation from 1.010 to 1.162 μm and three-level operation at 974 nm," *J. Mod. Opt.,* 1990, Vol. 37, pp. 517-525

[3] A. Liu, K. Ueda, "The absorption characteristics of circular, offset, and rectangular double-clad fibers," Optics com., 1996, vol. 132, pp.511-518.

[4] M. Muendel, B. Engstrom, D. Kea, B. Laliberte, R. Minns, R. Robinson, B. Rockney, Y. Zhang, R. Collins, P. Gavrilovic, A. Rowley, "35-watt CW singlemode Ytterbium Fibre laser at 1.1 μm", CLEO'98, 1998

[5] V. Dominic, S. MacCormack, R. Waarts, S. Sanders, S. Bicknese, R. Dohle, E. Wolak, P. S. Yeh, E. Zucker, "110 W fiber laser," Postdeadline paper, CPD 11, CLEO'99, Baltimore, 1999

PART I: HOW TO MAKE THE SYSTEM COMPACT

CHAPTER I: DIFFERENT OPTICAL LAUNCHING SYSTEMS

I INTRODUCTION

A laser is a system, which can be described by four subsystems. Figure 1 shows a schematic view of a laser system and a representation of a compact setup for a fibre laser.
-The pump, which feeds the system with the necessary energy to create lasing, can come either from an electrical process, a chemical process, or from light. In this work, the pump sources were high power laser diodes (pigtailed or not) operating at a wavelength corresponding to an absorption band for the active medium.
-The launching system couples the pump light into the active medium. In the experiments, presented in this thesis, it is composed of either one or two parts. There is always a part which couples the pump beam into a multimode fibre waveguide. In many cases, this is the DCF itself. Otherwise it is a multimode fibre. Then, in several experiments, a multimode coupler or a fibre arrangement were used. They coupled the pump light (from the multimode fibre) into the inner cladding of the DCF.

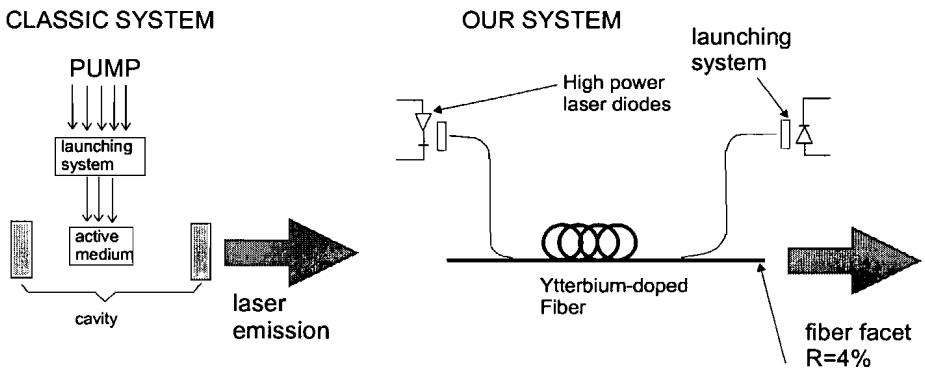

Figure I-1: Usual laser setup scheme, and a compact system scheme for fibre laser.

-The active medium transforms the pump energy into signal light via stimulated emission in this medium. For this work, the active medium is the Ytterbium-doped core of the DCF. It transforms the energy of the pump (light at 980 nm or 915 nm) to light at 1010-1100 nm or 975 nm.

-The cavity provides feedback for the system to facilitate laser operation. A cavity is usually composed of two mirrors. In the fibre-laser, the cavity is composed by the two cleaved facets of the fibre-ends, which reflect ~4% of the light. Either fibre Bragg gratings, external mirrors, or bulk gratings could also be used, to make the output unidirectional and/or tunable.

An amplifier is just composed of the first three subsystems, therefore, if one wants to create an amplifier with that system, one should "open" the cavity (i.e. supress feedback). It can be done with angle-cleaved fibre-ends, for example.

In this chapter, the different launching systems studied during this work will be described. These systems depend on the laser-diodes, used as pump source, the inner-cladding diameter and profile of the multimode fibre. A launching system is needed so that as much pump light as possible is coupled into the multimode inner-cladding of the fibre. The purpose of the launching system is to match the beam waist and the divergence of the source, with the inner-cladding diameter and the NA of the multimode fibre. Four launching systems were considered for circular and rectangular inner-cladding.

(1)-a bulk optic conception

(2)-a LIMO coupler micro-optic

(3)-a LIMO collimator micro-optic.

(4)-a fibre lens

Note that LIMO GmbH is a company making microlenses and that this name will be used in this thesis for all the launching systems using this type of lenses. All the systems mentioned above gave at least a launching efficiency of 50%. This launching efficiency strongly depends on the laser-diode used, and it can go up to 80%. Finally, all these systems are reasonably compact.

II PUMP SOURCE: LASER DIODES

As stated in the introduction the pump sources were laser diodes.
Since the main dopant utilized was ytterbium, diodes emitting at 915 nm and 980 nm (the two main absorption bands for this dopant) were used.
Singlemode laser diodes produce high brightness (diffraction limited) beams but relatively low power. To obtain higher power one can use large area laser diodes but they will have a much lower brightness and a multimode output, therefore it would not be possible to launch the output beam of such a diode into a singlemode fibre. That is the principal reason why a double cladding configuration is used for high power fibre lasers.

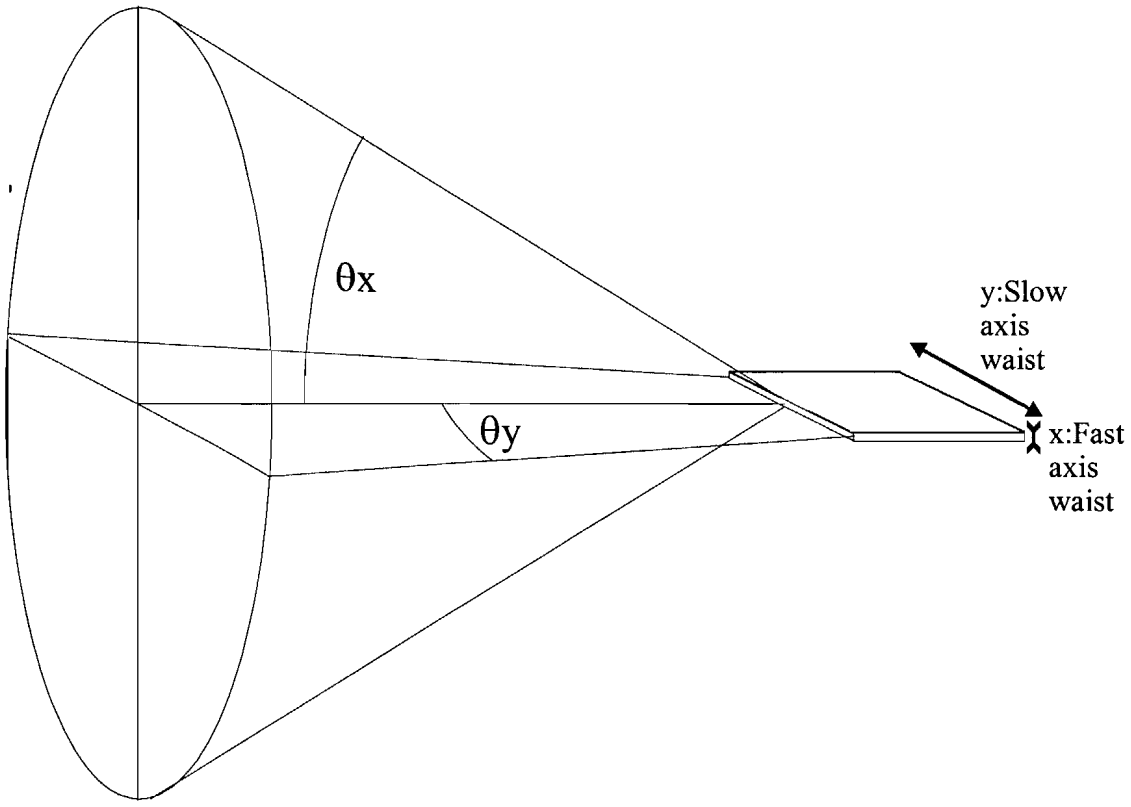

Figure I-2 Classical beam output for a diode stripe

Three different types of diodes were used:

-Single stripe diodes of 100, 200, 300, 400μm slow axis waist. The output power was from 1 to 8 W. Figure 2 shows in a schematic view the important parameters for laser diodes. There are four important parameters (figure 2.): The fast axis and slow axis, waists and divergences. The fast axis waist of these diodes was always approximately 1 μm and the divergences were 12 degrees (FWMH) in the slow axis and about 70 degrees for the fast one, except for a couple of diodes with 90 degrees of divergence. Some of those diodes were pigtailed to a 60 μm core diameter fibre (0.22 NA) with an output of 1.5 W. In this case the parameters of the pigtailed fibre are the important point to consider when designing the launching setup.

-Single stripe diode array either combined with prisms in a single output of 25 W (DIOMED-HIRAFS), or pigtailed with a 100 μm core multimode fibre (0.22 NA), which gives an output of 7 W at 915 nm (MILON source). Again for this last one, the fibre parameters are the only ones to be important for choosing the launching optics.

- Beam-shaped diode bars [1], generating 35W at 915nm. In this case the beam shaping permits an equalized output beam with an almost square shape to be obtained (one axis is slightly more divergent than the other).

III THE BULK OPTIC SCHEME

III-1 For a diode stripe

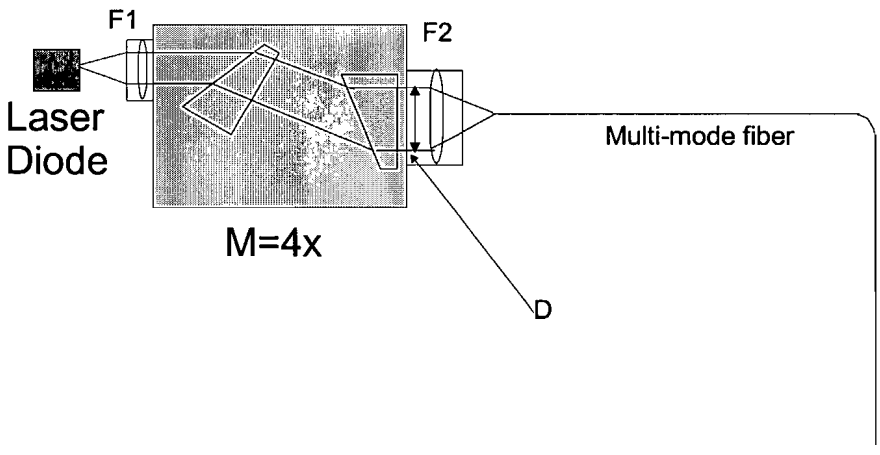

Figure I-3 Bulk optic configuration, with a collimating lens, two prisms, and a focusing lens

To launch the light from a diode stripe into a circular inner cladding, one can use a classic design, shown in figure 3. It comprises: a collimating lens (focal length = F_1), anamorphic prisms (magnification = M), and a focusing lens (focal length = F_2). The focal lengths and magnification can be matched to optimise the image spot sizes for the fast and the slow axis (y_2, y_2') and the image-beam numerical apertures. This can be done using the following formulas where y_1 and y_1' are the spot sizes of the fast and the slow axis of the laser-diode and NA_1 and NA_1' are the numerical apertures of the fast and slow axis:

$$y_2 = \frac{F_2}{F_1} \cdot y_1,\ y_2' = \frac{F_2}{F_1 \cdot M} \cdot y_1',\ NA_2 = NA_1 \cdot \frac{F_1}{F_2},\ NA_2' = NA_1' \cdot \frac{F_1 \cdot M}{F_2}.$$

A major problem comes from the first lens. Its NA was 0.5 and the fast axis divergence was 0.6, thus losses were observed. In fact, the losses were measured to be around 15%. Then with large diodes (300 μm stripe width) 35% more was lost in the prisms and in the second lens, this means the launching efficiency is between 80% and 50%. Therefore for 1W diodes (100 μm) about 800mW was launched in the multimode fibre and for 3W diodes (300 μm) about 1.5 W was launched experimentally. The following parameters were for 1x100 (1) and 1x300 μm diodes (2), respectively. Both diodes had a NA of 0.6 on the fast axis and 0.1 on the slow axis:

(1)-F_1=6.8mm F_2=14.6 or 25.8mm M=x4.

This gave respectively, y_2= 2x54 μm or 3.9x95 μm and NA= 0.3x0.2 or 0.18x0.1

(2)-f1=6.8mm f2=14.6mm M=x6

This gave y_2= 2x108 μm and NA=0.3x0.3

Therefore with such setups all the pump power should be launched in any fibre with a diameter more than 110 μm and NA more than 0.3. In the experiments 150 μm fibres with a silicone rubber coating were used, which in theory gave about NA=0.4, therefore the launching efficiency should have been good.

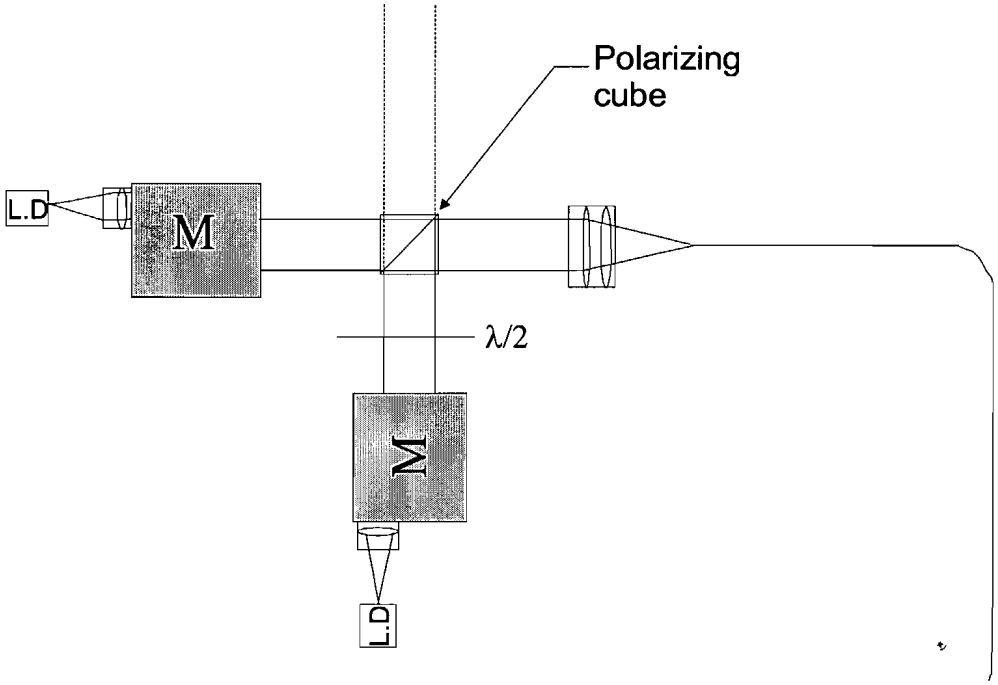

Figure I-4 Complete compact bulk optic configuration. With a polarising cube to combine the two beams which have crossed polarisation.

Using the setup shown in figure 4, utilizing polarization multiplexing, 3W of pump power was launched into the DCF from two diode stripes of 300 μm (3W output), with a launching efficiency around 50%, as expected. This design has the advantage to be easy to align but it has not the best compactness obtainable. It is a good experimental setup, which will easily permit the testing of amplifiers and lasers.
If the multimode fibre has a rectangular shape then one has to think more carefully of the setup and calculate for each axis what will be the result of the combination of lenses. One can as well use cylindrical lenses (for each axis) and use a similar setup as before. In this case two sets of two lenses will be needed; one set for the fast axis and one set for the other one.

III-2 For a pigtailed diode

This is the simplest setup. In this case, the numerical apertures and diameters of both the fibres are known (the fibre pigtailed to the diode laser and the inner cladding of the DCF). then, one just needs a simple set of two lenses to match the parameters like in figure 5.
This also allows the use of polarisation multiplexing (insofar as polarization is preserved in the pigtail) or wavelength multiplexing.

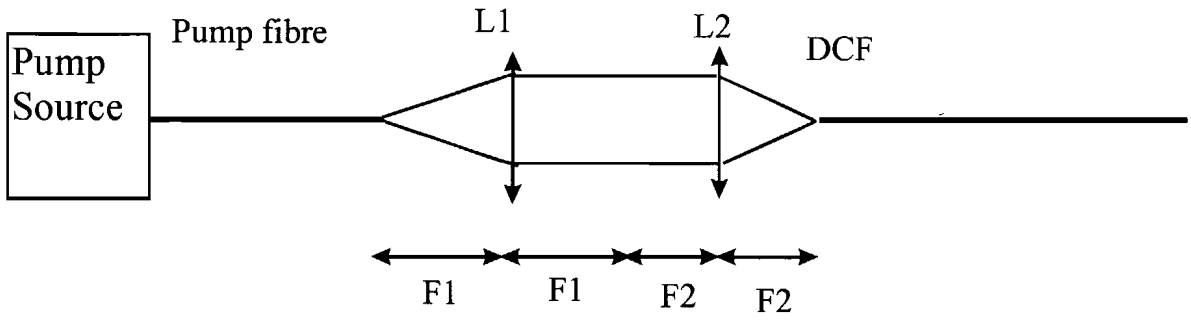

Figure I-5 Simple telescope setup to launch from a pigtailed diode

With such a setup the image of the fibre output will be given by:

$$Y_2 = \frac{F_2}{F_1} Y_1, \qquad NA_2 = \frac{F_1}{F_2} NA_1,$$

where NA_1 is the pump fibre NA and Y_1 is the pump fibre core diameter.
The main problem in this case is the mismatch between the pump parameters and the multimode fibre physical size (core and NA). As a rule of thumb, to be able to launch most of the signal into a multimode fibre, one should have:

$$D_f \cdot NA_f \geq D_i \cdot NA_i,$$

where D_i, NA_i are the source's fibre characteristics and D_f, NA_f are the multimode fibre characteristics.
When this condition is matched more than 80% of launching efficiency can be achieved.
If one wants to launch light in a rectangular cladding from such a source, then the limitation will be the shorter dimension (if the NA is the same for all directions) as if one has a circular inner cladding of this dimension. If by some means (glass structure and doping, holes…) one can manage to have a different NA for each direction then the choice of lenses should be done for each axis and cylindrical lenses should probably be used.

III-3 For a Diode bar

The output of the beam-shaped diode bar [1] is roughly squared, but there is still a small astigmatism, which needs to be corrected, thus a single cylindrical lens to collimate the slow

axis can be used. Then a spherical lens is used to focus the beam into the fibre, as in figure 6. Alternatively, an aspherical lens would be a better solution to reduce aberrations.

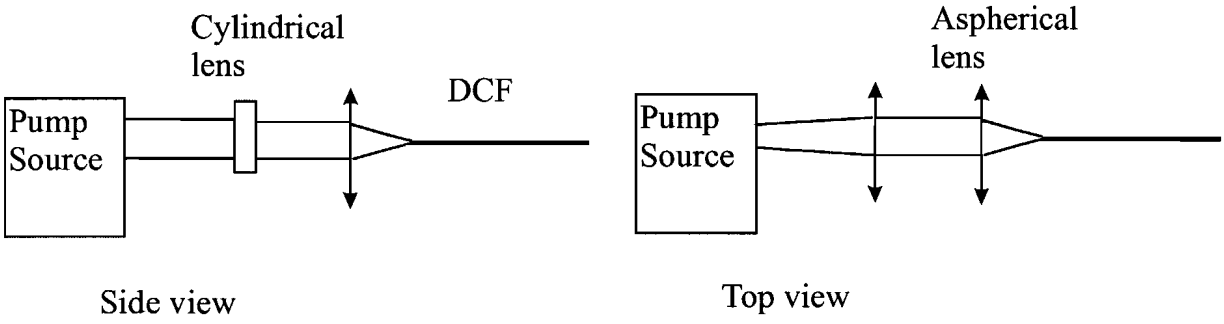

Figure I-6: typical launching setup for a diode bar with beam shaping.

In this setup the launching efficiency could reach up to 70% for a 200 μm inner cladding. The main disadvantage of this system is its size (water cooling of the diode bars). However it was very useful to test the different fibre's performances at high power and it was used to reach high energy in Q-switched regimes.

IV LIMO COUPLER AND COLLIMATOR

IV-1 The LIMO coupler

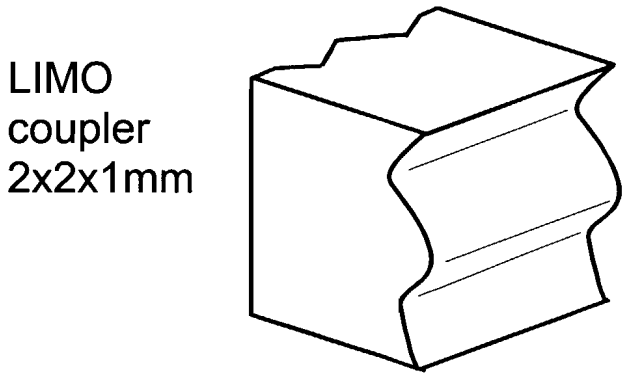

Figure I-7: The LIMO coupler is a combination of two crossed cylindrical lenses. This has almost the same effect as the bulk-optic system.

The LIMO coupler is a micro lens (2x2x1mm), which is composed of two crossed cylindrical lenses (figure 7). This lens gives images of the fast and slow axis separately. The one used

for this experiment is designed for launching the light from a 1x100 microns diode into 100 microns core fibre with an efficiency of more than 90%.
Launching efficiencies between 80 and 50% were obtained, for different diodes and fibres. The main problem is the mismatch between the size of the fibre and the size of the diode. For this lens, the waist size in the slow axis should be smaller or equal to the diameter of the fibre. For example, with a 3W output power diode (1x300 microns), 80 % of launching efficiency was obtained in a fibre of 300 microns core-diameter and 50% in a fibre of 150 microns core-diameter.
Due to their physical size, the LIMO couplers have a limited incident angle of about 70 degrees (full width), therefore the divergence of the diode fast axis is an important parameter too. This effect was observed by measuring the launching efficiency with a 1W diode (1x100 μm) into a 150 μm core-diameter fibre. The diode had a beam divergence of 90 degrees (FWHM), and a launching efficiency of 50% was obtained.

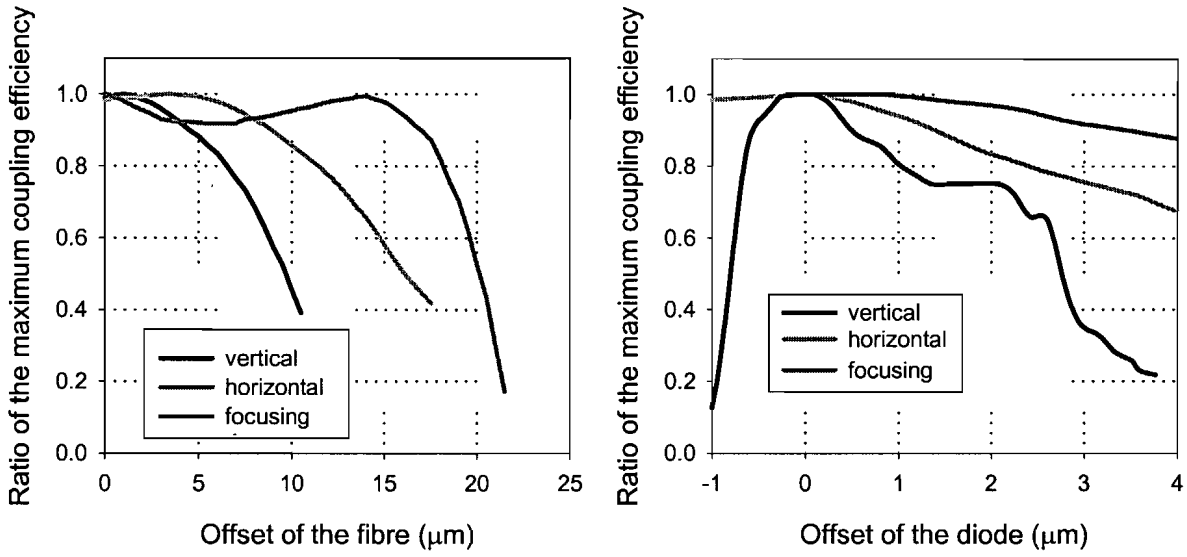

Figure I-8: Tolerance in alignment for the fibre and the diode with a LIMO coupler

The main problem associated with the use of LIMO lenses is that tolerances on this lens position are very stringent. Figure 8 shows experimental results in launching efficiency with LIMO coupler depending on alignment.

Of course, the design of those lenses might be changed to match any particular pairs of diodes-fibre, even if the fibre has a rectangular shape. The main advantage of this lens is the

compactness obtainable with a very high launching efficiency. Therefore this system of launching seems to be very good from the point of view of constructing a very compact source.

IV-2 The LIMO collimator

The LIMO collimator is based on the same concept as the LIMO coupler. Its main objective is to collimate the beam. So in this case, the idea is to collimate several beams and condense them with a second lens. It should permit several pump beams to launched in the multimode fibre.

With three different diodes from different manufacturers (SLI and GEC-Marconi) the following spot sizes were obtained at 25cm after the collimator:

SLI 1x100 μm:	2.2x2.2 cm	(divergence: 5x5 °)
SLI 1x200μm:	2x4 cm	(divergence: 4.6x9°)
GEC1x300 μm:	2x6 cm	(divergence: 4.6x13.5°)

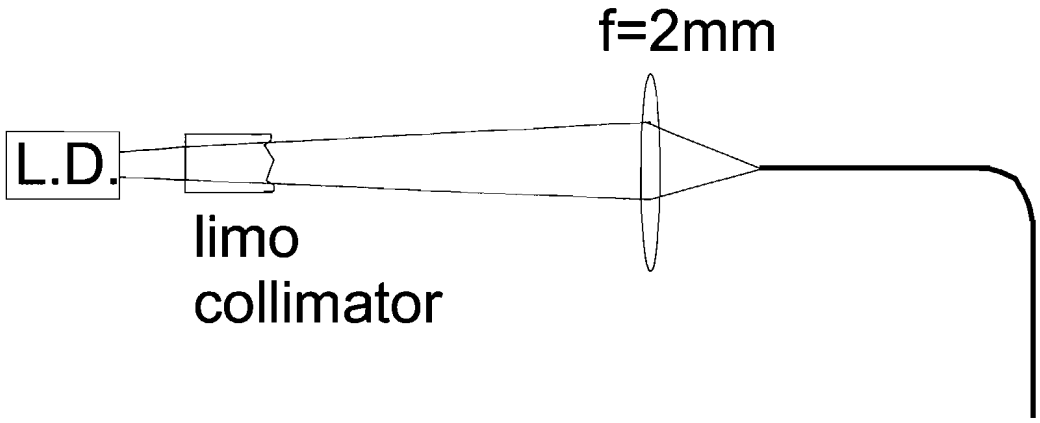

Figure I-9 LIMO collimator setup. The focal length of the focusing lens is 2 mm

The divergences are pretty high for a collimator but this is mainly due to the fact that their fast axes divergence was large.

The lens which should be associated with this collimator, for launching into a 150 μm diameter fibre, (in regard of the focal lengths of the LIMO collimator, and the fact that the system should remain compact) should have a focal length around 2 mm, and a NA of less than 0.4 (the NA of the fibres). The lens used has a clear aperture diameter about 2mm, the

NA was 0.5 but the spot size on the lens was limiting the output beam NA to 0.4. Therefore the distance between the lens and the collimator should be less than 2.5cm.
To launch the beam in the fibre the setup shown in figure 9 was used. With this setup and a distance between the lens and the collimator of either 1 or 2 cm, the following launching efficiencies were obtained:

SLI (1x100) microns: 70% for 1cm and 70% for 2 cm
SLI (1x200) microns: 50% for 1cm and 45% for 2 cm
GEC(1x300)microns: 57% for 1cm and 46% for 2 cm

The launching efficiencies obtained are comparable with the one obtained with LIMO-couplers, and a high level of compactness can still be reached. In this case, more than one diode can be used via polarization or wavelength multiplexing. For example two beams (with a polarising cube) from 3W diodes can be launched in the multimode fibre with a launching efficiency of 50%. It means that the same results, as with bulk optic configuration, can be achieved but with a system five times smaller in volume. As with the bulk optic system, if the last spherical lens is replaced by a set of two cylindrical lenses, one will be able to efficiently launch light in a rectangular shaped fibre. Therefore this concept seems to be interesting for the compact source configuration as well. It will enable more pump power in the cavity. So with that configuration a more powerful laser than with the LIMO-coupler configuration should be obtainable.

V FIBRE LENS SYSTEM

One other way of launching the light from a diode stripe, in a compact system, is to use a fibre lens, as in figure 10.
As a rule of thumb the diameter of the collimated beam (fast axis) is given by the fibre lens diameter, and the size of the slow axis after the lens is determined by the increase due to divergence through an amount of space roughly equal to the fibre lens diameter.
This system has the advantage of permitting a launching efficiency of more than 90% when the diameter of the multimode fibre is slightly bigger than the slow axis waist. It also excites the fibres with a small input angle (as will be seen in the next chapter it is quite important when multimode couplers are used). In addition, it allows the fibre to be tapered down

(increase the intensity). For example, the launched NA is about 0.12 (and the fibre NA is nominally 0.4), therefore, if one starts with a fibre diameter of 125 µm, one can go down to about 40 µm diameter with low losses. This means, about a ten times higher intensity. A higher intensity in a smaller multimode waveguide would be usefull for 3-level laser operation.

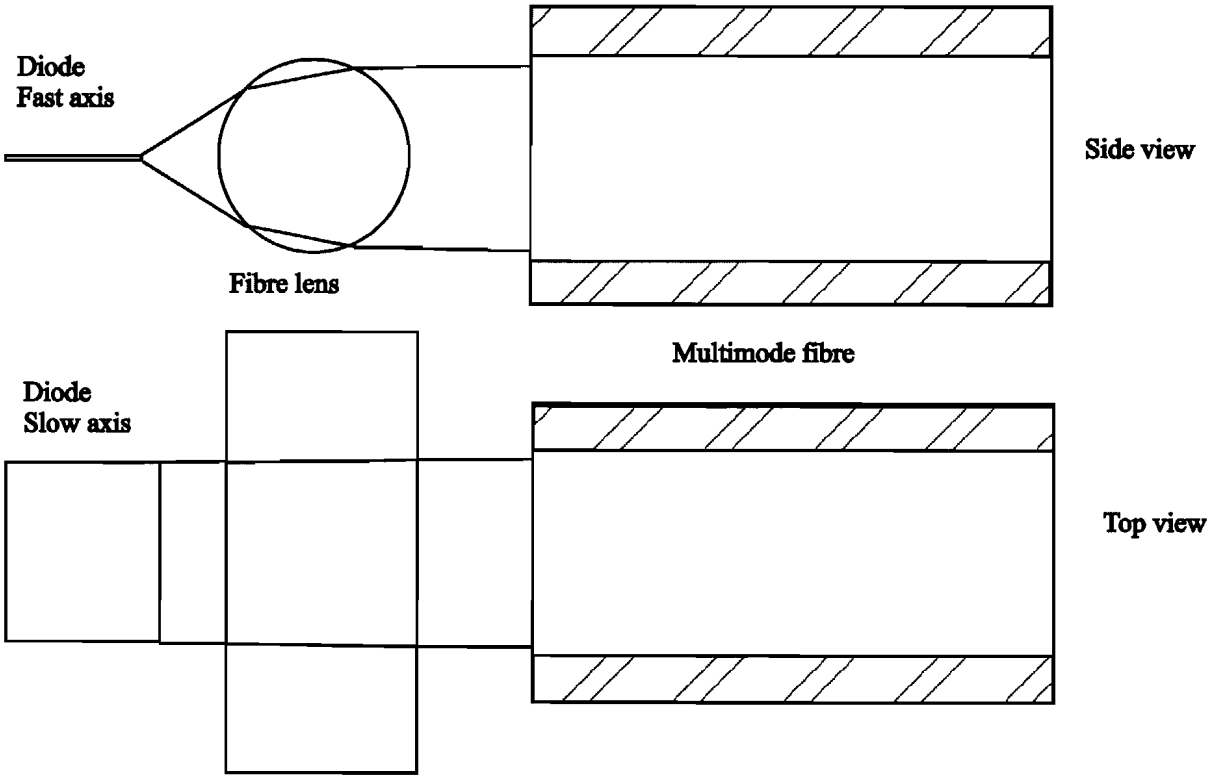

Figure I-10: Fibre lens setup.

VI CONCLUSION

In this chapter, the different launching setups used for this work were described. More than 70 % launching efficiency was achieved for each source and fibre combination with the different setups with a good level of compactness.

In most cases, the use of a LIMO coupler seems the best solution since they offer a high launching efficiency and they can be design to provide good launching for any pair diode/fibre", however for a diode-stripe and a circular geometry fibre slightly bigger than the slow axis of the laser diode, it can be seen that the fibre lens is a cheaper and simpler setup.

REFERENCE

[1] A. Clarkson and D. C. Hanna, "Two-mirror beam-shaping technique for high-power diode bars," Optics Lett., 1996, Vol.21, No.6, pp.375-377

CHAPTER II: THE MULTIMODE COUPLER

I INTRODUCTION

Now that an optical system is set for launching the laser diode's light, it seems reasonable to think about coupling the light efficiently into the doped fibre.

The first obvious solution is to end-pump it, then the only problem is the geometrical parameters of the fibre, and one has to choose an appropriate pumping scheme as describe in chapter I.

This is not the most convenient, because it makes it hard to introduce other components in the cavity. What will be called an end-free laser (the pump and the signal are not propagating in the same guides at the outputs) seems more interesting. For core pumping devices, this scheme is provided by WDM couplers, but for higher power i.e. cladding pumping, since the pump and the signal are propagating in two different (embedded) guides, this is not possible, and there are not many solutions available.

One of them is the use of V-groove side pumping (figure 1). The main disadvantage of this system is the fact that the maximum power, which can be launched, is limited [1-3] by the size of the fibre and the V-groove. Another solution is the use of multimode couplers. The final one is to use some multiple fibre arrangements. During this work, only the last two

solutions have been investigated. This chapter will describe the multimode coupler and the next one the multifibre arrangements.

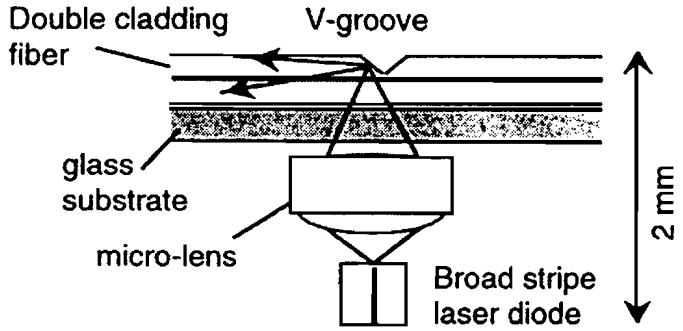

Figure II-1: V-groove side pumping [1]

II PRINCIPLE

As it can be seen in figure 2, multimode couplers are composed of a pump fibre (a silica rod -this term will be used to describe a coreless fibre in this thesis- with a low index coating) which is stripped and tapered down and side spliced to the double clad fibre (a standard doped fibre with a low index coating, stripped and slightly tapered as well), thus there is optical contact between the silica rod and the inner cladding of the DCF. Note that the side splicing occurs only at the taper waist, which is made long enough for good coupling. This results in optical coupling of the pump light, launched in the silica road, into the inner cladding of the doped fibre. The tapering permits an increase in the coupling efficiency.

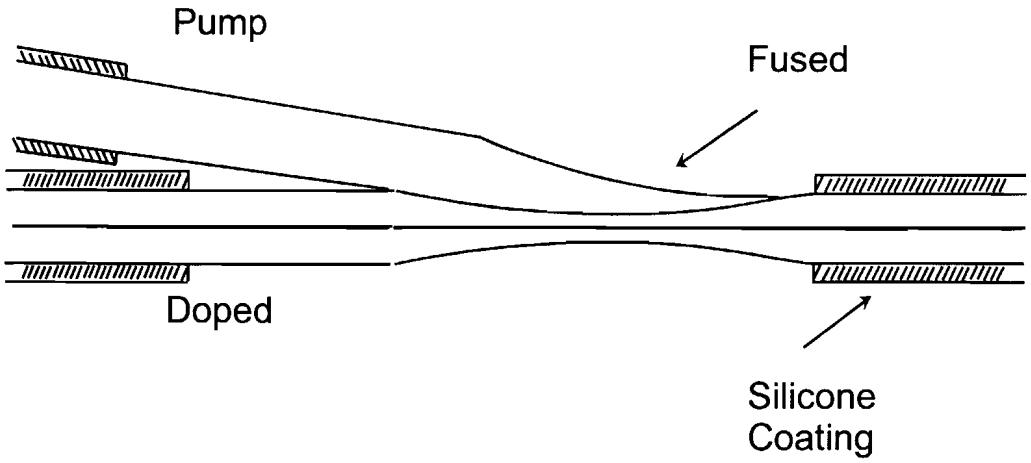

Figure II-2: Schematic view of the multimode coupler (The real proportions are not respected)

By manufacturing couplers in both ends of a DCF it is possible use double end pumping. In fact, one can use any number of couplers but they are lossy for the pump light propagating in the DCF, so they should be separated by at least two pump absorption lengths. These couplers allow the pump to be separated from the signal. Then there will be no laser emission going into the laser diodes to perturb their emission and even destroy the semiconductor facet.

Different problems occurred with these couplers, one was the choice of the diameter of the launching fibre and the other was regarding the launching beam aperture.

In the coupler the two multimode guides (silica rod and inner cladding) are fused together. Since they are both composed of pure silica, light should be expected to travel freely from one guide to the other. Practically, the contact is not as good as expected, and it is more an evanescent field type of coupling for each mode that is observed. In this case the higher order modes (high angle) are the first to couple in or out, thus it is needed to increase the amount of high angle modes, therefore the tapering is advantageous. It is also important to notice that, as a rule of thumb with these multimode guides, the coupling ratio is given by the area ratio. Therefore, if both guides are tapered to the same size there will be only a 50% coupling ratio, hence half of the pump will remain unused. On the other hand, if the pump guide is tapered much more than the doped fibre, then the coupling ratio will be high, but the high order modes will be the ones to be excited by the coupling. The problem will be that they may not cross the core hence giving low absorption. It means that the doped fibre will have to be bent to provide some mode mixing in the inner cladding, or the core will have to be offset.

Furthermore, if the taper is too strong for the silica rod, high angle modes will be excited in the waist. These modes will be coupled out of the inner cladding, when the low index coating reappears after the up-tapered section, if the taper for the doped fibre is not big enough to reduce the NA in the up-tapered section. For example if one has both pump and doped fibre with an outer diameter of 300 μm (NA with coating 0.35 in theory) and the doped fibre is tapered down to 100 μm, and the pump fibre down to 30 μm. One should have a coupling ratio of 99% (300/330) but up to NA=1 will be excited, when the doped fibre will only accept 0.7, since when untapered and with coating, the NA will be 0.35. This means up to 36% loss. One other example will be to have both fibres with the same level of tapering, in this case there would be no loss from the taper but only 50% of the pump would be coupled.

Therefore, a trade off should be found to obtain the best coupling. Furthermore, this was just a first approach of the problem, and some other factors can be taken into account, like the quality of the taper itself (if it is not perfectly adiabatic, some losses will occur) or the fact that by side splicing the two fibres together they will be embedded in only one fibre at the end (this increases the coupling and reduce the loss).
In the next parts, the different experimental issues for those multimode couplers will be described. The first was the choice of the pump fibre, since if one takes a smaller one; it needs to be less tapered to obtain a good level of coupling without inducing losses. The second was the excitation of the pump fibre, since if one excites it with a lower NA; one will have a good coupling and avoid the losses due to the taper.

III THE PUMP FIBRE SIZE

As explained in the previous section, it seems that it would be better to have a pump fibre with a smaller outer diameter than of the doped fibre. It seemed then that it was important to measure different couplers and see how this will affect their performances.
So in a first attempt, 300 μm diameter fibres were used with GEC diodes (stripe of 1x100 μm). In this case, the diameter of the multimode fibre was the same as the diameter of the inner cladding of the doped fibre (DCF) and since the fibre was bent before the coupler, all the silica rod NA was filled thanks to the mode mixing induced by bending. Both fibres were tapered the same way to the same diameter. With this coupler, the coupling efficiency was around 50% as expected in such a design. When the pump fibre was tapered much more, to have a supposed coupling ratio of 90 %, the effective coupling was still 50 %. Looking directly at the coupler, a high level of scattering was observed at the point where the coating restarts. As predicted all the very high order modes are lost in the low index coating.
Therefore, it seems that a smaller outer-diameter pump fibre should be used. Then a 150 μm outer diameter silica rod was used. With that, the coupling-efficiency reached about 90 % (launching the light with a NA<0.2 in the silica rod). This time, no scattered light was observed, where the coating reappears, only the uncoupled light coming out of the silica rod after the side splice was observed. This means that all the light coupled into the DCF excites modes, which will be propagated when the coating reappears.
This is exactly the type of coupling results expected to make a compact and efficient system. This type of coupler associated with the best launching system will allow coupling of 75% of

the laser diode (1W single stripe of 100 μm) output into the doped fibre, which means for a double end pumping scheme, 1.5 W launched into the fibre at least (it can be even 3W if 2W stripes are used). Now, for ytterbium, as a rule of thumb the output power is about half of the input power, it means that one can already expect quite a high power laser in a very compact setup.

But as it will be described in the next part the couplers are not as good as predicted, since they start to be lossy when the NA of the light launched into the pump fibre increases.

IV LAUNCHING IN THE PUMP FIBRE

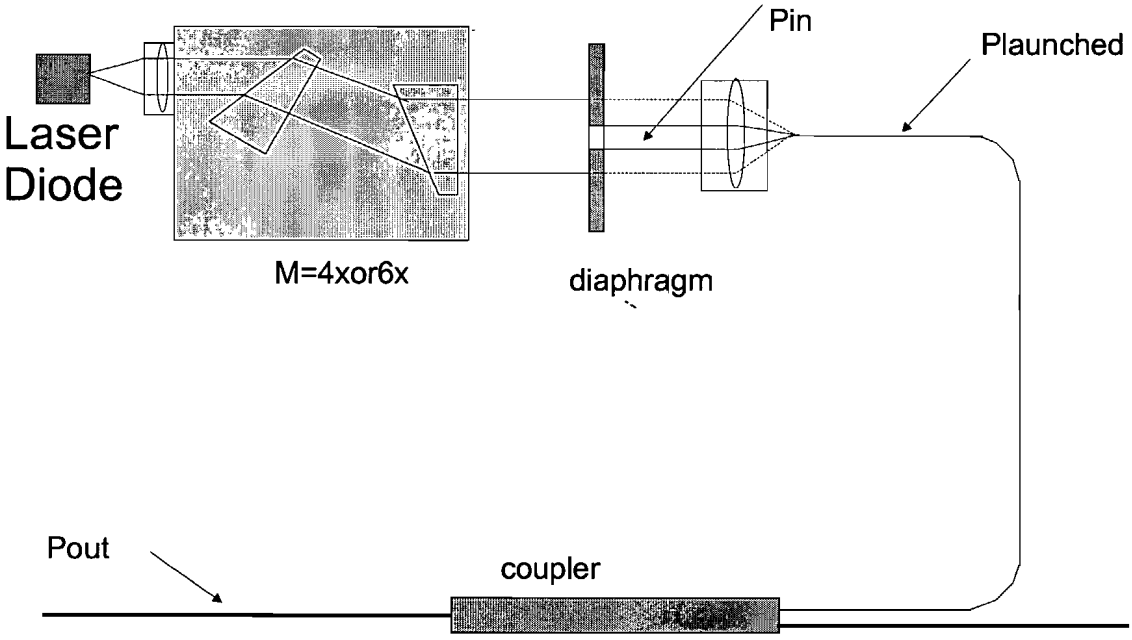

Figure II-3 Setup for measuring coupler's dependence on launching beam aperture.

With the best coupler the silica rod was tapered with a waist (50 μm diameter) of 1/3 of the waist of the doped fibre (150 μm diameter). This gave a ratio of 1 to 9 for the areas (silica rod compared to the DCF at the waist of the taper), to obtain a 90% coupling efficiency. Both fibres had NA of 0.35 with coating, and the silica rod diameter was half of the DCF diameter (300 μm). Since the NA of the DCF with coating is the limit, in the taper the limit NA will be 0.7 (300 μm down to 150 μm). It is the same limit for the silica rod at the waist, so untapered the limit NA for the silica rod is 0.23. It means that everything above 0.2 will be lost. Therefore if the pump fibre is excited with less than 0.2 aperture, no losses should be

observed. To have a more quantitative idea of this effect some measurements were done with the setup shown in figure 3. The powers (W) were measured with thermal power-meters, which give a relative error of 5% for the measurment. This setup was mainly based on the bulk optic launching system described in chapter I. The main difference was that a large aperture lens was used to launch the light in the doped fibre and a diaphragm used to effectively measure the dependence on aperture. Note that at full aperture of the diaphragm the pump beam homogeneously covered the lens. To know which aperture was used, the power was measured after the lens for each chosen position of the diaphragm and those powers were compared to the maximum (Maximal aperture). Then the power launched into the silica rod was checked. Finally, the silica rod was spliced to the coupler and the output was measured for each given aperture. With this, the results shown in figure 4 were obtained.

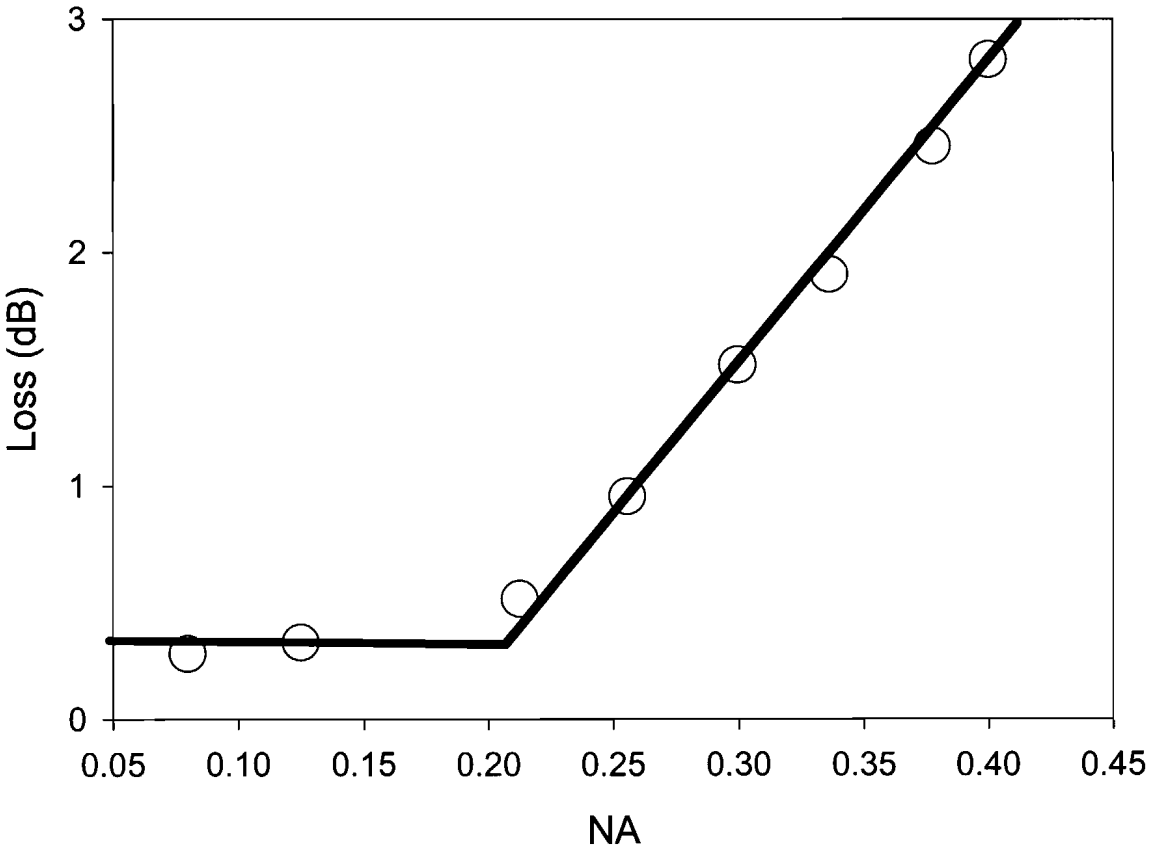

Figure II-4 losses in the coupler depending on incoming beam NA.

As expected, there is a lower coupling efficiency when the incoming pump beam aperture goes above 0.2. This proves that for the setup to be efficient, the incoming beam convergence should be controlled. To be more precise the best launching system for those

couplers, would be to use fibre lenses since they provide an incoming aperture around 0.12. Furthermore this is an important limitation for the fibre laser because it limits the amount of pump one can launch into the system. However, the brightness of the broad stripe laser diodes is becoming sufficiently good to overcome the limitation. For example, now one can find 100μm stripe with 4W output and standard divergence (12 degrees in the slow axis and 35 degrees in the fast axis). It means that with a fibre lens one should be able to couple up to 3.2 W of the pump light into the doped fibre. Actually this was good enough, because most of the power lost into the coupler is turned into heat. Therefore, when very high power is launched, the coupler will burn, as happened when diode bars were used and up to 10W was launched into the coupler.

V LOSSES IN THE CORE

As will be described in the second part of the thesis (Chapter V), a lower efficiency was experienced when a fibre with one or two couplers was used. It seems that the couplers are introducing some losses for the signal into the core. There are three possible ways of explaining this. The first one is that the signal is scattered out of the core or coupled into the cladding. The second is that since the outer modes are coupling first and they are rarely crossing the core, the absorption of the pump is much less efficient, and so is the laser operation. The third possible explanation might be that the side fusion splice might deteriorate the core structure and induce loss for the signal. For the second one, by bending the fibre, there should be enough mode-mixing for the pump to have a good absorption and a good lasing operation. Obviously it should not be bent too tight to avoid loss in the core. However, results (Chapter V) were mostly obtained with bent (wound in a kidney shape) fibre, therefore the loss in efficiency is probably not due to this problem.

An electric arc was used to make the coupler. It generates very high temperature. It then switches off quickly from this high temperature to room temperature. This sort of process may generate a permanent crystallisation site in silica. This effect will obviously increase the scattering loss. Furthermore the fibre is tapered, and the signal mode in the core will have an important evanescent field, which makes it much more sensitive to scattering losses.
To test if the third effect was the problem, an Er/Yb fibre was used with two different types of couplers. The first type of coupler was a standard one like the best one described earlier. The second one was made with two tapered fibres wrapped together without side splicing

them. This last one was less good in coupling (bad optical contact) but the core should not be perturbed by side splicing or bending (the rate of wrapping did not induce high bending: 1 turn over 10 cm). The results are shown in figure 5. It has to be noticed that the increase in slope is due to the Ytterbium, which started to lase instead of Erbium.

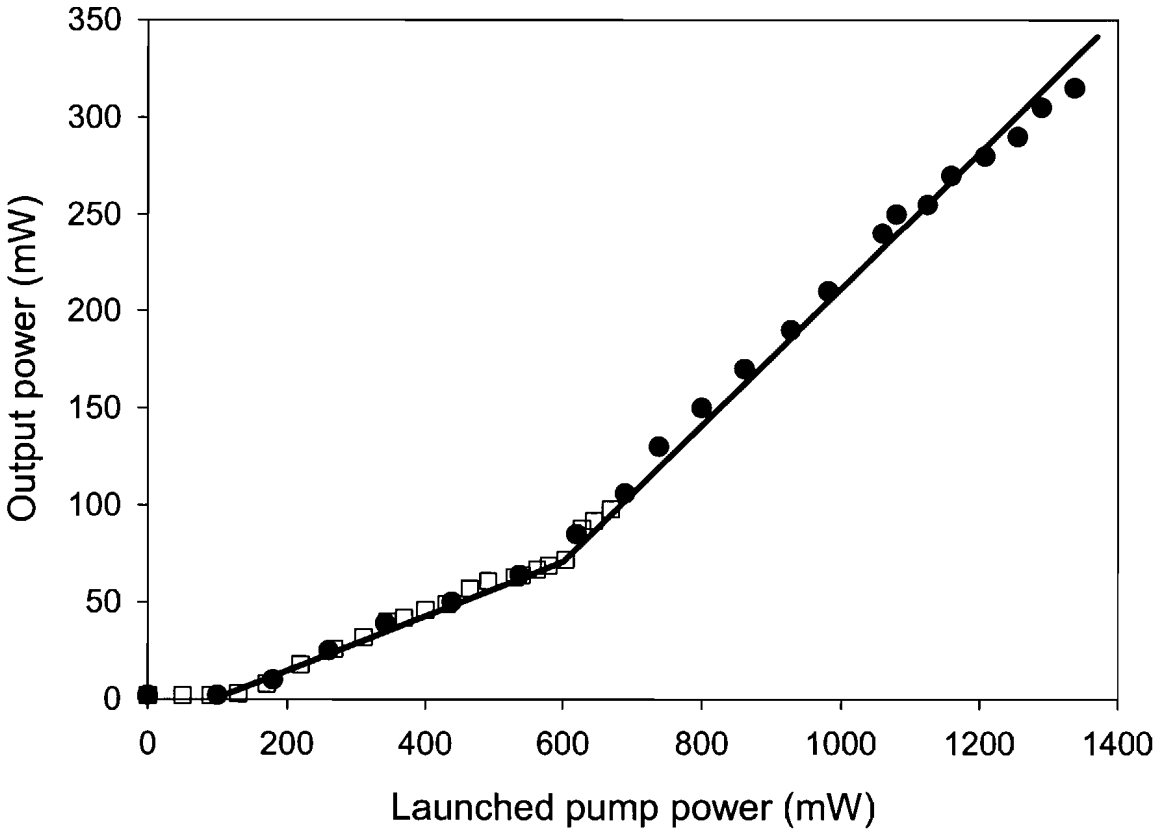

Figure II-5 Lasing results with two different types of couplers. Standard coupler (Black dot) and coupler without side splicing (white square)

This shows that for an equivalent level of launched pump power there is no difference between the two couplers. It proves that the losses are induced by the tapering of the fibre and not the side splicing.

This seems to prove that the losses are only due to the tapering and the crystallisation of silica, since it is the last possible source of losses in the coupler. Those losses might be avoided if one uses a tapering rig with a flame or furnace instead of an arc (like the rigs used for WDM couplers), since it provides a smoother change in temperature. In this case, the crystallisation of silica should be avoided.

VI CONCLUSION.

In this chapter, the importance of having a laser with free ends was discussed, and one solution was proposed; the multimode coupler. It proved to be quite efficient, around 90% coupling efficiency. To some extent, it can also be pushed further by using several silica rods associated with a single mode fibre all side spliced together and tapered down to be end spliced with the double clad fibre like in [4].
However, the use of couplers has some limitations; it introduces losses for the signal in the core and to obtain the maximum coupling efficiency one needs to control the pump launching aperture. Therefore the full aperture of the pump silica rod was not used. Furthermore those couplers cannot support very high power since the losses (at least 10%) are turned into heat and can destroy the coupler if the pump power is more than 10W.

REFERENCES

[1] J. P. Koplow, L. Goldberg, D. A. V. Kliner, "Compact 1-W Yb-doped double-cladding fibre amplifier using V-groove side-pumping," *IEEE Photonics Technology Lett.*, 1998, Vol.10, No.6, pp.793-795

[2] M. Hofer, M. E. Fermann, L. Goldberg, "High-power side-pumped passively mode-locked Er-Yb fibre laser," *IEEE Photonics Technology Lett*, 1998, Vol.10, No.9, pp.1247-1249

[3] L. Goldberg, J. P. Koplow, R. P. Moeller, D. A. V. Kliner, "High-power superfluorescent source with a side-pumped Yb-doped double-cladding fibre," *Optics Lett.*, 1998, Vol.23, No.13, pp.1037-1039

[4] US patent No: US 5,864,644 "Tapered fiber bundles for coupling light into and out of cladding-pumped fiber devices."

[5] A. B. Grudinin, J. Nilsson, P. W. Turner, W. A. Clarkson and D. N. Payne, "Single clad coiled optical fibre for high power lasers and amplifiers," Postdeadline papers, CPD 26, CLEO'99, Baltimore, 1999.

CHAPTER III: MULTI FIBRE ARRANGEMENT

I THE PRINCIPLE

As illustrated in the previous chapter, it is a great improvement to have an end-free fibre laser. The problems observed with the multimode couplers combined with difficulties in their fabrication, suggest that a better solution is needed.

To extend the idea of the coupler, two (or more) fibres could be placed side by side, thus evanescent field coupling from one fibre to the other should occur for the multimode propagation of the pump, until an equilibrium point is reached, which is linked to the relative areas of both fibres. In this case, the length of coupling will be longer than for coupler and will be strongly dependant on the distance between the two fibres.

For this compact system, two different ways of utilising this process were investigated. First, by using bare coiled fibres (single cladding), and then, by using two fibres twisted around each other inside the same coating (figure 1).

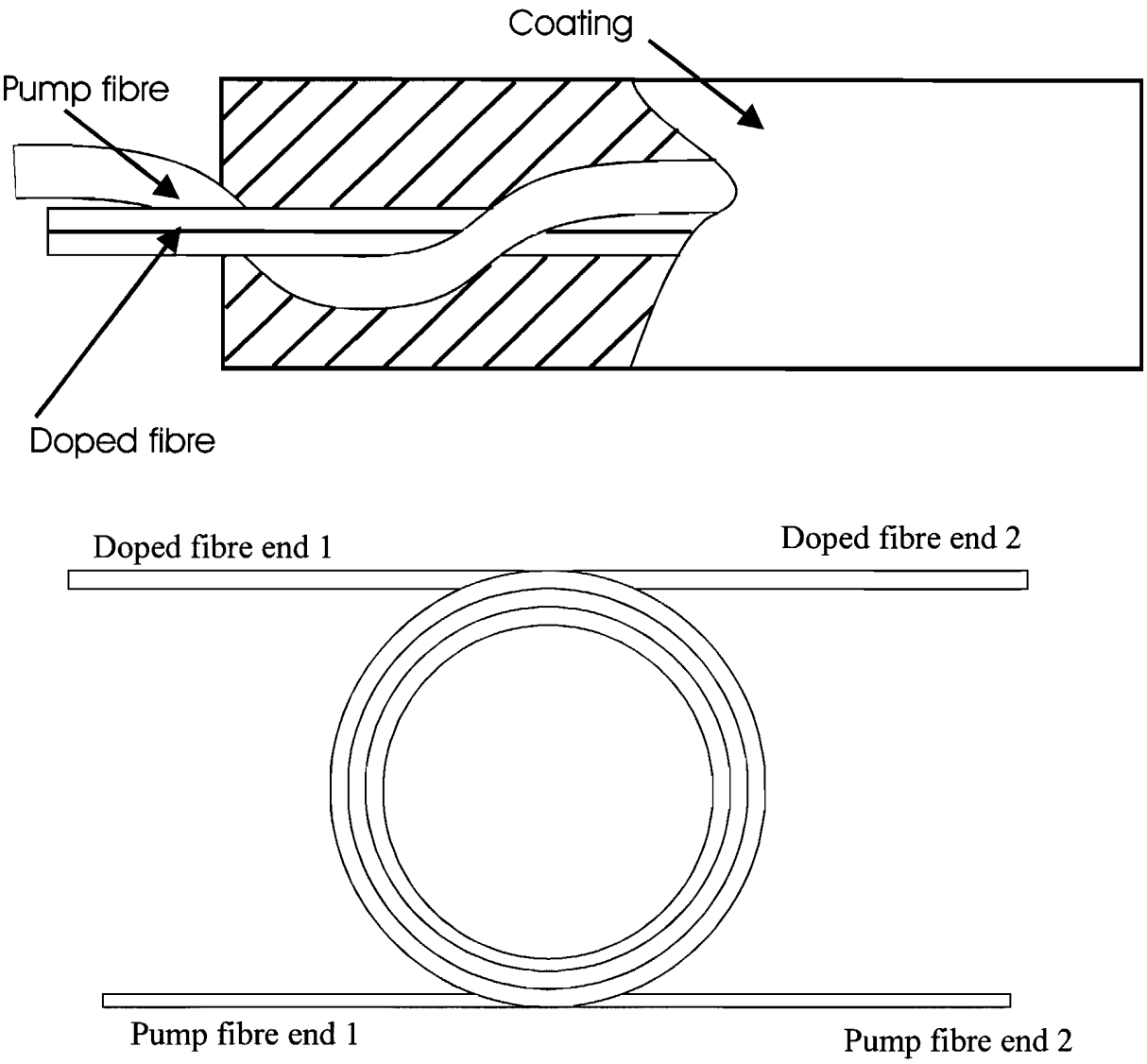

Figure III-1: The two different types of fibre arrangement.

In this chapter, a simple theoretical model is developed, to describe the interaction between two fibres twisted together, and some experimental measurements for comparison with this theory will be shown. The lasing results will be described in Chapter V (Part II).

II A SIMPLE THEORETICAL APPROACH

II-1 The coupling

The multimode coupling between two silica rods is the main problem described in the following part. Here, a beam propagating through the fibres with a certain shape filling the

NA of the fibre (Gaussian or square) will be considered. This is a very simple way of describing the system, however it proved to be a good approximation, and an exact calculation of the modes and their propagation in such a big fibre demands a lot of computing resources, for which I did not have access.

The model used, is taken from [1], and is defined by the equations below. Note that it is considered that the two rods are in contact, thus there is no factor including dependence on the distance between the two rods. The first equation gives the power in the second rod as a function of the power in the first rod where the light is launched. The second equation gives the expression for the coupling coefficient for a given angle of propagation within the NA.

$$P_2(z) = P_1(0) \cdot \frac{A_2}{A_2 + A_1} \cdot \frac{\int_0^{\theta_c} f(\theta) \cdot [1 - \frac{\sin(C(\theta) \cdot z)}{C(\theta) \cdot z}] d\theta}{\int_0^{\theta_c} f(\theta) d\theta} \quad (1),$$

$$C(\theta) = \frac{\theta^2}{\theta_c} \cdot (\frac{4}{\pi \cdot V})^{1/2} \cdot \frac{1}{\rho} \quad (2),$$

where the coefficients are:

P_i: Power in fibre i=1 or 2 (W)

z: position along the fibre (m)

A_i: area of fibre i, $A_i=\pi\rho_i^2$ (m^2)

θ_c: Compliment of the critical angle of the fibre; $\sin\theta_c=NA/n$ (rad)

V: V number of the guide (see Appendix A)

ρ: average of the two fibre radius $\rho_{1,2}$ (m)

$f(\theta)$: propagating beam shape

The propagating beam shape is defined depending on the twist rate of the fibre (r). It was decided to make it tend to a beam, which equally fills all the angle of acceptance of the multimode guide, starting from a Gaussian shape with a $1/e^2$ waist equal to the fibre diameter. The purpose was to take into account the mode mixing. To make it as close as possible to reality the experimental results were fitted to find the right functionnal dependence on the twist rate (r). Note that the experimental twist rates are included between 50 and 500 turn/m. This gives the following formula for the propagating beam shape.

$$f(\theta) = \exp(-(\frac{\theta}{\theta_c})^2 \cdot \frac{2}{(1+r/r_0)^{1/2}}) \quad (3).$$

In this function r_0 is a normalization factor equal to 1 turn/m. As $n \to \infty$, the function becomes flat (while $\theta < \theta_c$). The following results (figure 2) were obtained for the coupling efficiency, which is given by averaging the coupling coefficients $C(\theta)$, over the beam shape, as a function of the twist rate of the dual fibre. Note that two identical silica rods of 100 μm diameter were used in the calculation, and that the results are only valid above a rate of 50 turns/m since the fitting was done between 50 and 500 turns per meter.

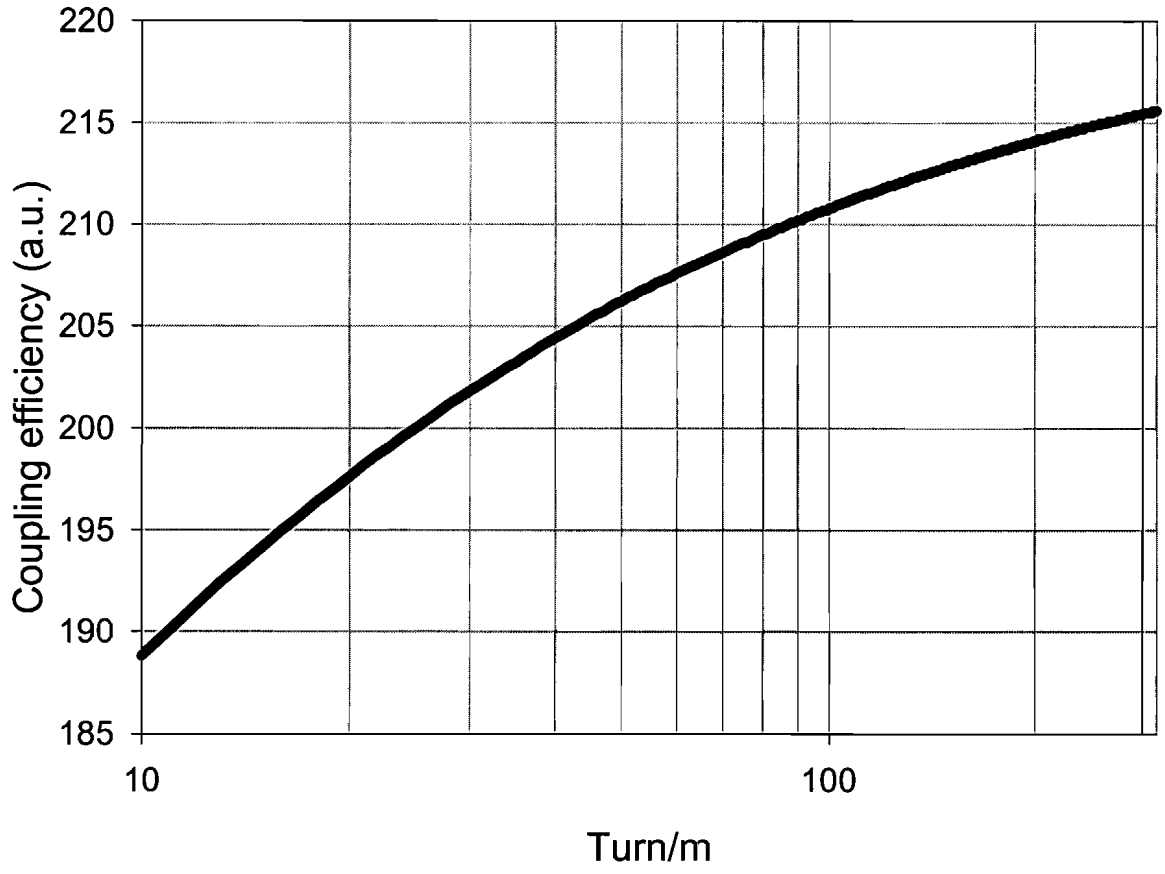

Figure III-2: Dependence of the coupling with the twist rate.

Then, the calculations were performed for the two extreme types of propagation, the square shape and the Gaussian one. In figure 3, the length dependence of the coupled light for those two shapes is shown. For those calculations, both rods had the same size of 100 μm diameter.

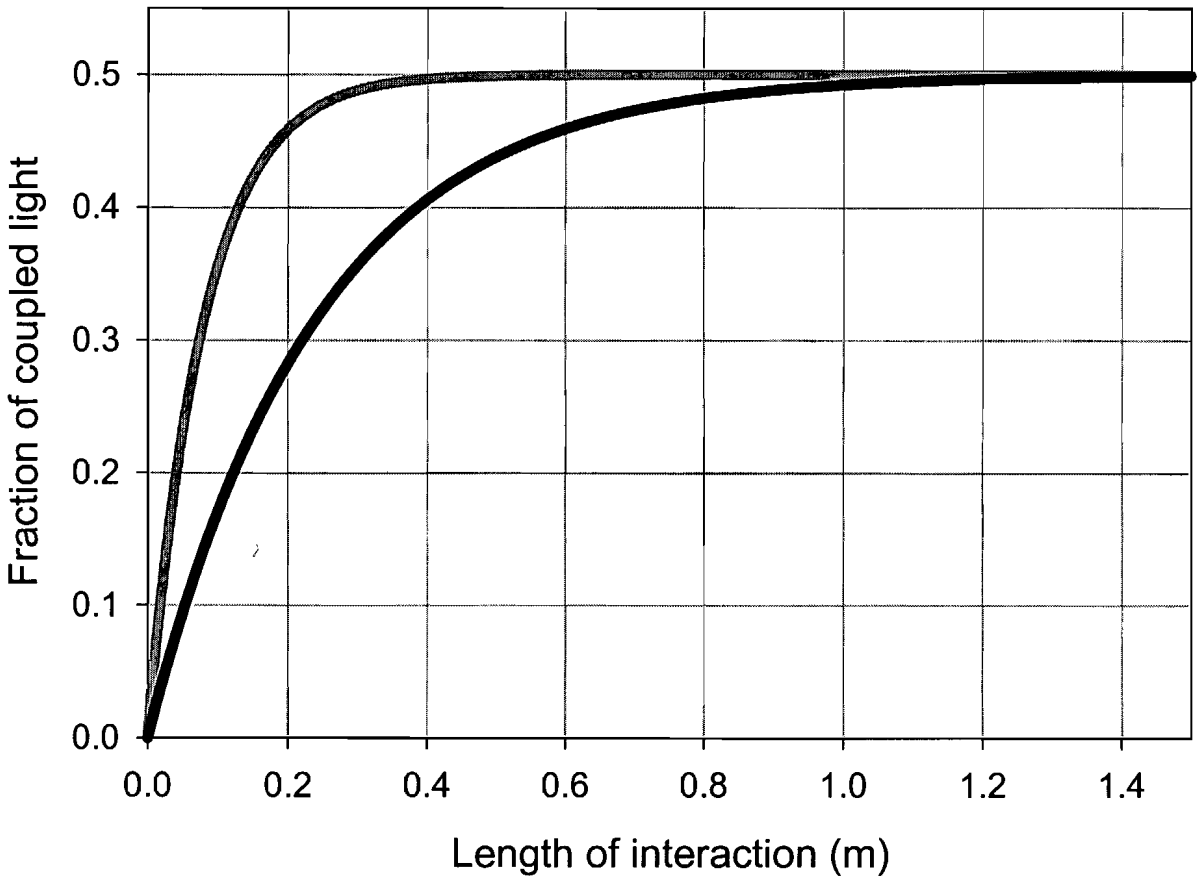

Figure III-3: Length dependence for coupled light. When there is a Gaussian beam (r=0) propagating (black) and when there is a square shape beam (r→∞) propagating (grey).

As it can be seen from figure 3, the coupling depends on the twist rate and provides a coupling length short enough to obtain a laser device. Note that the coupling is wavelength dependant (V is directly related to the wavelength), however for the wavelengths of the sources used in the experiments (633nm up to 975 nm) the relative difference does not excess 10%. All the above calculations were made for λ=915nm.

This model can be extended for more than two fibres. Then one has to take into account what fibre is in contact with the other. Mainly, it is practically difficult to have contact between more than two fibres. Therefore, it seems reasonable to consider that all fibres are side by side to model the behaviour of a multifibre (more than 2 fibres), thus each fibre is in contact with either one or two other fibres.

II-2 The bend losses

Since the fibres are twisted together some bending losses may occur both for the pump and the signal depending on the twist frequency.
Here, the best way of studying the losses for the pump would have been to use a beam propagation method along a helix path defined by the size of the other fibre and the twist frequency. However such a method is prohibitively complicated to compute and time consuming; therefore it was considered that all the NA was filled with the signal and that each step of calculation, the part out of the critical angle was removed because of the displacement due to the bending. Then because of the helix path it was considered that the NA was still equally filled because of high mode coupling induced by the twisting. The helix path amplitude was defined by the size of the fibres and the period by the twist rate. Of course the losses were only calculated over half a period, since after that they will repeat themselves. Such a method was hoped to overestimate the losses. The change of angle per step dz of length for a helix path is given by:

$$\delta\theta(z,r) = dz \cdot 2 \cdot \rho \cdot (2 \cdot \pi \cdot r)^2 \quad (4),$$

which leads to the following to compute the losses:

$$L_{dB/m}(r) = r \cdot 10 \log\left(\prod_{i=0}^{N} \frac{2 \cdot \theta_c - |\delta\theta(i \cdot dz, r)|}{2 \cdot \theta_c}\right) \quad (5),$$

where dz is the integration step, ρ is the fibre radius, i the iteration step, and N the number of iterations (dz would be given by 1/2rN). Again r is the twist rate and θ_c the critical angle. This gave the following results, shown in figure 4). These formulas are for two fibres, of the same outer diameter of 100 μm, twisted together.
For most of the experimental fibres, periods of 1-2cm were used for the twisting (50-100 turn/m) which with this model corresponds to a loss of 0.15-0.35 dB/m.
Next, one can consider the effect of changing the size of the doped fibre. Diameters of 80, 100 and 125 μm were considered. The results are shown in figure 5.

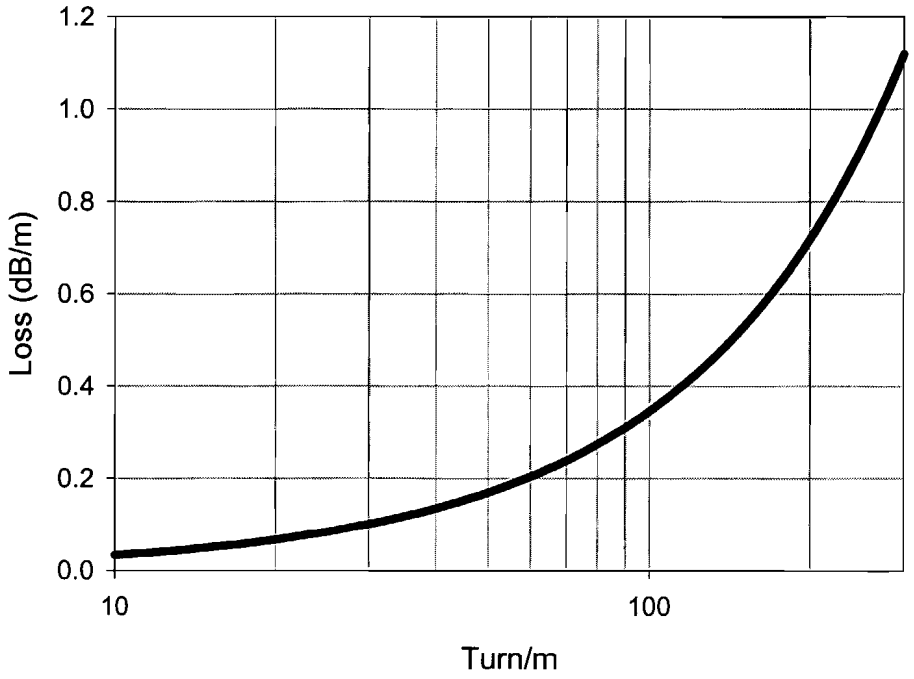

Figure III-4: Bending losses for the pump propagation depending on the twist rate for two silica rods of 100 µm.

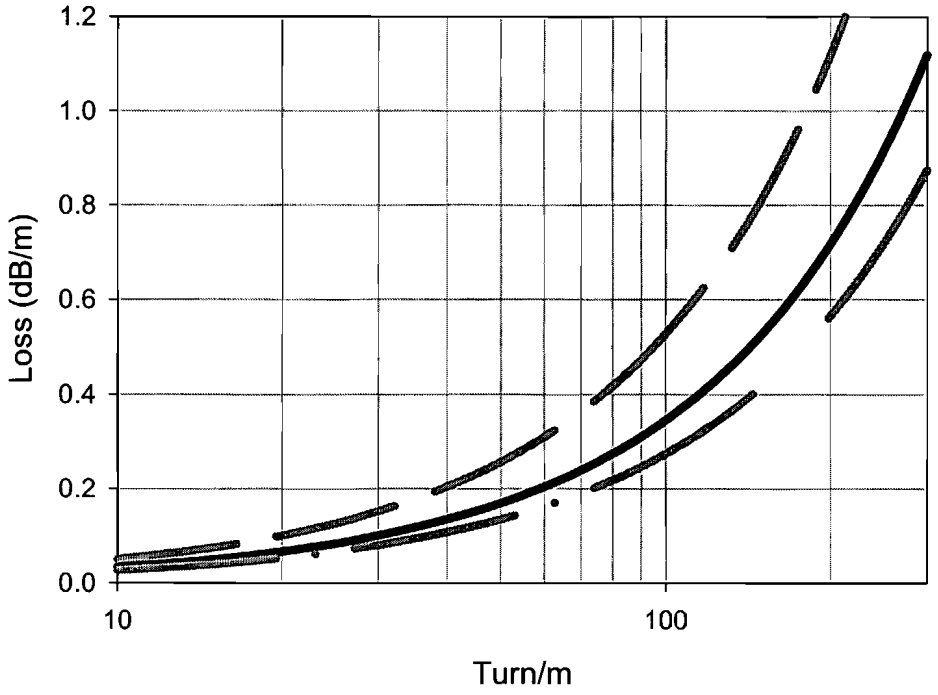

Figure III-5: Losses for the pump versus twist rate. The pump rod was always 100 µm of diameter. The grey dash-curve is with a 125 µm diameter doped fibre; the grey dot-dash curve is with a 80 µm diameter doped fibre. The solid line is for a 100 µm doped fibre.

This shows that the smaller the doped fibre is, the less losses are observed, since in this case the amplitude of the helix path is smaller.

The losses for the signal propagating in the core were then studied. A modal model described by the following equations [2] was used.

$$\alpha_{dB/m}(R) = \frac{4.34}{\sqrt{\pi \cdot a \cdot R \cdot W}} \cdot \left(\frac{U}{V}\right)^2 \cdot \exp\left(-\frac{4}{3} \cdot \frac{W^3}{V^2} \cdot \Delta \cdot \frac{R}{a}\right) \quad (6),$$

where R is the radius of bending curvature, a is the singlemode core radius, U, W, Δ and V are parameters to describe the propagation in the fibre core. They will be detailed in Appendix A.

These results are shown as a function of the radius of curvature. Once again a helical path was consider and the average radius of curvature was calculated over the length of half a twist period. The NA of the fibre ($\Delta=NA^2/2$) was fixed to 0.1 and the core radius was 3 µm since most of the fibres had this NA and core size. The results are shown in figure 6, for the cut off wavelength, and for two identical fibres with an outer diameter of 100 µm.

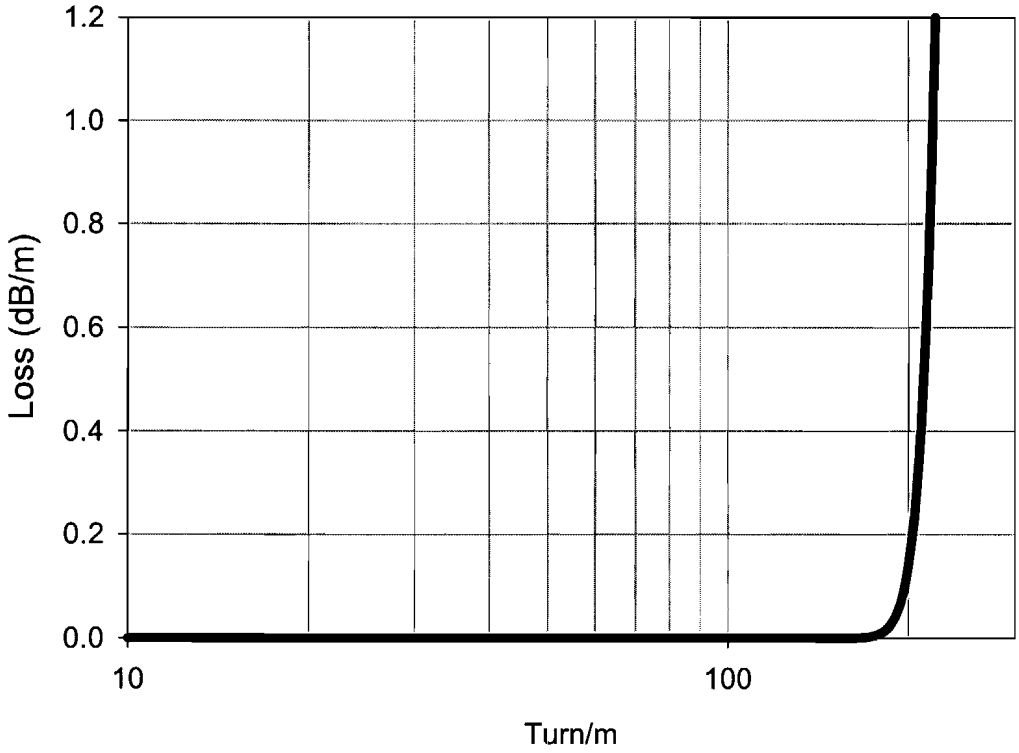

Figure III-6: Core losses at the cutoff wavelength for two fibres of 100 µm diameter twisted together.

The wavelength dependence of these losses (wavelength compared with the cut-off)is shown in figure 7. Note that the wavelength dependence is due to dispersion in silica for the index and the fact that V is directly dependent on the wavelength. Therefore, the dispersion of pure silica [3] was used for the calculation, even if in the fibre experimentally used there was also germanium and aluminium in the core, which change the dispersion slightly. Once again the NA was chosen to be 0.1.

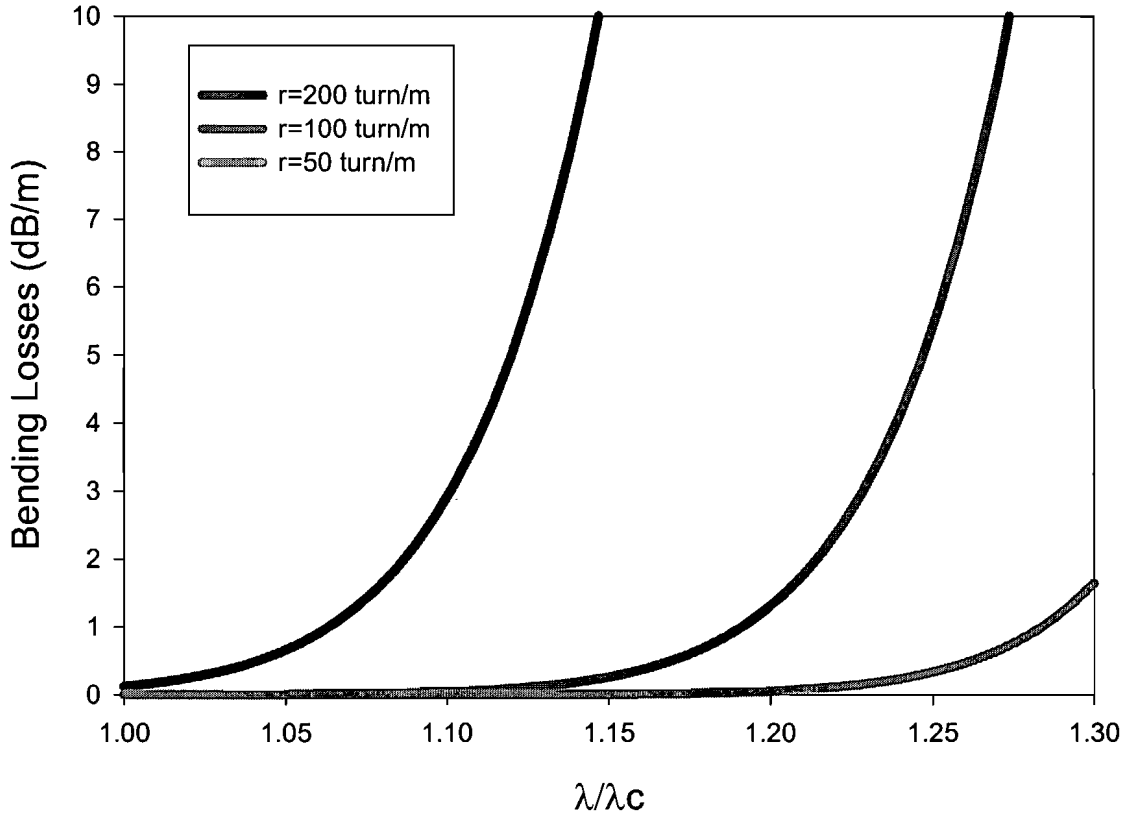

Figure III-7: Bending losses in the core depending on signal wavelength compared to the cutoff.

This demonstrates the importance of the choice of the cut-off wavelength for this type of fibre, since the losses can become too big if the signal wavelength is too far from the cut-off. For instance, if one consider a Er/Yb amplifier with a cutoff at 1240 nm, and a twist rate (standard) of one turn per centimetre, the losses for the signal at 1550 nm will be around 6dB/m. This shows that if one wants to have a high twist rate, either the cutoff needs to be kept as close to the signal wavelength as possible, or the NA needs to be increased to improve the mode confinement.

Once again the results for different pump fibre size were compared and as expected the smaller the pump fibre is the lower are the losses, for the same reason as stated earlier.

It should be emphasised that the twist rate is important because it creates mode coupling for the pump modes inside one rod which constantly excites the higher order modes, which thus have a better coupling coefficient with the other rod. This means that twisting enhanced the coupling of the multifibre configuration. It is quite important to have good coupling to obtain a good lasing operation, because if it is bad an important part of the doped-fibre would not be pumped, thus reabsorption of the signal would be important and the threshold would be higher than with a better coupling. Therefore one has to find a twist rate for which the losses in the core are low enough and the coupling is good enough. The calculations performed above suggest that a period of 1-2cm (rate of 50 or 100 turn per meter) seems the most suitable to have low loss and high coupling, if the signal wavelength is not too far from the cutoff wavelength.

As stated previously, these results were expected to overestimate the losses for the pump, therefore it was decided to make some comparative measurements to test the model, as it will be detailed later in part III of this chapter.

II-3 Lasing with a multifibre configuration

To simulate lasing with a multifibre configuration, the model of coupling described in this chapter and a simple numerical model based on the rate equation described in chapter IV were combined.

The main purpose of these calculations is to give a comparison between end pumping and multifibre configurations. For those calculations the multifibre was considered to be composed of a silica rod of 100 μm diameter, and a doped fibre with an outer diameter of 100 μm, a core of 6 μm diameter, and a NA of 0.1. The dopant concentration was calculated to obtain an absorption of 3 dB/m for the pump (the pump is considered to be at 920 nm). The twist rate was considered to be 2 turn per centimetre, thus there were no bend losses for the signal at 1080 nm (ytterbium doped fibre was considered as it is more likely to lase at 1040 nm). The fibre length was chosen to give an overall 20 dB pump absorption. The standard double clad fibre (end-pumping) had the same core characteristics as the multifibre arrangement. The cladding size was calculated to obtain the same area of silica as in the multifibre arrangement, hence the cladding diameter was 141.4 μm. In this configuration the fibre absorption was exactly the same (3 dB/m), and again the fibre length was calculated to obtain a total absorption of 20 dB. Both fibres were pumped from one end only. The

parameters for ytterbium and a detailed rate equation model will be given in Chapter IV. With these considerations the calculation results shown in figure 8 were obtained.

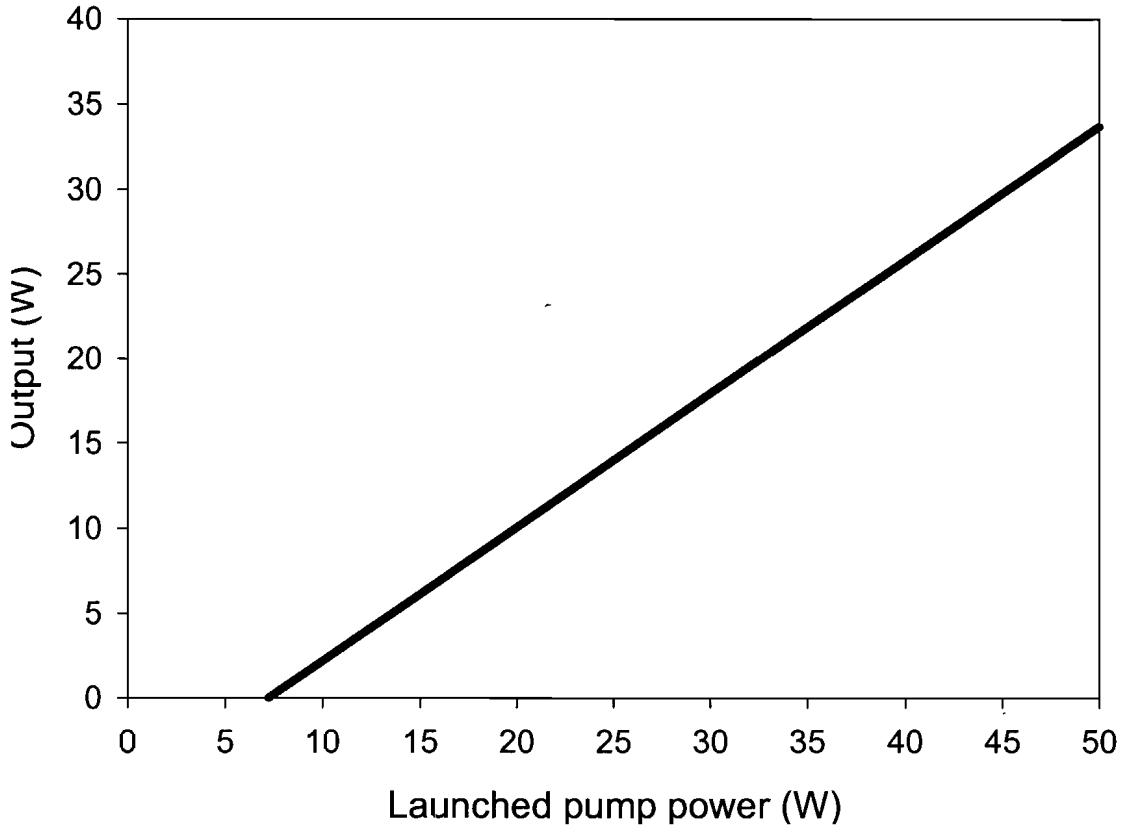

Figure III-8: Result of calculation for lasing with a 141.4 µm end pumped cladding pumped fibre laser, and for a double fibre arrangement with two 100 µm fibres (the pump silica rod and the doped fibre). There is no difference between the two curves.

It can be seen from figure 8, that there is no significant difference between the end pumping and the multifibre configuration. In fact, just the threshold is slightly higher for the multifibre configuration; 7.45 W instead of 7.3 W. The threshold is high because the fibre is very long and reabsorption is strong at 1040 nm.

This is mainly due to the short unpumped part of the fibre, thus it reabsorbed the signal. It seems therefore that in theory the multifibre configuration is a good solution for a cladding pumped fibre laser.

III EXPERIMENTAL RESULTS

III-1 The coupling

To test the coupling interaction for this type of device, a fibre arrangement consisting of two silica rods twisted together was first used. One rod was 100 μm diameter the other was 125 μm diameter. The twist rate was approximately 2 turns per centimetre, which means that the mode mixing should be good.

To test the fibre, a He-Ne laser (633 nm) was used to launch light in one of the two silica-rods. The light was launched through a set of two lenses. This was done in order to have a large input NA for this pump, and to be able to insert a diaphragm to test the effect of changing the input NA. Note that these fibres will be used at either 915 nm or 975 nm, therefore the coupling will be different since the measurement is done at 633 nm.

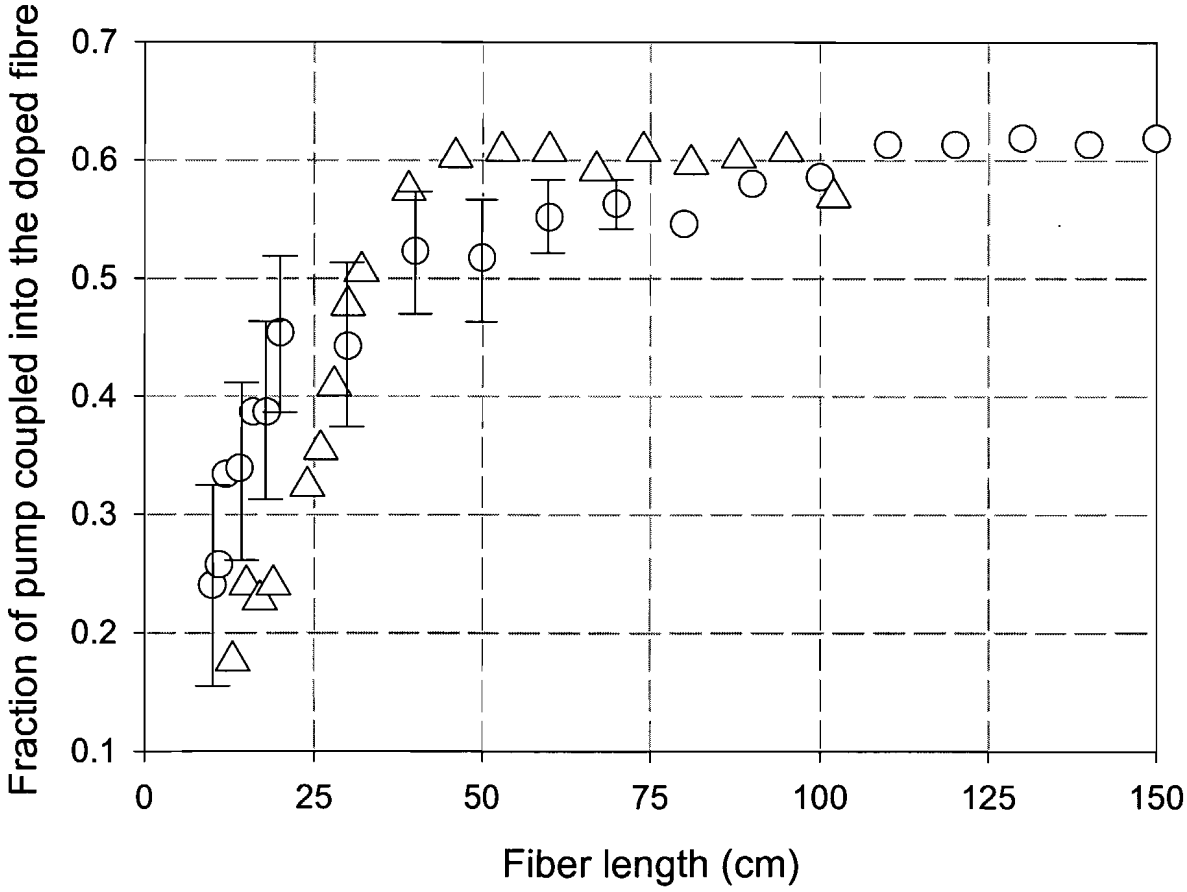

Figure III-9: Experimental result of coupling length when half the pump fibre NA (circle), and all the pump fibre NA (triangle) is excited.

The results, as shown in figure 9, demonstrate good agreement with the simple theoretical model described above. A final coupling ratio of 60% was measured, which corresponds to the fibres relative sizes. Around half a meter of coupling length was also measured. It is also interesting to notice that, even with good mode-mixing due to the twist rate, the coupling length will be longer if the NA of the silica rod is not filled with the launched beam.

III-2 The bend losses

The simple theoretical model described previously predicts that losses due to the bending of the multimode fibre should occur. Then, it was decided to check if the theory was accurate enough. For this three different types of measurement were used for the pump losses and one for the signal losses.

A 3 m long section of fibre was excited with a diode laser source emitting at 808 nm into either the core or in the cladding. The fibres were either a 125 μm silica rod or a 125 μm diameter doped fibre with a core diameter of 6 μm and a NA of 0.1 to match the conditions of the calculation.

For the first test, one end was fixed for the launching setup and the other in a bare fibre adapter. Two fibres of 125 μm diameter were twisted together counting the number of turns and then measuring the losses. The main problem associated with this method, was the difficulty in maintaining a uniform twist rate along the fibre, thus for high twist rate the measurement was imprecise. It was next decided to exchange the twisting by simply coiling the fibre around a fixed diameter cylinder. Here the error is less important and the cylinder diameter can be related to the twist rate. However, in this case, there were still problems with the bare fibre adapter (a 125 μm adapter) as movement of the fibre within the adapter might alter the measurement. The fibre adapter was then fixed with a short length fibre, which was spliced to the coiled fibre. In this last method, there was no problem for both the precision of twisting and the movement in the fibre adaptor. The last method of measurement was the only one used for the signal losses in the core. It has to be noted that the cutoff wavelength was almost the same as the source wavelength, thus the bending losses are lower than would occur in the laser emitting at 1080 nm.

The results for the last test are shown in figure 10 for the multimode propagation and in figure 11 for the single mode propagation. On each graph, the theoretical estimation from the model described above has been plotted.

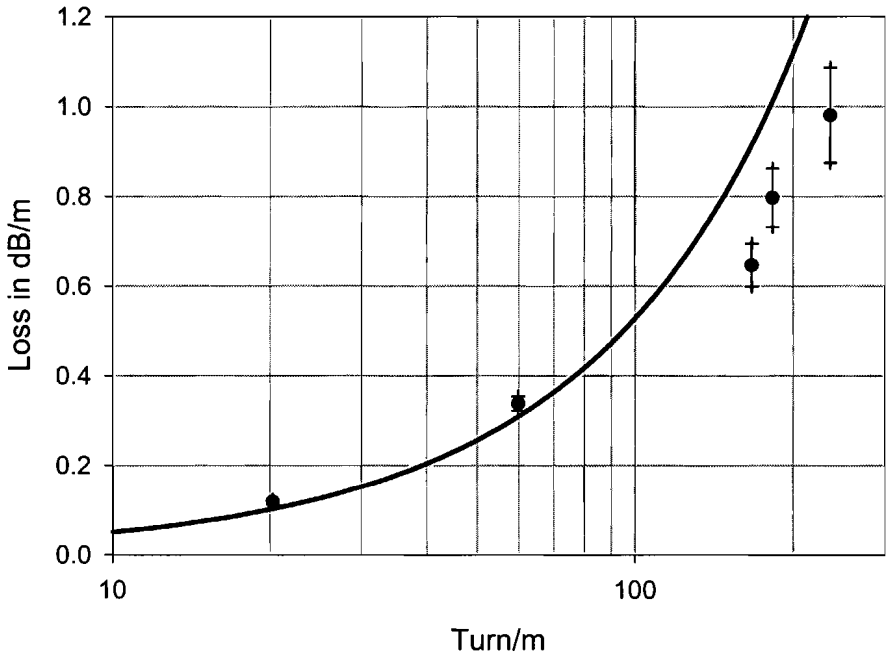

Figure III-10: Measured bend losses at 808 nm in the silica rod. The solid curve is the calculated loss for two 125 µm diameter fibres twisted together.

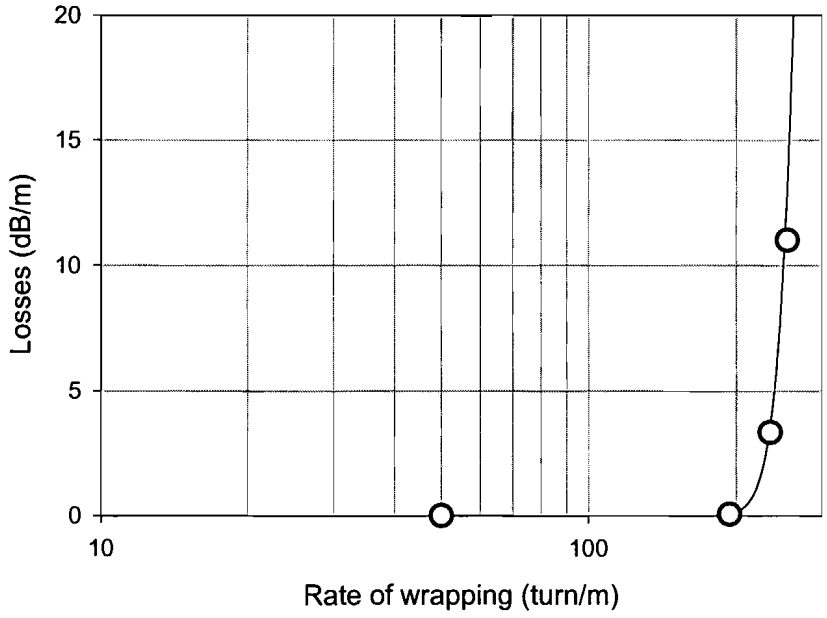

Figure III-11: Bending losses (808 nm) measurement results, for the core propagation. The solid line is the calculated losses for the same size fibre (125 µm). The error bars cannot be seen in this figure they are around 0.1 dB/m maximum.

These two plots demonstrate a good agreement with theory. Note also that for multimode propagation, the theory seems to slightly overestimate the real losses, as predicted since in reality the NA of the multimode fibre is never homogeneously filled by the pump power as assumed for the calculations. Hopefully, this model can, therefore, be used to have a better idea of a reasonable twist rate.

IV DISCUSSION

IV-1 Main advantage of the multifibre arrangement

The obvious advantage of this arrangement is the end-free running system. Furthermore, the twisting induces mode mixing in the multimode guide. This has two advantages, first it enhances the coupling, secondly it gives a good absorption length for the doped fibre, since it is not necessary to bend the fibre to increase the mode mixing for the pump modes (This is necessary for good absorption in centro-symmetric circular shaped DCF). In the case of the air-clad system, the NA should be so high that one should be able to launch light from quite low brightness high power sources, with the only limitation being the lenses.
This sort of scheme for a fibre laser should give results comparable with an end pumped double clad fibre laser. However some limitations were also found.

IV-2 Main problems of the multifibre arrangement

The main problems are the losses due to the twisting for the pump and the signal. About 0.2 dB/m was measured for the pump and the signal might depend strongly on cut-off and bending. On the other hand, if the twisting is too low then the coupling for lower order modes starts to be very weak, and the first modes coupled are not crossing the core therefore the pumping is less efficient and the gain medium is not saturated. In this case, one would have to use a long fibre, and the reabsorption of signal (in the core) will start to be significant, thus the threshold will be higher and the efficiency lower. For the core, if the signal wavelength is too far from the cutoff then important losses can be observed (more than 5 dB) with the standard twist rate (1-2 turns per centimetre). Furthermore, for the air clad system the obvious problem is the environmental sensitivity of such a device: any dust on the fibre will generate scattering losses, which results in a large decrease of the efficiency of the source.

V CONCLUSION

This type of device provides apparently an efficient system to couple the light into the doped fibre. The main advantage of this system is that one can use even more fibres and then launch even more light. This system is mainly limited by bending losses. Some solution should be therefore found to avoid this. It seems that the twisting is necessary for a good coupling and efficiency however it is inducing bending losses. The losses for the core can be easily avoided by a careful design of the fibre and its cut off. For the pump the bending losses always occur, but they can be kept as low as 0.2 dB/m for a good twist rate with good mode mixing. Then, with a highly doped fibre (absorption of 5dB/m for instance), the device length will be short and the bending losses for the pump can be neglected.

REFERENCES

[1] A. W. Snyder and J. D. Love, "Optical waveguide theory," Chapman and Hall, London, 1983

[2] K. Morishita, M. S. Yataki, W. A. Gambling, "In-line optical fibre filters using dispersive materials," Electronics lett., vol.23, pp.319-21, 1987.

PART II: BACKGROUND THEORY AND RESULTS

CHAPTER IV: BACKGROUND THEORY: CW LASING

I INTRODUCTION

The purpose of this chapter is to give some theoretical ideas of how a fibre laser works. The other aim was to present some calculation results to have a first estimation of what one could expect from the fibre laser used in this work. To achieve that, a model based on rate equations [1-5] was used.

First, since during this work ytterbium was the main dopant for the fibre laser, the Yb^{3+} ion will be described. The following part will present an analytical model [6] and the results it gives for lasing around 1060 nm with an Yb-doped fibre laser. Finally, the limitations of such a model for the emission at 980 nm are discussed, and the results of numerical calculation for this emission are presented.

These calculations were useful for choosing the type of fibre to be used in experimental work and for seeing what one can expect to achieve, even if for all of the models, limitations such as background losses, Rayleigh backscattering [7], or lifetime quenching [8], were not included. It has also to be noticed that, for DCF, it is important to consider the pump mode repartition, since some of the modes might not cross the core, thus they would not interact with the ytterbium ions. For the following models it will be considered that the fibres will have a sufficient mode-mixing to have all the pump modes interacting with the doped core.

II YTTERBIUM ION AND RATE EQUATION MODEL

II-1 The Ytterbium ion

Ytterbium is a rare earth like neodymium, and erbium. It can be described by a simple energy level scheme. The energy levels involved are $^2F_{5/2}$ (excited state) and $^2F_{7/2}$ (ground state), which consist of three and four sub-levels respectively. From those levels one can extract a simplified scheme with four energy levels involved (see figure 1).

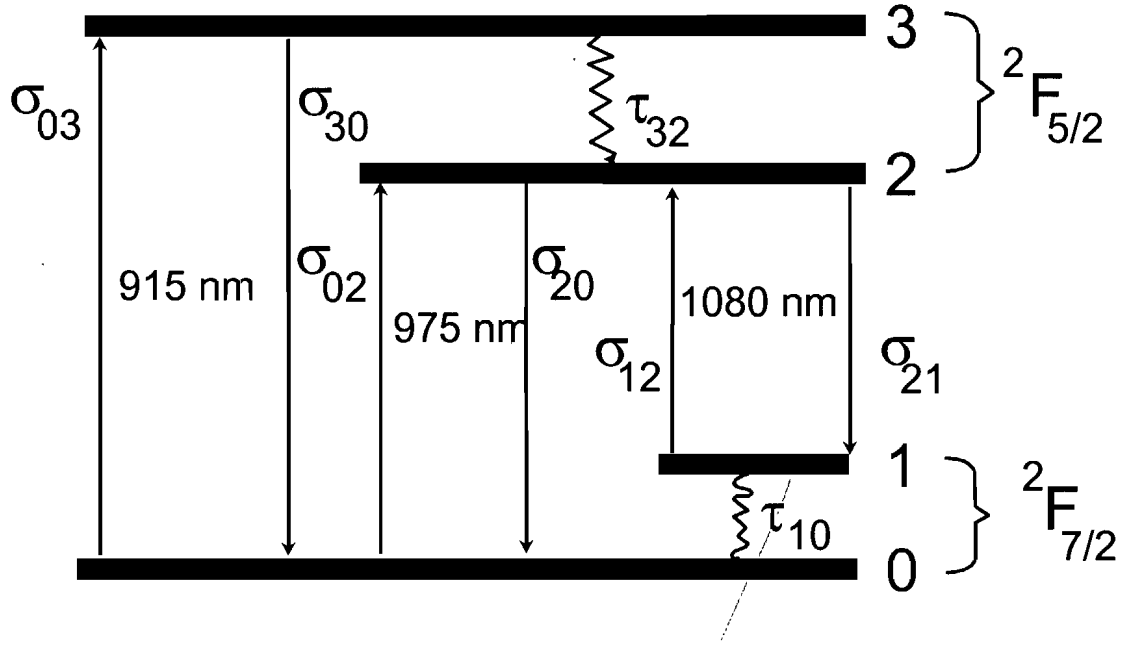

Figure IV-1 Energy band diagrams for Yb^{3+} ion

λ	cross sections (pm^2)	decay times
915 nm	σ_{03}=0.8 σ_{30}=0.025	τ_{32}<<1ns
975 nm	σ_{02}= 2.7 σ_{20}=2.7	τ_{21}=840μs
1080 nm	σ_{21}=0.25 σ_{12}=0.0014	τ_{20}=840 μs τ_{10}<<1ns

Table IV-1: Spectroscopic data for Yb^{3+} in germano-alumino-silicate glass [10].

The spectroscopic data for ytterbium in silica are shown in Table 1. The σ_i are the different cross sections and τ_i the relaxation times (spontaneous emission). The different wavelengths for emission (976 and 1080 nm) are chosen since they are the more likely to be emitted when there is no wavelength selection.

It is better to describe the system as a two level system since the decay times $\tau_{10,32}$ cannot be evaluated precisely. Then to be more precise on the different cross sections, one can have a look the spectral dependence in figure 2:

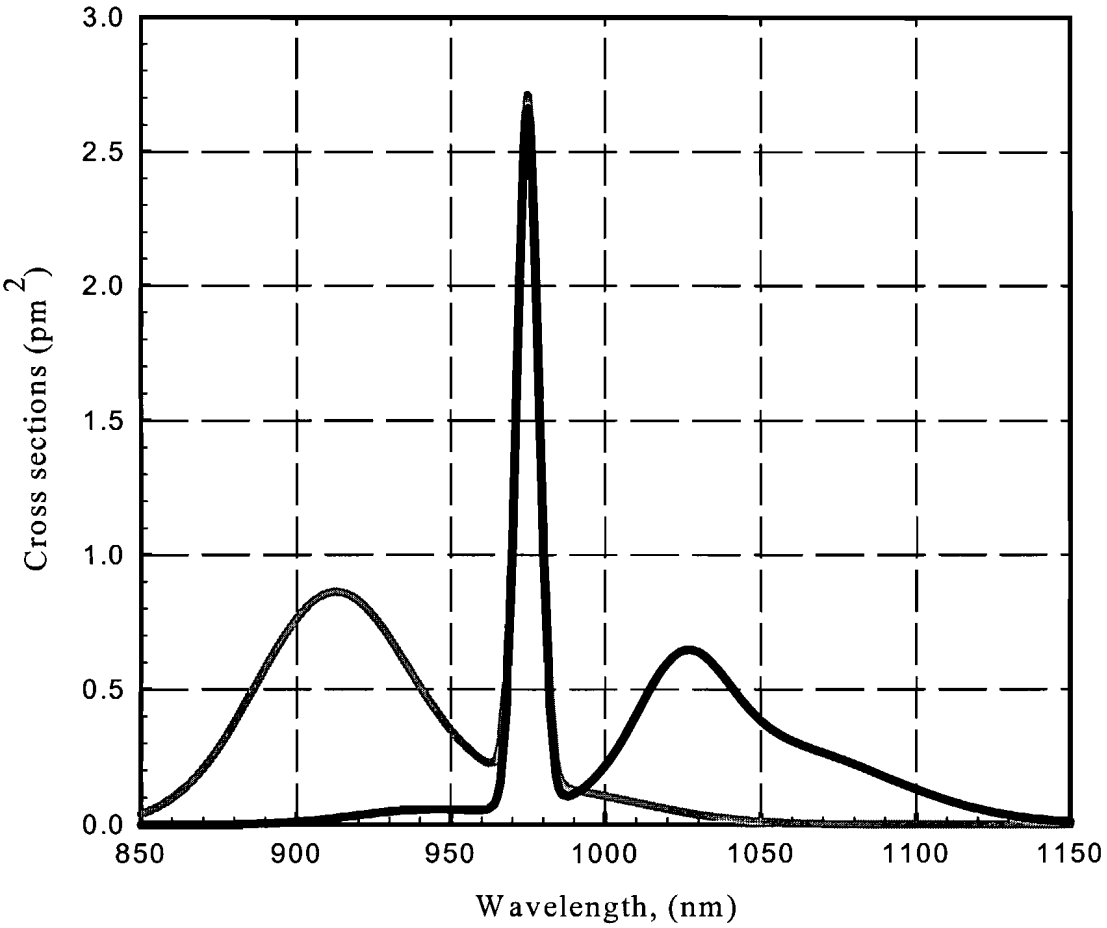

Figure IV-2: Emission (black) and absorption (grey) cross-sections versus wavelength in germano-alumino-silicate. Note the two peaks of absorption (915 and 975 nm) and the two areas of emission (around 980nm and from 1020 to 1150 nm).

This shows that the system can be pumped at either 915 nm (broad range), 975 nm (sharp peak, and higher absorption level) or around 1040 nm (broad absorption spectrum), and the

possible wavelengths for amplified stimulated emission are at 975 nm or around 1060 nm (broad emission spectrum). In the experiments, the system was pumped either at 975 nm or 920 nm, and it emitted at either 1020-1100 nm or 975 nm. To describe this process, a rate equation model will be used.

II-2 A rate equation model

As described above, there are two possible pump wavelengths and two possible emission wavelengths. First, the full rate equations involving all the different signals involved [1-5] are described. Those equations should be written as a two level system:

$$N_T = N_0 + N_2 \quad (1),$$

$$\frac{dN_2}{dt} = I_{915} \cdot (\sigma_{03} \cdot N_0 - \sigma_{30} \cdot N_2) + I_{975} \cdot (\sigma_{02} \cdot N_0 - \sigma_{20} \cdot N_2) + \ldots$$

$$\ldots I_{1080} \cdot (-\sigma_{21} \cdot N_2) - \frac{N_2}{\tau_{21}} \quad (2).$$

Then the power rate equations for the pump (915 nm or 975 nm) and the signals (975 and/or 1080 nm) will be:

Pump:

$$\pm \frac{\partial I_{915}^{\pm}}{\partial z} + \frac{n_{co}}{c} \cdot \frac{\partial I_{915}^{\pm}}{\partial t} = (\sigma_{30} \cdot N_3 - \sigma_{03} \cdot N_0) \cdot I_{915}^{\pm} \quad (3),$$

$$\pm \frac{\partial I_{975}^{\pm}}{\partial z} + \frac{n_{co}}{c} \cdot \frac{\partial I_{975}^{\pm}}{\partial t} = (\sigma_{20} \cdot N_2 - \sigma_{02} \cdot N_0) \cdot I_{975}^{\pm} \quad (4).$$

Signal:

$$\pm \frac{\partial I_{975}^{\pm}}{\partial z} + \frac{n_{co}}{c} \cdot \frac{\partial I_{975}^{\pm}}{\partial t} = (\sigma_{20} \cdot N_2 - \sigma_{02} \cdot N_0) \cdot I_{975}^{\pm} + N_2 \cdot \sigma_{20} \cdot \frac{2 \cdot c \cdot \Delta\lambda_{ASE975}}{\lambda^2 \cdot A} \quad (5),$$

$$\pm \frac{\partial I_{1080}^{\pm}}{\partial z} + \frac{n_{co}}{c} \cdot \frac{\partial I_{1080}^{\pm}}{\partial t} = (\sigma_{21} \cdot N_2 - \sigma_{12} \cdot N_1) \cdot I_{1080}^{\pm} + N_2 \cdot \sigma_{21} \cdot \frac{2 \cdot c \cdot \Delta\lambda_{ASE1080}}{\lambda^2 \cdot A} \quad (6),$$

where the N_i are the different level population density (ions/m^3), the positive and negative signs represent the direction in which the light is propagating in the fibre, n_{co} is the silica index, c is the speed of light, h is the Plank constant and λ is the signal wavelength. $\Delta\lambda$ represents the ASE bandwidth and A is the core area. The last term in equations 5 and 6 represents the ASE contribution to the signal [4,5]. In most of the lasers this term can be neglected but if ytterbium lases at 975 nm, the ASE at 1080 nm may be strong, therefore it needs to be included in the model.

Continuous wave lasing is a steady state condition; therefore all the time derivatives are equal to zero in the above equations. This gives an expression of N_2 and N_0 as a function of N_t and the different signal power:

$$N_2 = N_T \cdot \frac{I_{915}\cdot\sigma_{03} + I_{975}\cdot\sigma_{02} + I_{1080}\cdot\sigma_{12}}{I_{915}\cdot(\sigma_{03}+\sigma_{30}) + I_{975}\cdot(\sigma_{02}+\sigma_{20}) + I_{1080}\cdot(\sigma_{12}+\sigma_{21}) + 1/\tau_{21}} \quad (7),$$

$$N_0 = N_T \cdot \frac{I_{915}\cdot\sigma_{30} + I_{975}\cdot\sigma_{20} + I_{1080}\cdot\sigma_{21} + 1/\tau_{21}}{I_{915}\cdot(\sigma_{03}+\sigma_{30}) + I_{975}\cdot(\sigma_{02}+\sigma_{20}) + I_{1080}\cdot(\sigma_{12}+\sigma_{21}) + 1/\tau_{21}} \quad (8).$$

From those equations a numerical model can be written knowing that the boundary conditions and I_i's are expressed as:

$$I_i = \frac{P_i \cdot \Gamma_i}{h \cdot \nu_i \cdot A_i} \quad (9),$$

$$P_i^+(z=0) = R_{1i} \cdot P_i^-(z=0) \quad (10),$$

$$P_i^-(z=L) = R_{2i} \cdot P_i^+(z=L) \quad (11),$$

where L is the length of the fibre, $R_{1,2i}$ are the reflectivities of the two output mirrors for the wavelength i, A_i is the core area, Γ_i are the overlap integrals with the core for the pump and the signal, ν is the frequency (pump and signal), and P is the power in W.

III CALCULATION RESULTS FOR EMISSION ABOVE 1 μm

As stated before for cw emission at 1060 nm, the effect of ASE can be neglected. This allows a simpler analytical model [6]. This model was used to perform the following calculation for emission above 1 μm.

To use this model, the concentration of doping ions in the core is needed. To gain a rough idea, one can use the value of the pump absorption along the fibre and, by using the cladding to core ratio and the absorption cross-section of the pump, the number of ytterbium ions per unit volume can be extracted. Note, that in this case, it is considered that the pump was evenly distributed in the cladding, thus all the pump light is in interaction with the core.

The model described in [6] gives two equations for the threshold value (P_{th}) and the slope efficiency (η) as functions of the parameters of ytterbium ions described above. The detailed equations of those parameters are given in appendix B. The evolution of lasing output power (P_l) as a function of pump power (P_p) can be written as follows when the pump power is above the threshold:

$$P_l = \eta \cdot (P_p - P_{th}) \qquad (12).$$

The purpose of this very simple model was to calculate the possible output, slope efficiency, threshold, and optimal length of a typical double-clad fibre.

Most of the fibres used in this work had a cladding size of 150 μm, a core of 10 μm, and absorption for the pump of 2 dB/m at 975 nm (in fact the best fibres described in the next chapter had higher absorption). In the compact system 2W of pump at 975 nm was launched into the inner cladding, therefore this level of pump will be taken as an example. The following results are just some examples of what the desired achievements were for this model. The optimal length for a given pump level (2W) was the first parameter to be calculated. The result is shown in figure 3.

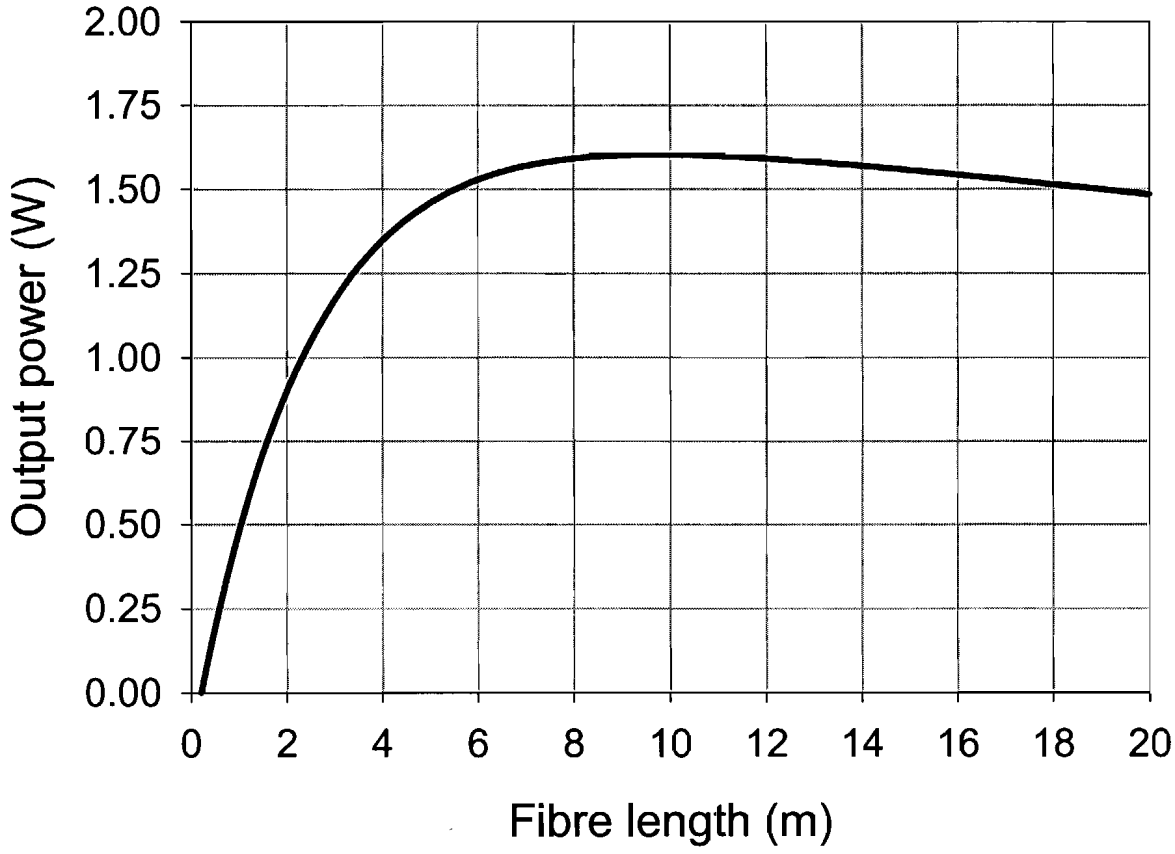

Figure IV-3: Calculation of the output power as a function of the length for a pump of 2W. The pump absorption was 2 dB/m.

For this pump power the optimal length seems to be 10 m, for an output of 1.6 W. Then the slope efficiency and the threshold for such a length were calculated. Figure 4 presents the results of these calculations for the same fibre as for the previous calculation with the optimum length. One output coupler was just a cleaved facet (4% reflectivity), the other was a high reflectivity mirror (assumed to have 100% reflectivity at the signal wavelength). The important parameters are the threshold of 192 mW and the slope efficiency of 88.9%. Note that the slope is theoretically very high because all the pump is absorbed and background losses along the fibre were not considered.

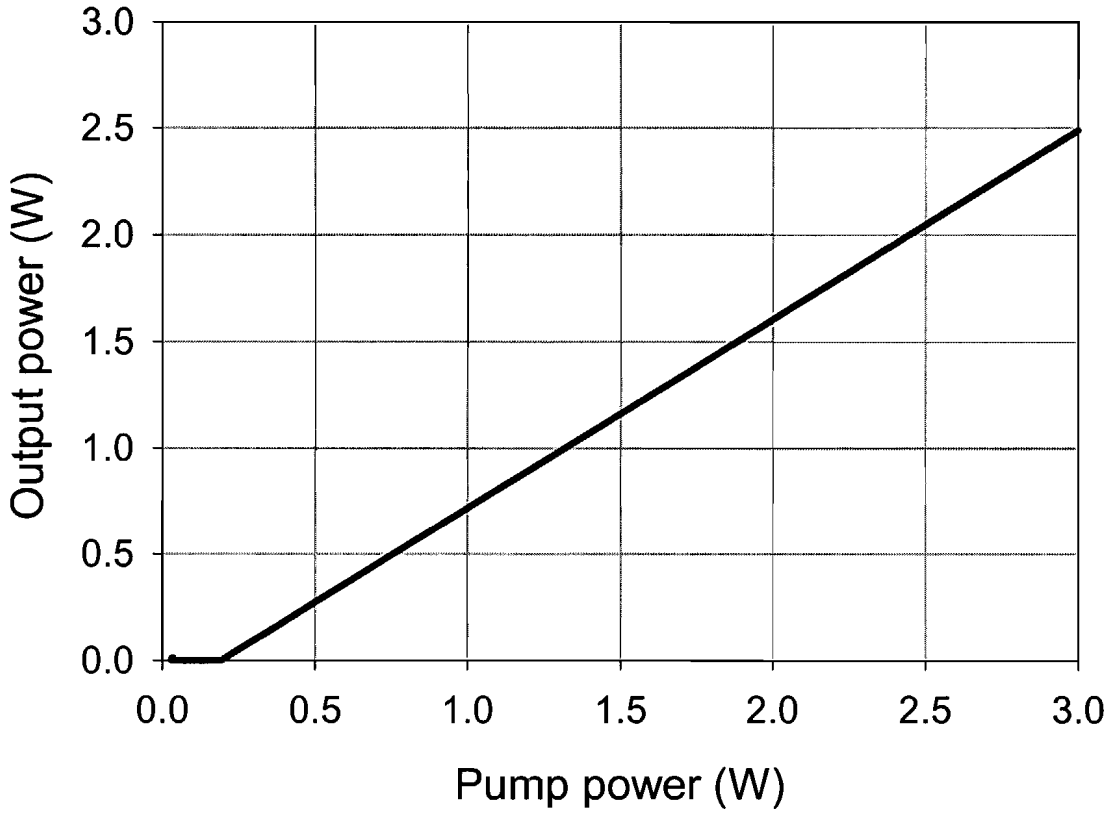

Figure IV-4: Calculation of the lasing behaviour of a typical double clad Yb-doped fibre laser.

Note that with a similar fibre, the experimental results were 1.3 W of output power for 10 m of fibre length, and 2W of pump power, the threshold being 200mW (Chapter V).
This model seems to be good enough to simulate Yb-doped double-clad fibre lasers when they emit at 1080 nm. It was therefore used to have a first idea of the threshold and output one will obtain for a given fibre.

IV CALCULATION RESULTS FOR EMISSION AT 980 nm

Ytterbium is more likely working above 1 μm, because of the strong reabsorption at 975 nm. In cladding pumped fibre this is even more an issue since for the same level of doping the fibre will be much longer than for core pumping. Therefore, it will be very hard to bleach all the fibre thus very hard to reach the threshold. This means that the fibre should be as short as possible. Thus, the core to cladding ratio should be high to increase the pump absorption. The following calculations were made with a numerical simulation based on the rate equations 1-11. Both emission at 975 nm and 1080 nm were considered (mainly ASE when

the lasing signal is at 980 nm). One of the cavity couplers had 100% reflectivity for 975 nm and 0% for 1080 nm. The other coupler had 4% reflectivity for both wavelengths. The fibre was pumped from one end. This pump power could be single or double-passed. A setup sketch can be found in the following chapter in figures V-19 and V-20.

The first important parameter is the cladding size (core size is fixed at 8 μm to keep the emission single mode) and its influence on the threshold value. Figure 5 shows the results of calculations of the threshold for different core to cladding ratios. The length of the fibre was chosen to absorb 10 dB of the pump single passed (No lasing occurring). Note that at most 5 dB of the pump will be absorbed when the fibre is lasing, since when Yb emits at 975 nm, it is essentially a 3 level operation. In fact the threshold depends on spontaneous emission and ASE above 1 μm, which could be considered as losses for the signal at 976 nm. The spontaneous emission is emitted in all directions, and part of it is coupled into the guide and will be amplified to generate ASE (much stronger).

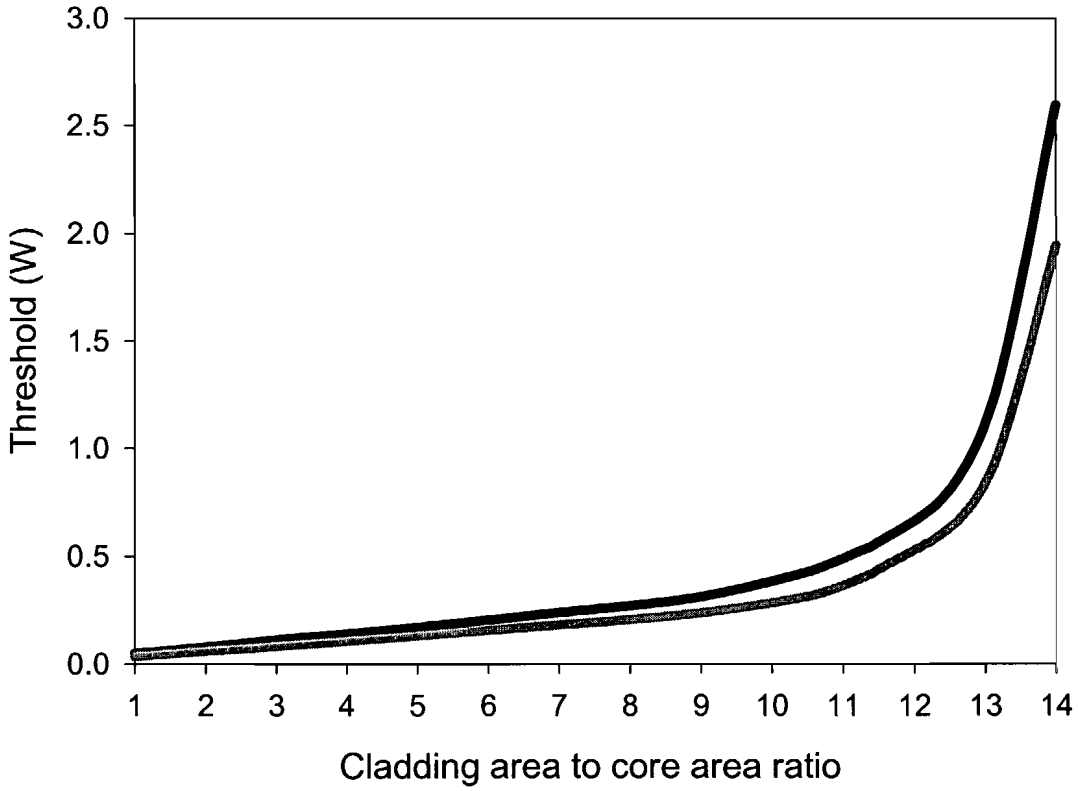

Figure IV-5: Calculated threshold pump power as a function of the cladding to core area ratio. The pump was either single passed (black) or double passed (grey).

This shows how important the cladding to core ratio is, since when it rises above 12 the threshold starts to reach a level which will be too high to practically realize a laser. This is

mainly due the 1080 nm ASE, which is depleting most of the upper level for this cladding to core ratio. It can also be seen that the threshold drops when the pump is double passed, but the improvement is not really significant. The slope efficiency of the laser depends more on the fact that the pump is double passed as is shown in figure 6. For this calculation, the length was again corresponding to 10dB absorption. The core had a 9 μm diameter (NA=0.08 then V_{980}=2.3, the fibre is single mode) and the cladding a 30 μm diameter.

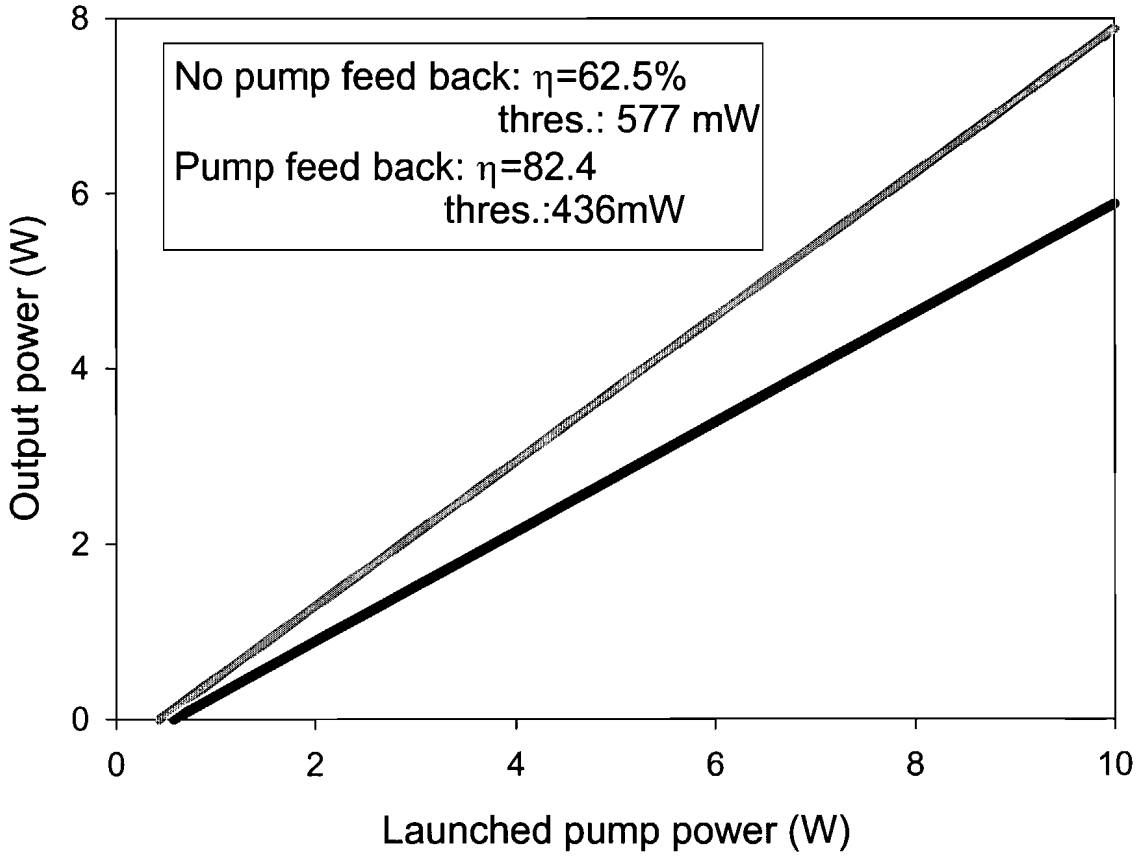

Figure IV-6: Calculation of lasing behaviour. The fibre had an inner-cladding diameter of 30 μm, a core of 9 μm. The fibre length was equivalent to a 10 dB absorption single passed. The pump was either single passed (black) or double passed (grey).

As it is seen in figure 6 the threshold does not differ much, but an important increase in slope efficiency was obtained. This is mainly due to the fact that much more pump is absorbed overall. In fact the slope efficiency with respect to absorbed pump power is about the same for both the single and double passed pump. This demonstrates how important the double passing of the pump is.

Now, for a given pump, the optimum length for such a laser can also be estimated. The same fibre parameters were used and the pump was fixed at 2W. The results are shown in figure 7.

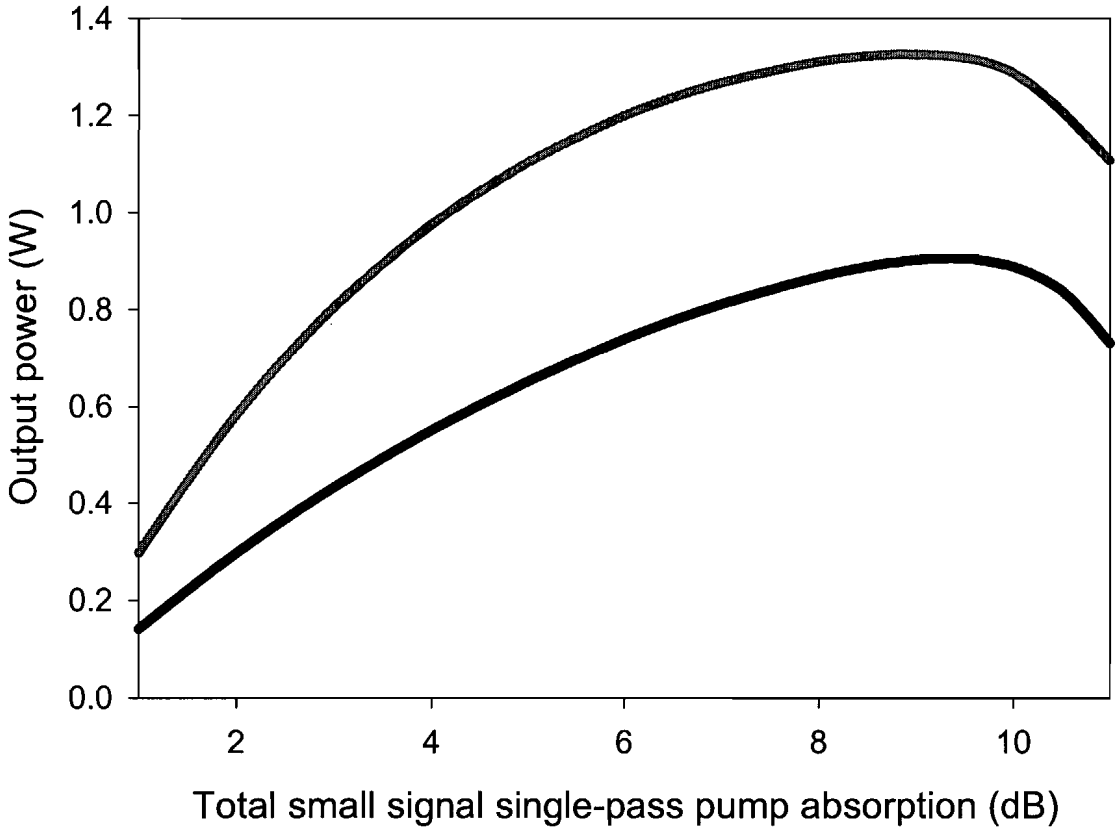

Figure IV-7: Calculation for the optimal fibre length. The fibre had an inner-cladding diameter of 30 µm, a core of 9 µm. The pump was 2W, and either single passed (black) or double passed (grey).

As it can be seen, the optimal length is around 9dB absorption for both single and double passed pump. However it should be noticed that for the double passed pump to be practical, less than 10% of the total pump power should come back to the pump source (diode laser facet can be destroyed by this feedback). This represents a length corresponding to 10 dB double passed operating absorption (when emission at 975 nm occurs). The threshold will become 690 mW and the output power is as shown in figure 8.

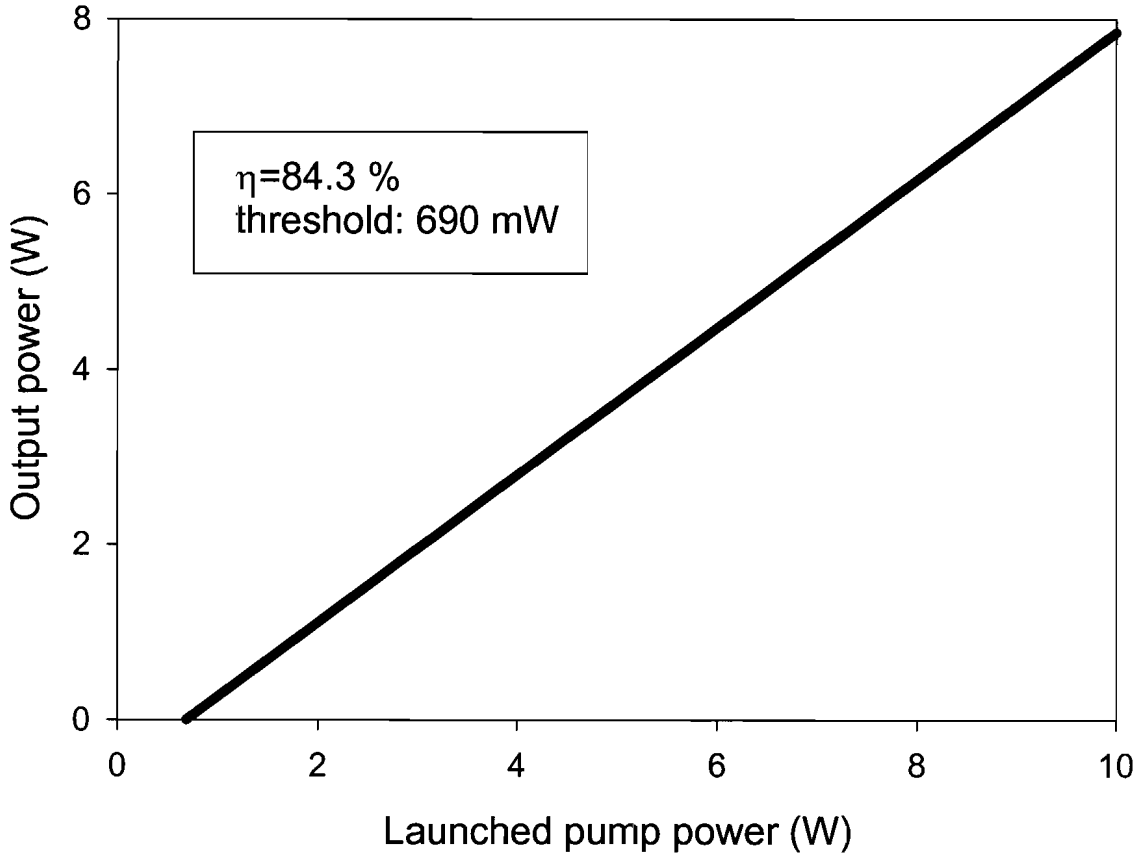

Figure IV-8: Calculated lasing behaviour for a 30μm diameter inner-cladding, and 9 μm core. The fibre had a length corresponding to 10 dB double passed absorption for the pump power, and the pump was double passed.

Therefore for very high power (when the threshold is less of an issue) double passing the pump will be a good solution to achieve very high slope efficiency. Since the efficiency against absorbed pump power is fixed (no background loss), the efficiency against launched pump power depends strongly on the fibre length.

This model seems to be good enough to design the fibres to generate 975 nm. This shows how important the cladding size, and the fibre length (if the fibre is too long the power drops quickly) will be. One has to note that it was assumed that pump was homogeneously covering the cladding area. This means that to approach the results obtained with those calculations with a real fibre, the pump should be homogeneously distributed across the waveguide by some means like flower shape or bending, which creates mode mixing. There is also another way to approach this problem; to reduce the reabsorption in the core, one can use ring doping

[9]. This solution can be simulated with the model by changing the way of calculating the overlap of the signal with the doped area and the overlap of the pump with the doped area. I choose not to use ring doping in the calculations since experimentally ring doping is harder to realize. The reasons are that, first, it is harder to make a ring doped preform than a standard step index core doped one, and secondly, some cladding modes (for cladding pumping) might have a higher overlap with the ring than the core mode, thus they would be the ones to lase.

V CONCLUSION

In this chapter, the basic theoretical knowledge of lasers was described for an ytterbium doped fibre laser. This information was used to simulate the fibre laser behaviour, and to have a good idea of what one can expect from the fibres used in this work. More precisely, a full set of calculations was performed for the emission at 975 nm. This allowed the evaluation of what the important parameters were in building such a source.
First it was proved that the cladding to core area-ratio should remain lower than 13-14, since around those values the threshold started to reach the Watt level. Furthermore it proved that it would be useful to double pass the pump for high output power. However, one should be very careful with a setup for double passing the pump, since it can induce damage on the facet of the pump laser diodes. In fact, the fibres will have to be longer than the optimum with the parameters chosen for this study.

REFERENCES

[1] A. Siegman, *Lasers*. Mill Valley, CA: Univ. Sci. Books, 1986, ch.26.

[2] W. Koechner, *Solid-state laser engineering*. Berlin, Germany: Springer-Verlag, 1996, vol.1, ch.8.

[3] M. J. F. Digonnet, Ed., *Rare Earth Doped Fibre Lasers and Amplifiers*, New York: Marcel Dekker, 1993.

[4] E. Desurvire, *Erbium-doped fibre amplifiers*, New York: Wiley-Interscience,1994, ch. 1.

[5] I. Kelson and A. Hardy, "Strongly pumped fibre lasers," IEEE J. of Quantum Electron., vol. 34, pp. 1570-1577, 1998

[6] C. Barnard, P. Mylinski, J. Chrostowsky, and M. Kavehrad, "Analytical Model for Rare-Earth-Doped Fibre Amplifiers and Lasers," *IEEE J. of Q. Elect.,* 1994, Vol. 30, No 8, pp. 1817-1829

[7] I. Kelson and A. Hardy, "Optimisation of strongly pumped fiber lasers," J. Lightwave Technol., vol. 17, pp. 891-897, 1999

[8] R. Paschotta, J. Nilsson, P. R. Barber, J. E. Caplen, A. C. Tropper, D. C. Hanna, " Lifetime quenching in Yb-doped fibres," Optics Com., 1997, Vol. 136, pp.375-378.

[9] J. Nilsson, J. D. Minelly, R. Paschotta, D. C. Hanna, and A. C. Tropper, "Ring-doped cladding-pumped single-mode three-level fiber laser", Opt. Lett., Vol. 23, pp. 355-357, 1998

[10] R. Paschotta, J. Nilsson, A. C. Tropper, D. C. Hanna, "Ytterbium-Doped Fibre Amplifiers," IEEE J. of Q. Elect., 1997, Vol.33, No.7, pp.1049-1056.

CHAPTER V: EXPERIMENTAL RESULTS IN CW LASING

I INTRODUCTION

Cladding pumped ytterbium doped fibre lasers in the continuous wave (cw) regime have proved to be very efficient for emission between 1020 nm and 1120 nm [1-3]. The purpose of the two works presented in this chapter was first to compare an end pumped double cladding fibre laser with a fibre laser with a coupler or in a multifibre configuration. This way one can validate the multimode couplers and the multifibre arrangement as a good system to build compact fibre lasers.

Then, since core pumped ytterbium fibre lasers proved to be an efficient source for emission at 975 nm, it was tried in a cladding pumped configuration to scale the power up. The main problem here is that the strong reabsorption of the signal in the core makes the threshold for emission at 975 nm prohibitively high as it has been seen in the previous chapter. Here, several solutions are described to build a small inner cladding fibre to obtain a low threshold for the 975 nm emission.

II CHARACTERISATION OF FIBRES.

Several fibres were tested, to find the most efficient one to be tested in a compact setup. Those fibres were:

Fibre #1: 7 μm-0.12 NA core with an offset of 1/3, 300 μm inner cladding
Fibre #2: 20 μm-centred 0.12 NA core, 150 μm inner cladding
Fibre #3: 12 μm-centred 0.12 NA core, 80 μm inner cladding
Fibre #4: 15 μm-centred 0.12 NA core, 150 μm inner cladding
Fibre #5: 12 μm-centred core 0.07 NA, 100 μm inner cladding
Fibre #6: 7 μm-centred core 0.11 NA, 80 μm inner cladding

Note that the fibre OD is the inner cladding diameter and that the outer cladding was the low index coating (silicone rubber or UV curing). To have an idea of their behaviours their absorption and their lasing operations without a coupler were measured for each fibre. To end-pump the fibre two different sources were used: the diode bar and the DIOMED HIRAFS. They are described in Chapter I.

II-1 Absorption.

To measure the spectral absorption of the fibres, white-light was launched into the inner cladding of a 10 m fibre (coiled in large loop of ~20 cm diameter) and the output was observed on a spectrum analyser. After a comparison with the white light source spectrum, the absorption of the DCF at any wavelength can be extracted. In fact with such a fibre the absorption may vary with length, since some modes are rarely interacting with the core. More precisely the modes which are crossing the core will be absorbed over a short length as the other modes will need a much longer fibre to be absorbed, thus the effective absorption seems to be stronger over the first meters of the fibre. To avoid this problem one has to increase the mode coupling for the pump modes. The solution chosen was to tightly bend the fibre. The measurements were therefore done a second time with a bent fibre (figure of eight or kidney shape with a typical bend radius of 2-3 cm). In this case the absorption should have less variation with the fibre length. The following absorptions were obtained at 975 nm:

Fibre #1: 0.8 dB/m, and 1.2dB/m (with mode mixing)

Fibre #2: 0.3 dB/m, and 0.6 dB/m (with mode mixing)

Fibre #3: 0.4 dB/m, and 0.7 dB/m (with mode mixing)

Fibre #4: 1dB/m, and 2dB/m (with mode mixing)

Fibre #5: 8dB/m, and 17dB/m (with mode mixing)

Fibre #6: 4 dB/m at 915 nm with mode mixing

To have a good lasing operation, the global absorption should be around 10dB, this gives the length of the fibre needed to build the laser cavity. This means that if all those fibres are used tightly bent, the lengths needed are: about 10 m for Fibre#1, about 15-20 m for Fibre #2/3, and 5 m for Fibre #4 and less than 1 m for Fibre #5. If those fibres are used without bending, then the length should be doubled for Fibre #2-5 and about the same for Fibre #1.

II-2 Yb fibre lasing with end pumping

For fibre #1 the test was done with a DIOMED-HIRAFS source, which gives an output power of 25W at 980 nm with a bandwidth of 5nm. With the setup shown in figure 1, about 11 W was launched into the inner cladding of the doped fibre.

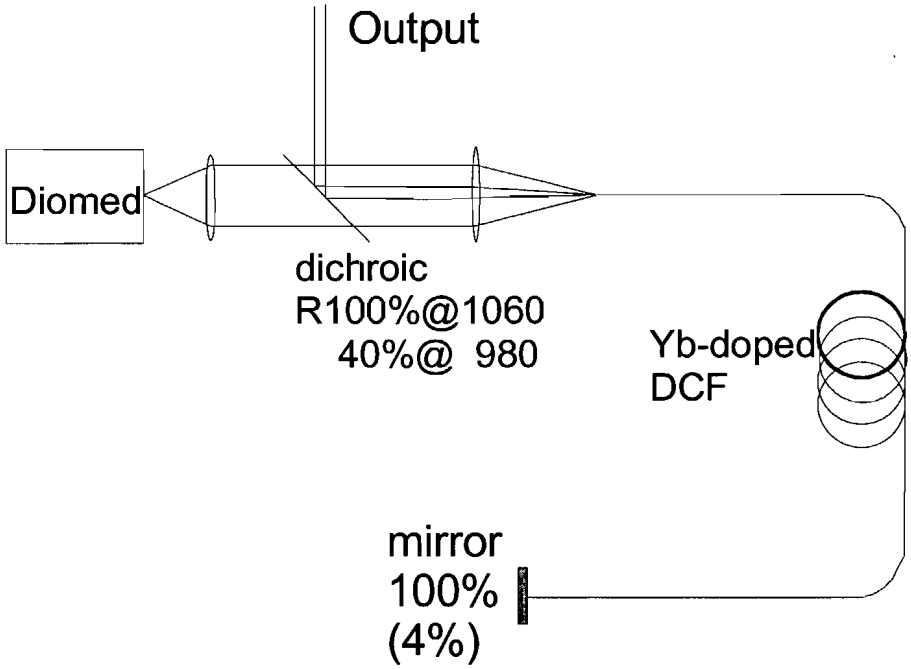

Figure V-1: Setup for testing fibres in lasing operation. The 4% reflections were assumed for a straight cleave. The mirror has a high reflectivity for both the pump and the signal.

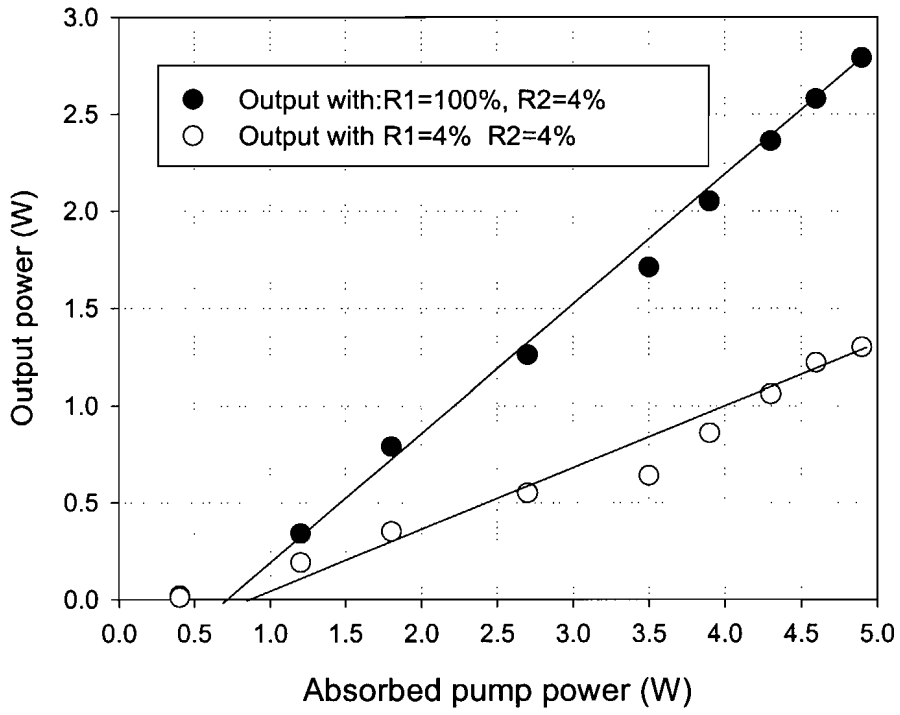

Figure V-2: Lasing results for 10 m of fibre #1. The threshold is 700 mW and the slope efficiency is 60% (black dot). The white dot curve represents a single output when the two output couplers are cleaved facet (4% reflection). The slope efficiency is 30% and the threshold 850 mW.

A threshold of 500 mW and a slope efficiency of 60% were obtained (see figure 2).
For the other fibres a diode bar with beam shaping [1] was used to replace the DIOMED HIRAFS source, which was not available at that time. Note that this source is emitting at 915 nm, thus about a three times longer fibre is needed to absorb the pump. The setup is shown in figure 3.

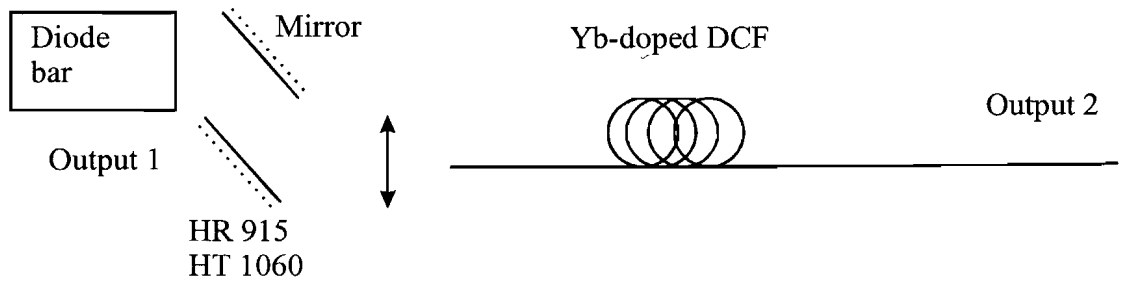

Figure V-3: Fibre characterisation setup with a beam shaped diode bar.

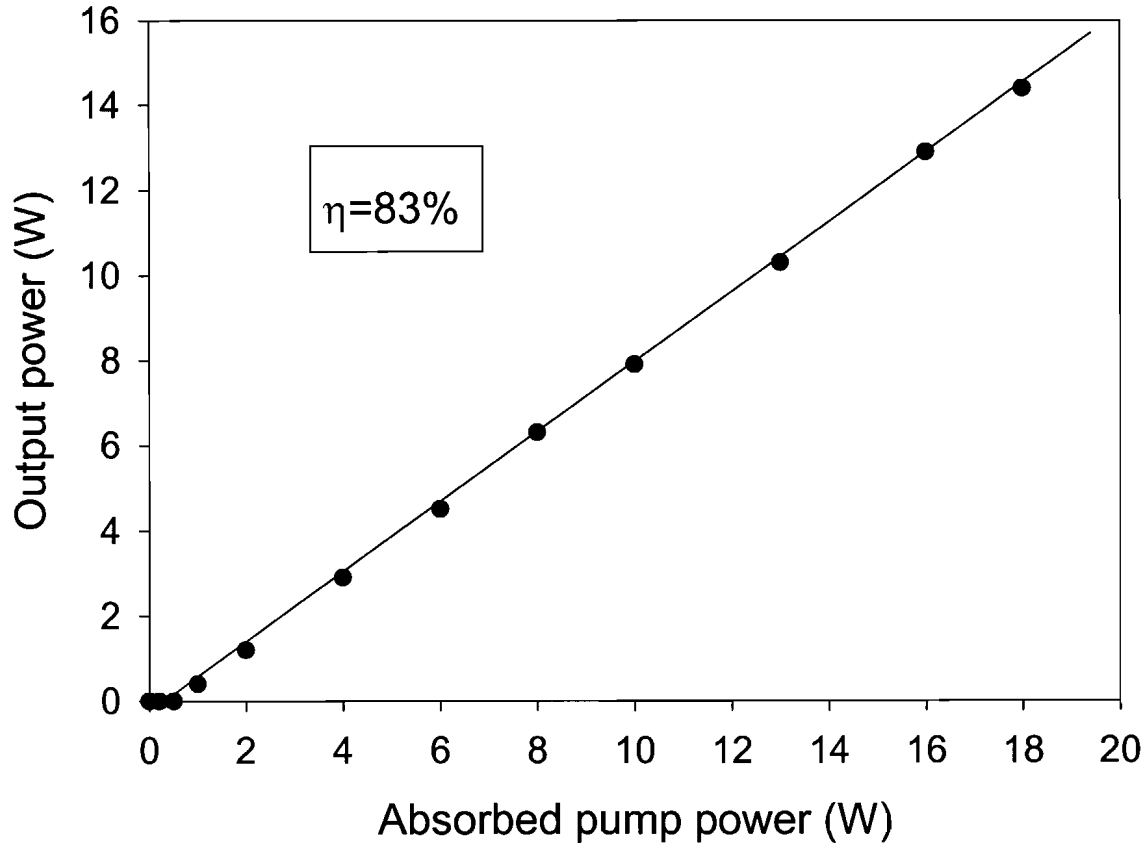

Figure V-4: Characterisation of 15m of fibre #4.

With this system 20 W were launched in the DCF. The results obtained with 15 m of Fibre #4 are shown in figure 4 as a typical example. It has to be noticed that for each fibre the slope efficiency is above 60% as shown in detail here in comparison with the absorbed pump power:

Fibre #1: 60% slope efficiency (pump 975 nm) threshold: 500 mW
Fibre #2: 70% slope efficiency (pump 915 nm) threshold: 700 mW
Fibre #3: 73% slope efficiency (pump 915 nm) threshold: 200 mW
Fibre #4: 83% slope efficiency (pump 915 nm) threshold: 500 mW
Fibre #5: 77% slope efficiency (pump 915 nm) threshold: 900 mW
Fibre #6: 84% slope efficiency (pump 915 nm) threshold: 400 mW

It has to be noticed that since some measurements have been done with a 915 nm pump, the comparison with the compact setup is not straightforward because in most of the experiments a 975 nm pump source was used. At this pump wavelength one should expect higher slope efficiency and a lower threshold.
Those tests showed that the most efficient fibres were Fibre #4 and #6 (83% and 84% of slope efficiency in respect with absorbed pump power). The fibres described previously are the most efficient ones from all the fibres used during this work. They were used in experiments depending on their chronological availability. Therefore fibre #1 and #4 were used with multimode couplers, and multifibre arrangements were made from fibre #3, #5 and #6.

III CW OPERATION IN COMPACT CONFIGURATION

III-1 Yb fibre with multimode couplers

In this compact configuration fibres #1 and #4 were tried. This compact system is composed of the DCF with multimode couplers and two pump sources as in figure 5; one (a laser diode with 3 W output at 975 nm) with a LIMO collimator (see figure 6 in Chapter I) and the other (two laser diodes with 3 W output at 975 nm) with the bulk optic configuration (figure 3 in Chapter I).

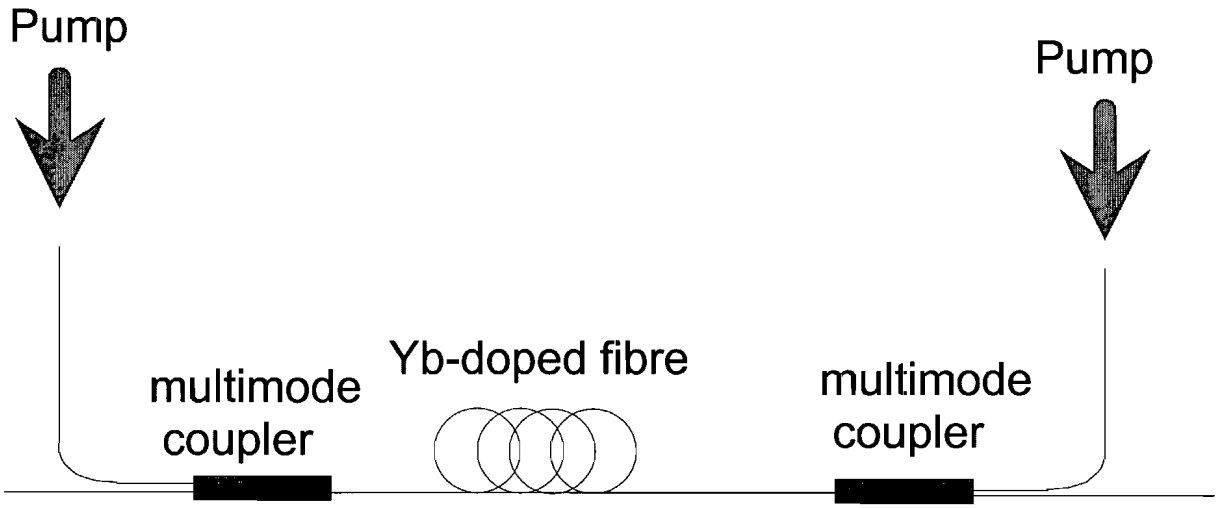

Figure V-5: Compact setup with multimode coupler. The pumps are as shown in Chapter I

The fibre #1 was tried in two configurations and with three generations of couplers. The two configurations are with either one or two couplers of the same generation. The three generations of couplers are two bought couplers (one with 50% coupling efficiency and one with 90% coupling efficiency), and a last coupler, which is homemade and has almost the same behaviour as the second generation of couplers.

For the first generation nothing was obtained because of the high losses in the coupler. In fact, the threshold was never reached.

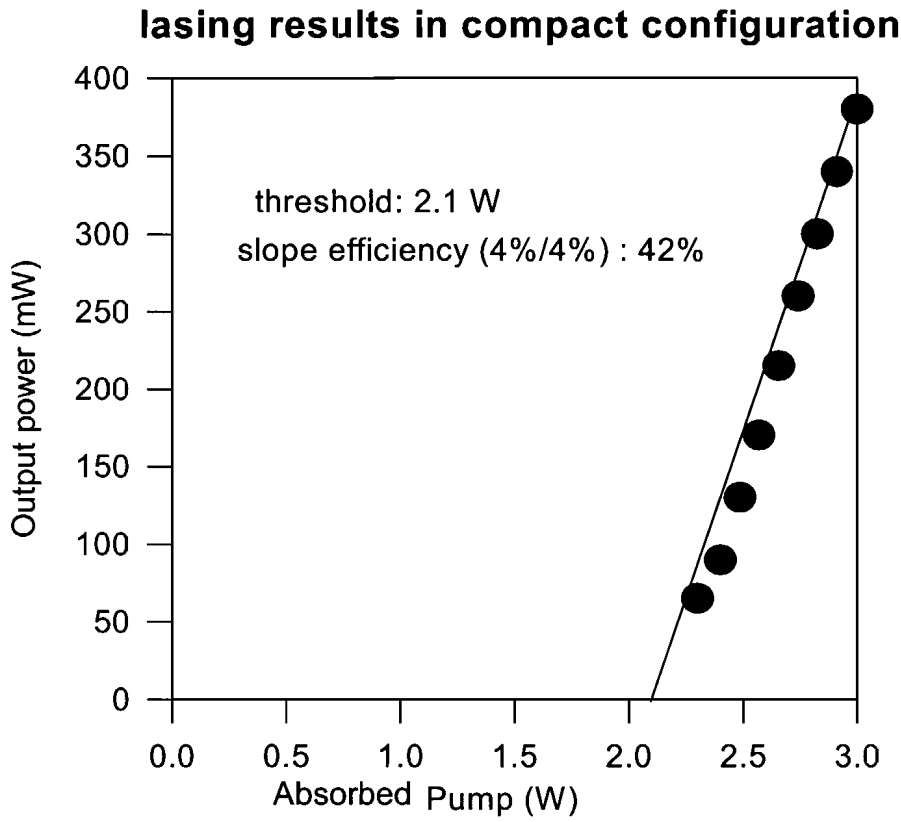

Figure V-6 Lasing results with the fibre #1 in compact configuration (two couplers). It is noticeable that the threshold is much higher than 500 mW

With the second generation coupler, as shown in figure 6, a threshold of 2.1W was obtained, instead of 500 mW and the slope efficiency is much lower (42% instead of 60 %). When an attempt with just one coupler was done, the threshold was lower but still higher than 500mW (980 mW) and the slope efficiency was 53%. Only one setup with the second generation of couplers gave a threshold of 500mW and a slope of 60%. As it was discussed in chapter II, it seems that the coupler is introducing losses for the signal, thus the threshold is higher.

With the best couplers and 10m of fibre #1, a measurement of the tunability was also performed. For this experiment one end of the DCF was angle-cleaved and a bulk grating (600 lines/mm blazed at 1μm) was used to force the laser to oscillate at one specific

wavelength (Figure 7). The grating reflected 70% of the signal in the first order. As it can be seen in figure 8, this laser is working between 1055 nm and 1095 nm with an output power between 200 and 300 mW for a pump of 1 W.

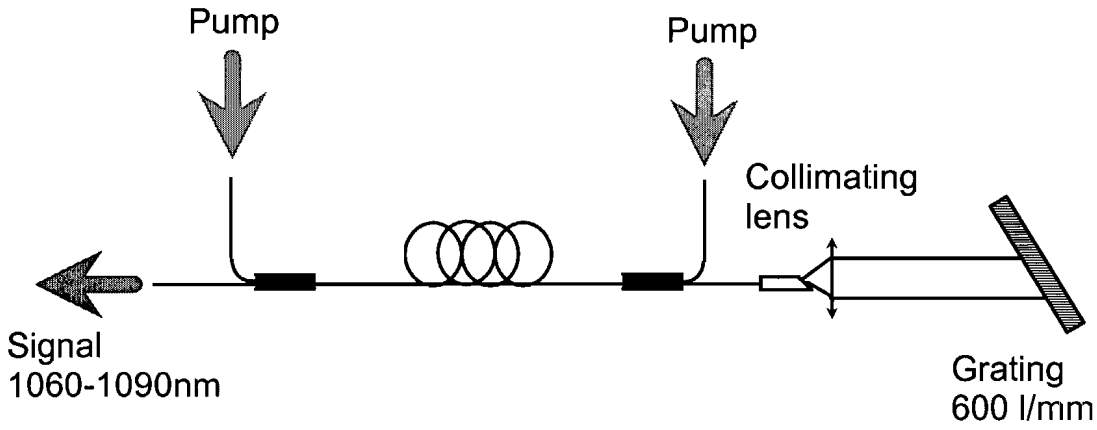

Figure V-7: Setup for testing the tunability. The 600 lines/mm grating blazed at 1 μm was used in Litrow incidence.

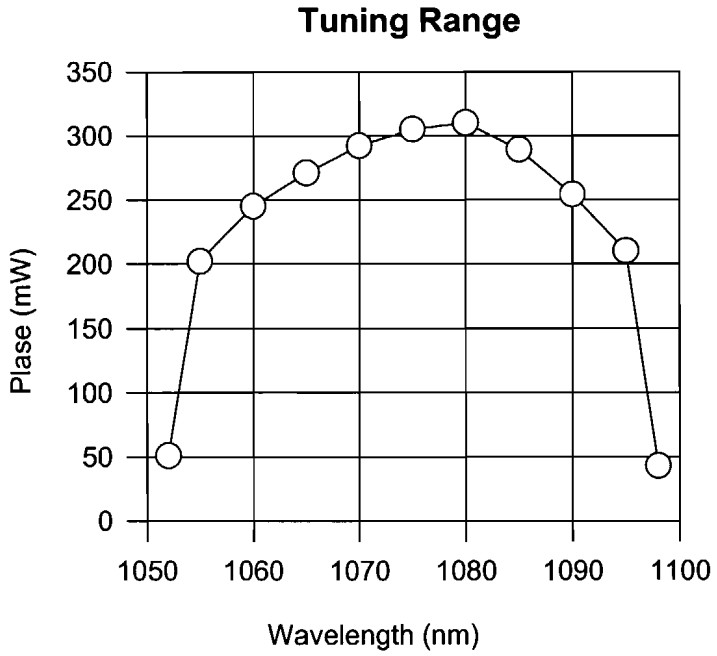

Figure V-8 Tuning range for the cw fibre laser (Fibre #1). The laser is operating between 1055 nm and 1095 nm

With fibre #4, the homemade couplers were used, and the results shown in figure 9 were obtained. The threshold was about 200 mW (good couplers) and the slope efficiency was 78%. This gives an output power of 1.4W, for a total pump power of 9W, essentially because the launching system is not really optimised; there is 50% loss through the optics and 50% through the couplers meaning that only 2.2 W is launched into the fibre. However, those results showed that with good couplers, a reasonably comparable threshold and slope efficiency as with an end pumping setup could be obtained, but with a much higher level of compactness. It should be noticed that if LIMO couplers are used with two 3 W diodes the output power should be substantially increased (70% (launching efficiency) of 6W means 4.2 W in the fibre, so about 3 W of output power). The tuning range of this laser is the same as for fibre #1(1055-1095 nm).

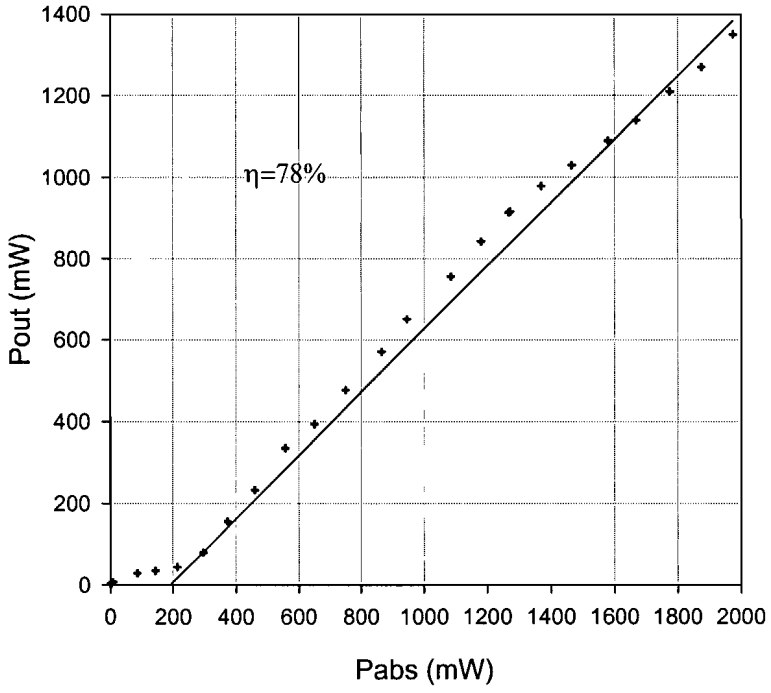

Figure V-9 Lasing operation results for fibre #4 in compact configuration. The threshold is 200 mW and the slope efficiency 78 %.

So, the laser based on the fibre #4, is really the best one, but the signal is still not diffraction limited. To force this laser in a single-mode operation, a monomode fibre was spliced at one end of the DCF. A diffraction limited output was effectively achieved, but the output power dropped to 1W; the splice introduces losses in the cavity, so a higher threshold (300 mW) and a lower efficiency (60%) were obtained. To obtain the diffraction limited output the ends of the fibre could be also tapered [2] (figure 10). It means that the core-diameter of both ends of the DCF will be reduced, to make it single-mode. With such a system, a selection of modes and lower losses can also be expected. In fact, a M^2 value of 1.4 was achieved with 1.2 W output. The threshold was 250 mW and the slope 69%, thus the taper was a better solution than the splice of a single mode fibre.

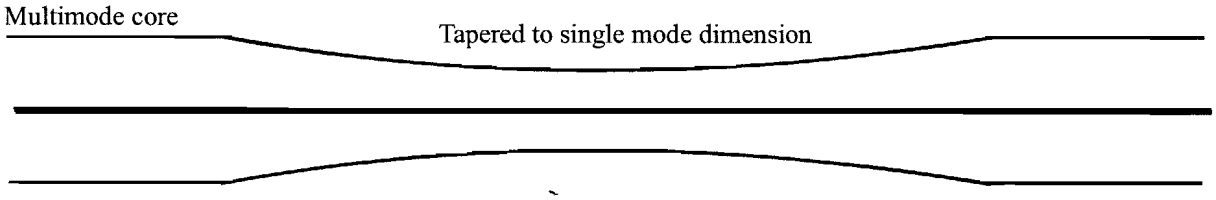

Figure V-10: Tapered fibre; a part of the fibre is reduced to obtain a single-mode core.

III-2 Yb doped fibre in the multifibre arrangement

In this case, the previously named fibres (#3,5 and 6) were used in the arrangements described in chapters II and III. There were two different approaches. The first was an air clad coiled fibre to have a high NA (theoretically around 1) pump fibre (more light could be launched into a smaller cladding)

III-2.1The coiled air-clad fibre

In this experiment fibre #5 was used in an arrangement like in figure 11.
The doped fibre surface was optically clean and coiled into a 4 cm tightly bound ring in such a way that adjacent turns were in close optical contact. To deliver pump power, two 80 μm silica-rods were implemented inside the laser coil. Note that only one end of each of those rods was used to inject pump, the other end was embedded in the coil. This way, the pump fibre interacts over a long surface with the doped fibre and it permits absorption of most of the launched pump power.

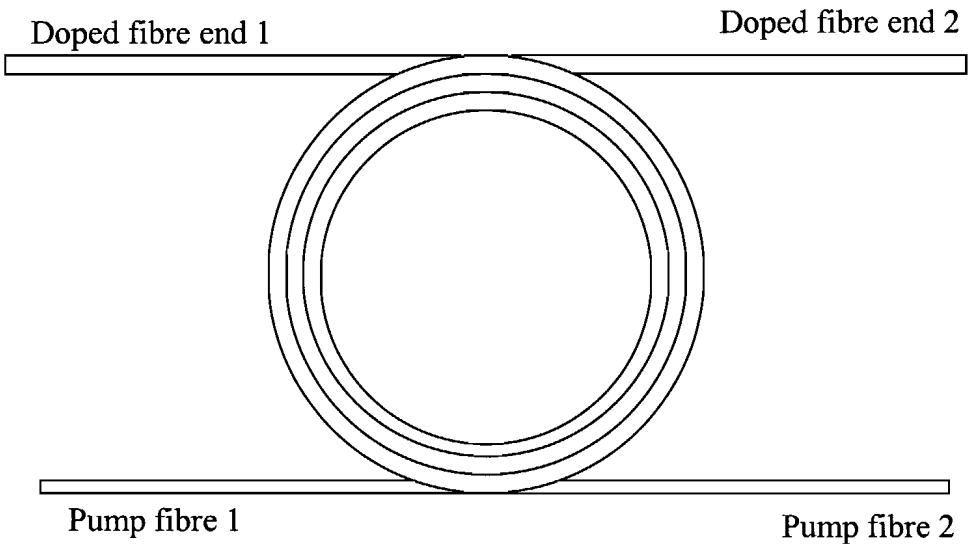

Figure V-11: Typical coiled air-clad configuration. Two pump silica rods and the doped fibre are tightly embedded together in a 4 cm diameter coil.

The setup shown in figure 12 was used. The pump sources were two diode bars with beam shapers [1] emitting at 915 nm. With these sources, up to 30 W pump power was launched into two 200 μm silica rods (with silicone rubber coating NA>0.3), which were tapered down to 80 μm and spliced with the two pump rods. Unfortunately it seemed to be impossible to obtain a good adiabatic coupler with those silica-rods (the silicone-rubber was hard to completely remove, thus there was silicone residue on the surface) and only 13 W of the pump was launched into the coil. The fibre was 2m long since the absorption at 915 nm was around 6dB/m.

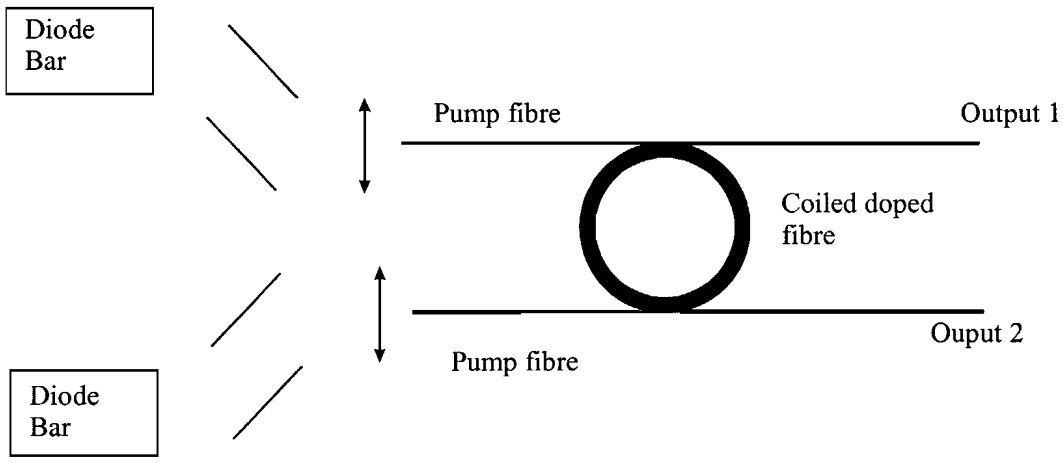

Figure V-12: Setup for a laser based on air clad coiled fibre pumped by two diode bars. The cavity was made by the two cleaved facets of the doped fibre

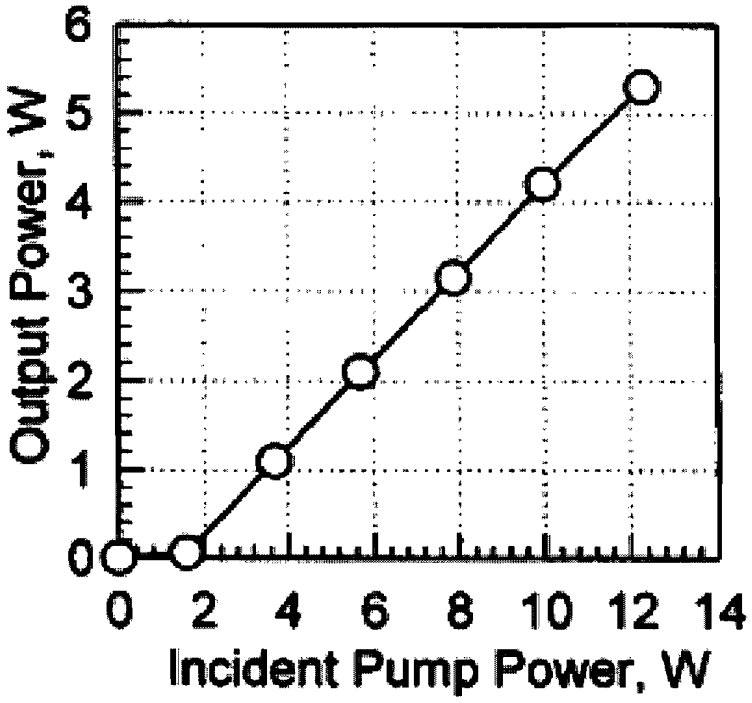

Figure V-13: Lasing result of the air clad coiled fibre. The slope efficiency was 60% and the threshold 1.8 W

The results shown in figure 13 were obtained. The signal wavelength was 1080 nm, the slope efficiency in respect to absorbed pump power was 60%, and the threshold was around 1.8W. For comparison, in an end-pumping configuration the slope efficiency was 77% and the threshold was 900 mW. The difference in this case is probably due to imperfections on the fibre surface, which induced pump losses, and bending losses for the signal in the core (NA is 0.07) mainly due to micro bending points in the coil.

This compact system has proved to be very efficient and permit once again the separation of the pump and the signal ends. However, this is very hard to manufacture (it needs to be perfectly clean) and to handle (bare silica is fragile, water sensitive, and any dirt might reduce the performances). Then, it was decided to lose the advantage of air cladding (high NA) to have a more realistic system from the handling point of view. This system should not be completely forgotten as a device, since an all glass structure would be very interesting for very high power devices (1 kW), without any damage problems (burning of the polymer coating).

III-2.2The dual coated fibre

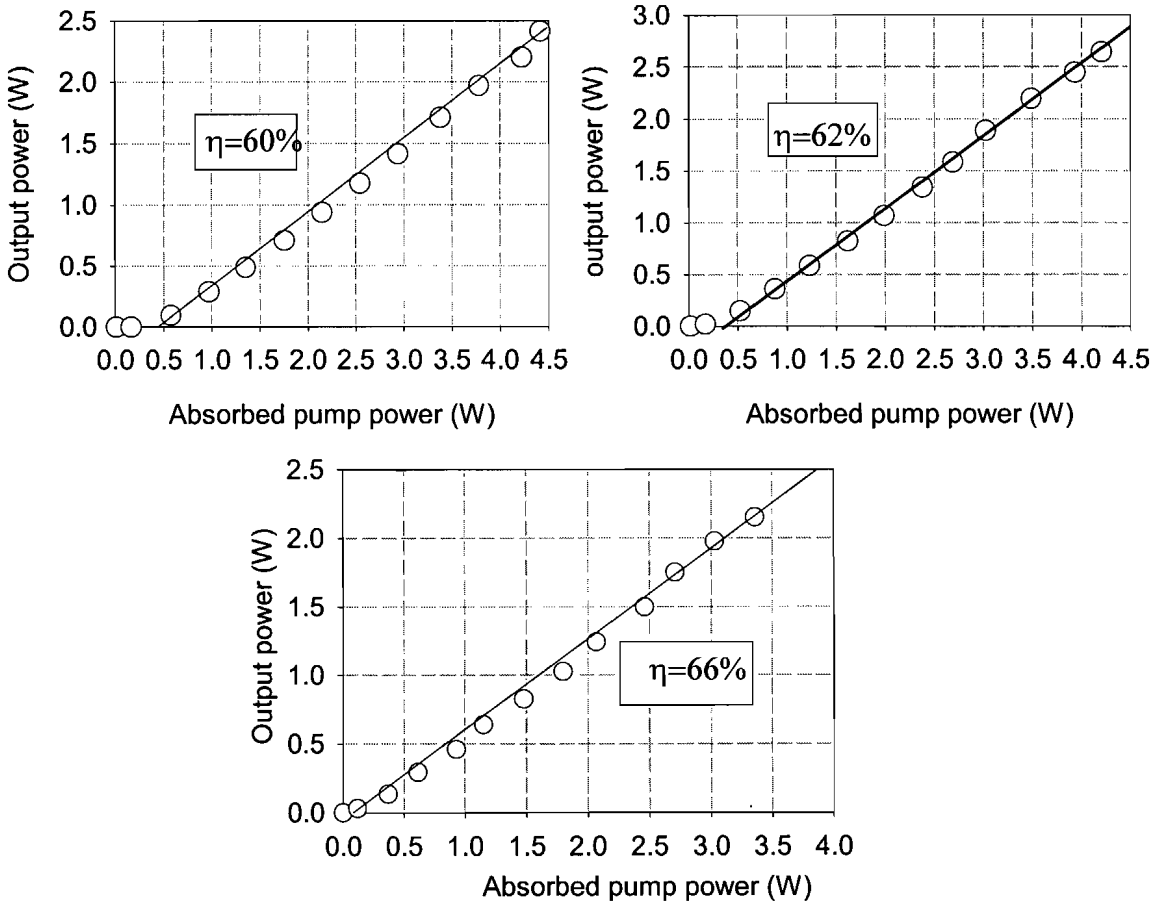

Figure V-14: Measure of a multifibre arrangement with different rates of wrapping between 50 to 100 turn/m. Top left is the higher rate and the bottom graph represents the lower rate.

This time, as described in chapter III, There were two fibres embedded in one coating. One fibre was a 100 μm diameter silica rod (or 80 μm) and the other one was a doped fibre (fibre #3 and fibre #6), with the same outer diameter.

For this experiment, the setup with diode bars was used as shown in figure 12, but with only one pump.

First, measurements were done with 15m of fibre #3 with different twist rates. The results are shown in figure 14.

As it can be seen the lower the wrapping rate, the closer the result is to a standard end pumped laser. In this case, a slope efficiency of 66% was measured instead of 73%. It can also be seen that the slope efficiency for the higher rate is much lower: 60%. Therefore, as

expected from theory, the pump losses due to bending have an effect on the laser performance, since in this case the fibre was relatively long, thus a shorter device length is needed, hence a higher pump absorption. Then, fibre #6 was tested with a length of 1.7 m. The results are shown in figure 15. The two fibres had a diameter of 80 μm and the core had a 8 μm diameter with NA=0.1.

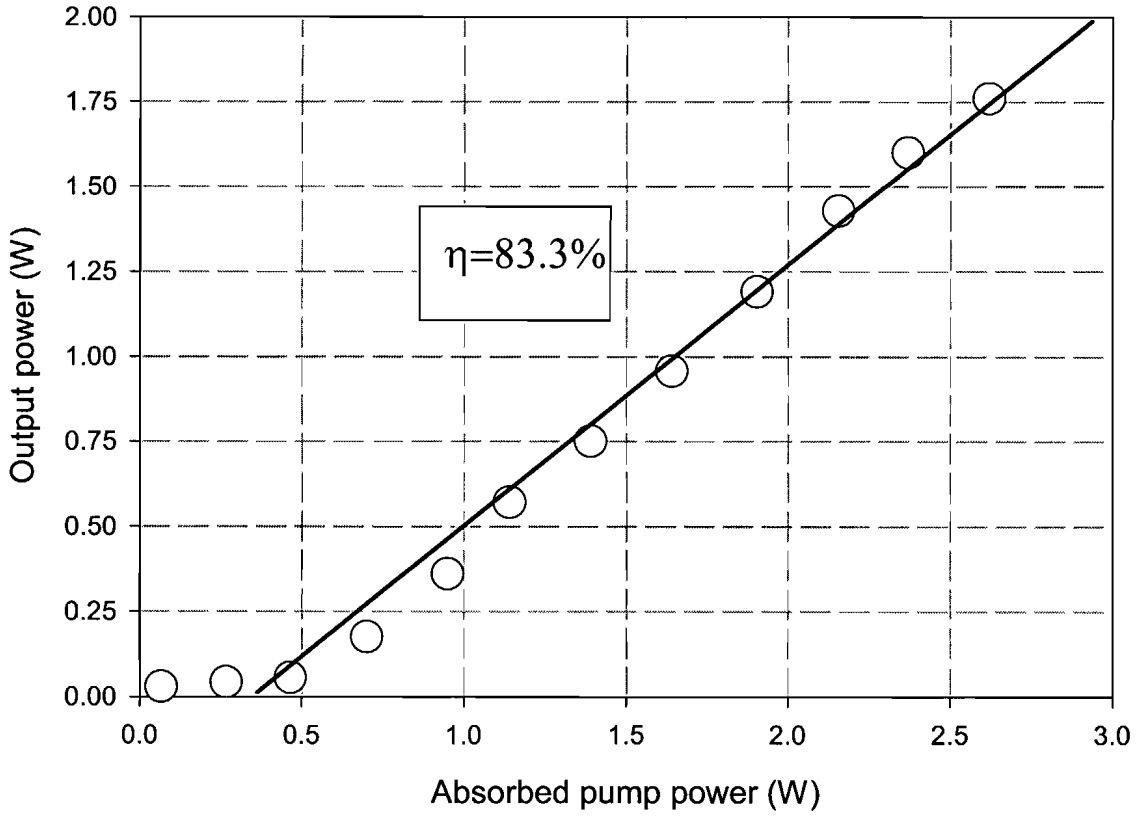

Figure V-15 Results with fibre #6 in a double fibre configuration. The fibre was 1.7 m long with a fairly low twist rate.

This time, exactly the same results as for an end pumping configuration were obtained; a slope efficiency of 83.3%, and a threshold of 400 mW.

However all those results are quite exceptions. In fact, in most cases the slope efficiency was around 50%. They were two reasons for that. The first one was that in the pulling process, some breaks appeared in either the doped fibre (no lasing) or the pump laser (low efficiency: 50% or less). Secondly, at some point there was coating between the two fibres; this means that the coupling was much lower hence the efficiency was dropping. Therefore before making a laser, the piece of fibre had to be carefully selected, and this was much easier with a short device length. However, highly doped fibres bring another problem: lifetime quenching

[3] which limits efficiency. It seems then important to find a way to increase the optical contact between the two fibres and avoid the bending which creates the mode mixing necessary to achieve good absorption and coupling. The best solution may be to pull a figure-of-eight fibre (like two fibres of 80 μm side spliced) and then splice at both ends an 80 μm pump fibre, and an 80 μm OD singlemode core fibre, as in figure 16.

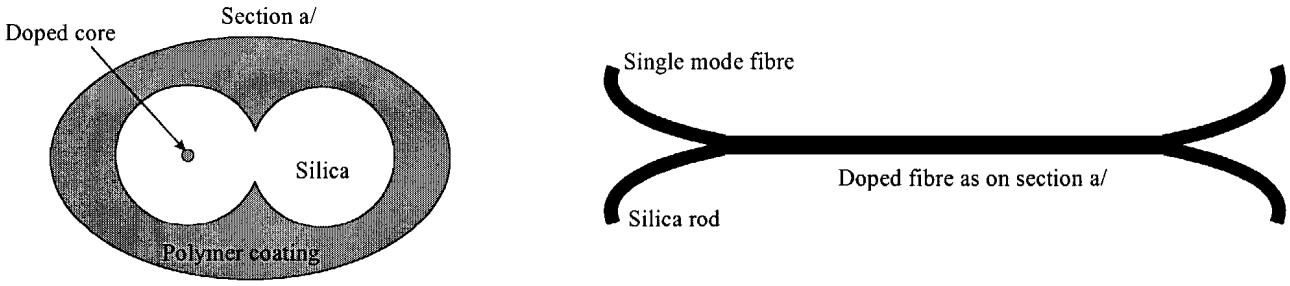

Figure V-16: One other solution to avoid bending losses and increase coupling and mode mixing.

IV LASING AT 975 nm

IV-1 Introduction

As it was discussed previously, having a powerful source emitting at 976 nm with a fibre coupled single mode signal output is an important issue for telecommunications (pump for EDFAs). Ytterbium seems to be a good contender for such a source [4-6]; however, the lasing at this wavelength operates as a three level system and the threshold is usually very high. As stated in chapter IV, one needs a small cladding to reduce this threshold and obtain a good lasing effect in double cladding configuration.
In the following part, different fibre designs will be discussed and the experimental results will be presented.

IV-2 Fibre design

For a small inner cladding, a high numerical aperture is needed to launch enough power and obtain high pump intensity. The cladding can be shaped to match the pump laser diodes output beam characteristics. In fact, three different types of diodes were considered for this

experiment: two types of diode stripes (1x100 μm and 1x200 μm emitting 2 W and 4 W respectively) or a pigtailed source offering 7 W in a 100 μm core fibre with an NA of 0.22. For the first experimental tests the pigtailed source was used. Therefore the best design should be a circular fibre as in [6] with cladding of 50 μm or less and NA of more than 0.2. Figure 17 shows an example of such a design. The core size is designed to be quite large (increasing the core to cladding ratio) and slightly multimode (14 μm 0.1 NA or more).

Figure V-17 First fibre design: The core (4) is 14 μm with NA around 0.1, the inner cladding (3) is 50 μm with NA> 0.2 with respect to the outer cladding (2, OD=125 μm). (1) is a high index polymer coating

To increase the mode mixing and optimise the absorption, it would be better to mill off one of the facets of the fibre. Finally in this sort of setup a way to increase the NA and the mode mixing is to drill holes all around the inner cladding as in figure 18, or to use a jacketed air clad structure [10] (the inner cladding is surrounded by capillaries in the preform, thus when it is pulled there are holes around the inner cladding). In this case, the NA of the inner cladding should be more than 0.4 and the inner cladding should not have a circular shape. Note that in this case the silica wall between the holes should remain thin to obtain a high air-filled fraction around the inner cladding, thus a high NA.

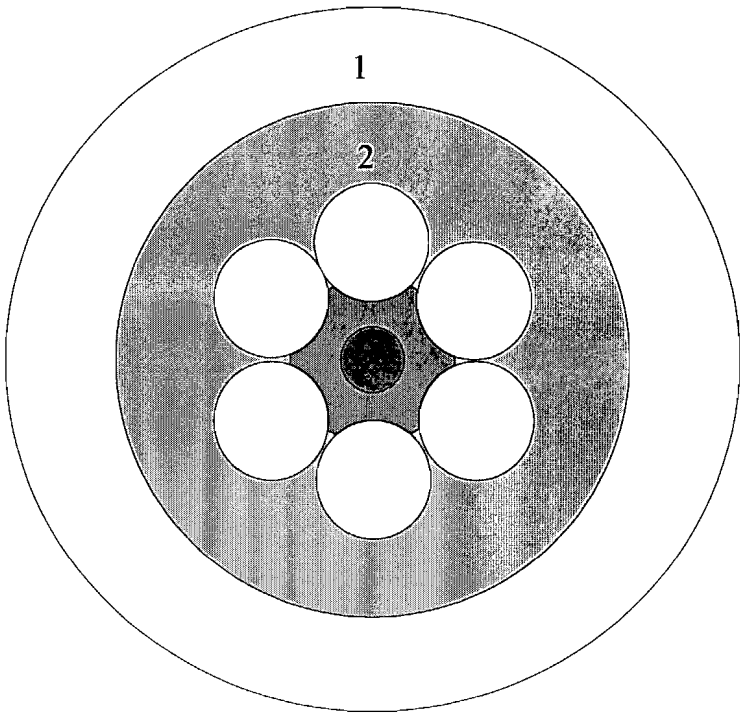

Figure V-18. The same design as previously described, but air holes are drilled around the inner cladding to increase its effective NA and the mode coupling for the pump modes.

Therefore, most of the signal from the pigtailed source should be launched into an inner cladding of 50 μm diameter.

To make the system more compact, one can use diode stripes, which provide a higher brightness. For these, the best design will be a thin rectangular inner cladding. The NA of each axis should be different to match the output NA of the pump laser diodes and the spot dimension. The physical dimension of this inner cladding should be as small as possible (given the limitation due to the lenses, and diffraction). With such a design, one should be able to launch most of the power from the diode stripes. However, when the fibre is too long then the NA will be the same for both axes (due to twisting of the fibre and mode-mixing). With a thin inner cladding, the absorption will probably be tremendous, and the device length should be less than a metre thus this should not be an issue.

The last problem in the fibre design is the lifetime quenching [3], which is more critical in this three level operation. Once again, the design is favourable: since the core to cladding ratio is large, the absorption will be high and the device length will be short, even with a low Yb concentration in the core. Hence, the quenching should remain very low.

IV-3 Experimental setups

The same basic setup was used for all the sources. This was an end-pumping setup, with the appropriate optics for the sources used. The fibre could be either used in a setup with an external grating as in figure 19a or with a spliced fibre Bragg grating as in figure 19b. For the external feedback one of the end must be angle polished or cleaved to avoid any reflections at 1030 nm, the other end in both cases is straight cleaved to provide the nominally 3.5% Fresnel reflection.

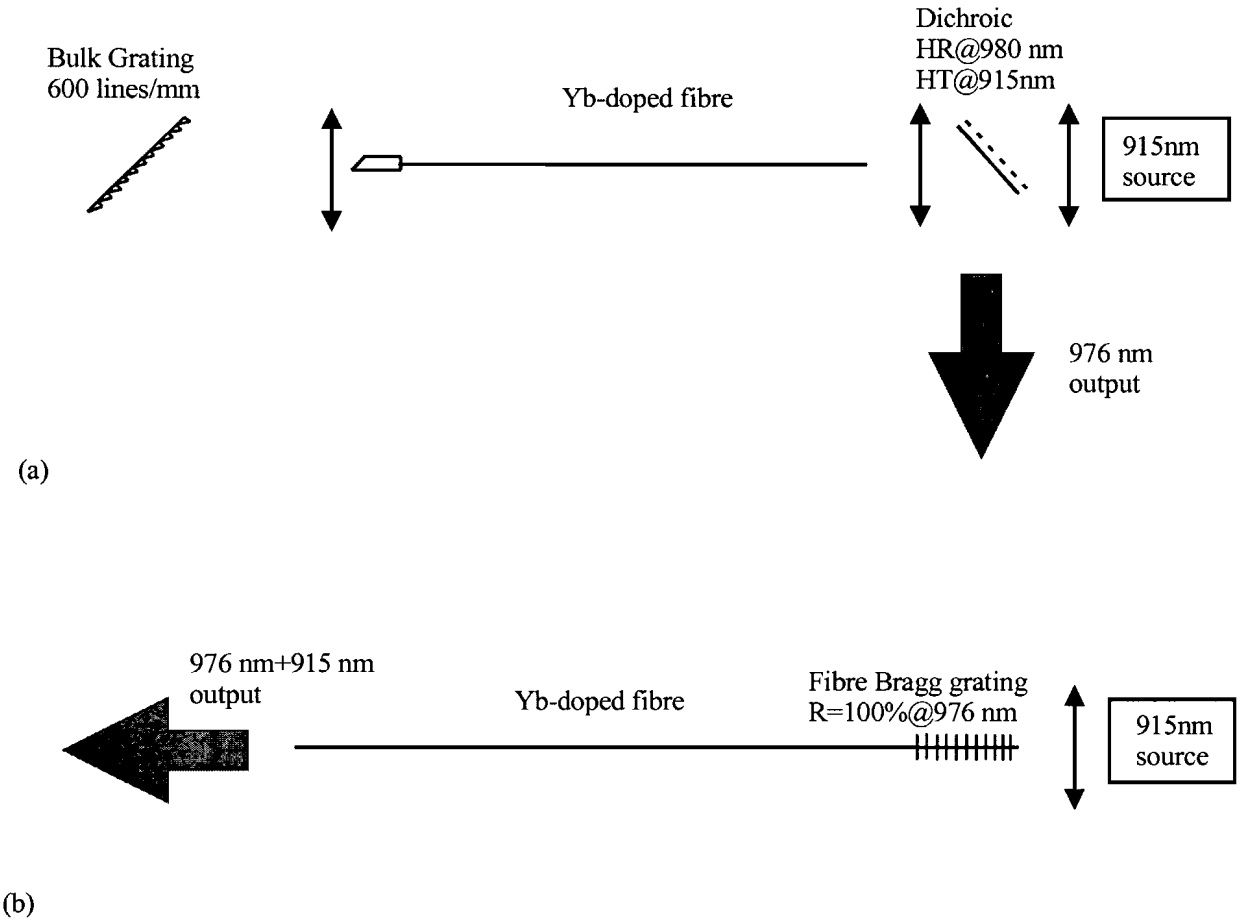

Figure V-19 Experimental setups for the 980 nm Yb-doped fibre laser. a/ with an external bulk grating, b/ with a fibre Bragg grating.

It is important to notice that the effective absorption, when the laser is operating, is less than half of the measured absorption with no emission because of the three level operation; thus, for most of the pump to be absorbed, the pump should be double-passed. The final setup, then, is as follows (figure 20a/b). The best solution will be to use a fibre with a Bragg grating at the pump end and an external feedback for the pump at the far end, but for the following

experiment, there was no fibre Bragg grating available. Therefore, for the first tests, the setups in figures 19a and 20a were used with an external grating for the signal.

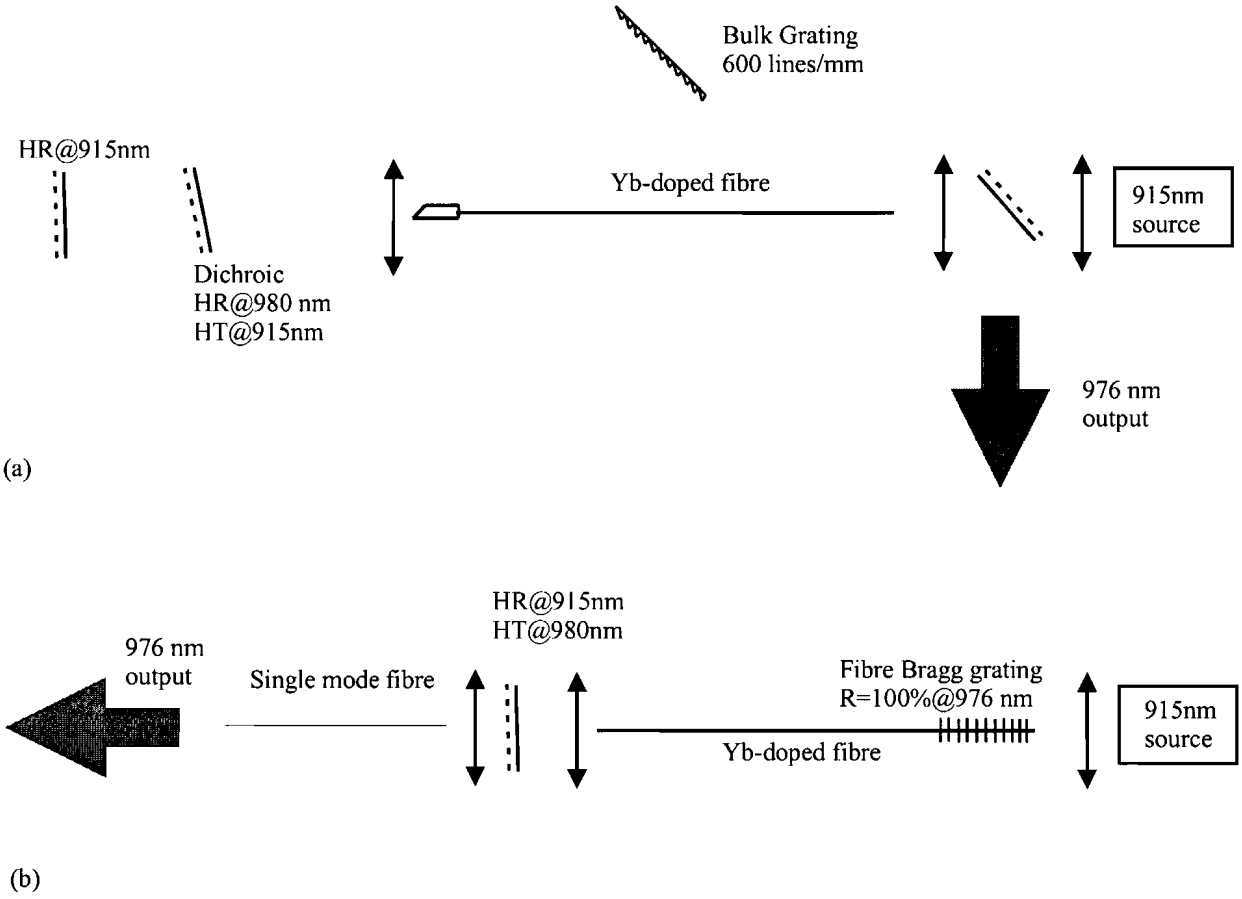

Figure V-20 experimental setups for the 980 nm Yb-doped fibre laser, with pump feedback.

To make a ytterbium doped fibre laser emitting at 975 nm one can also try to increase the threshold for emission above 1 μm. This means that a filter needs to be introduced in the fibre to filter those wavelengths out of the core. Solutions for this filter could be either the use of chirped blazed gratings scattered along the fibre to filter out the emission between 1020 and 1100 (probably several filters of 5 nm bandwidth each for example), the use of a long period grating [7], or fibre bending [8] as filters for long wavelength. This will have the advantage of reducing the ASE at 1035 nm, thus the threshold at 975 nm should be lower.

IV-4 Fibre characterisation and Lasing results

The first results obtained were with the setup in figure 19a. The fibre (fibre #7) was an all-glass structure with an inner cladding of 42 μm (NA= 0.2) and a core of around 14 μm

(NA=0.15). The pump source was the pigtailed array of diodes (MILON), which gave an output of 7W in a 100 μm core fibre (NA=0.22) at 915 nm. The main problem was the low level of pump power launched into the inner cladding. First the dichroic was only transmitting 5.6W of the pump. Secondly, the size mismatch between the DCF and the pump fibre allowed only launching up to 1.4 W in theory. Experimentally, 1.3 W of pump power was launched into the inner cladding.

However the first results shown in figure 21, proved that the right choice in terms of dopant concentration was made, since to obtain such efficiency the quenching rate should be very low.

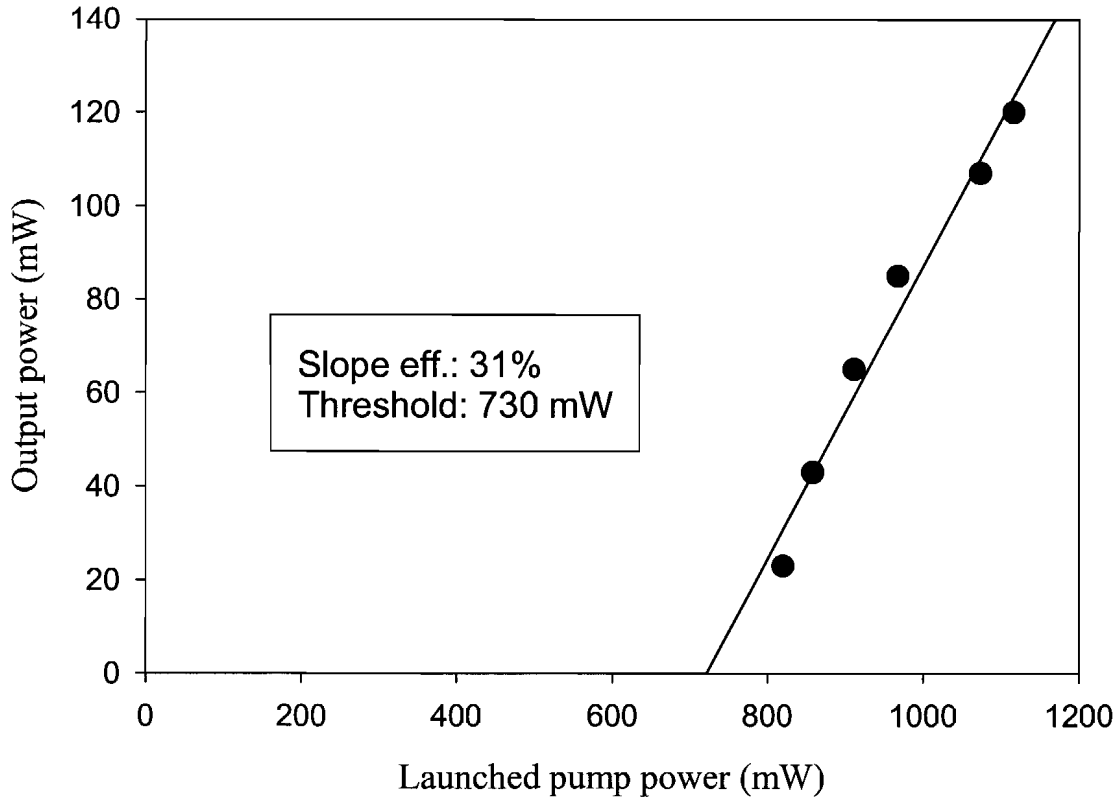

Figure V-21: Lasing results with one way pumping as in figure 20a. It should be noted that only 40 % of the pump was absorbed. The fibre was 40 cm long.

This showed the necessity of using a double pass setup for the pump, since the fibre was only absorbing 40% of the pump.

As a consequence, the setup shown in figure 20a was used. In this case, using longer fibre (no lasing at 980 nm in single pass configuration), the results shown in figure 22 were obtained.

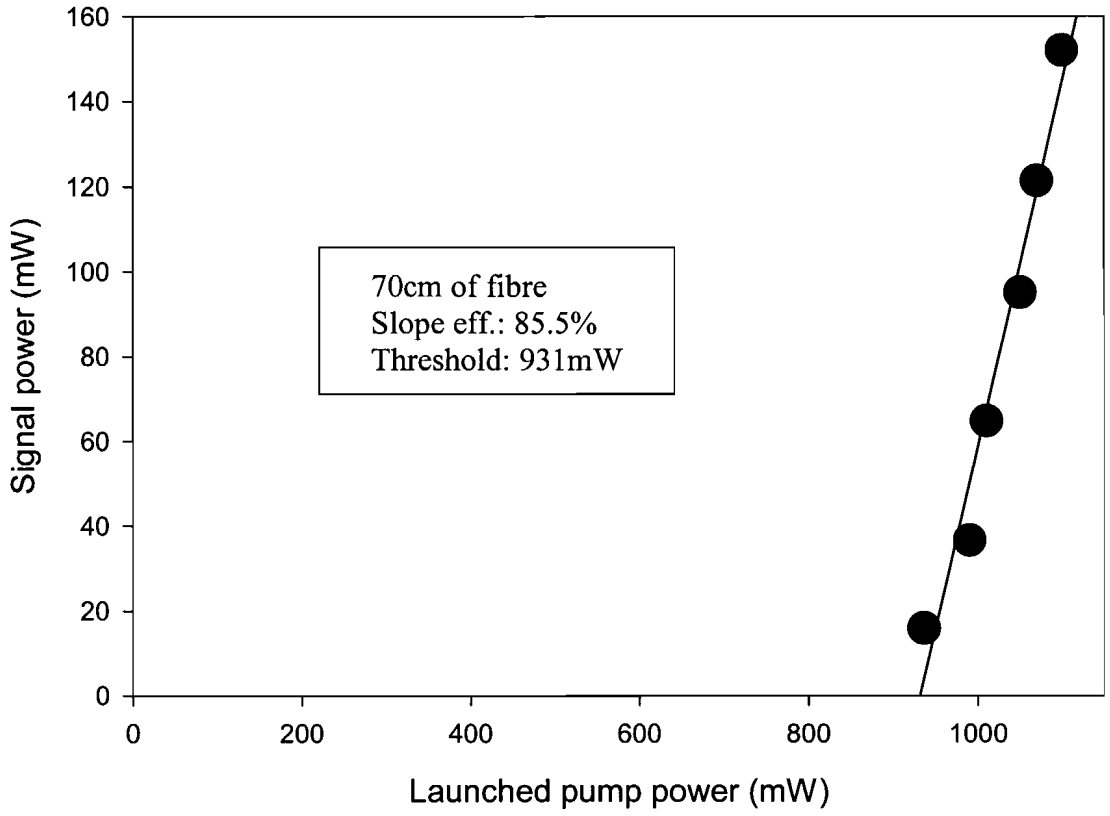

Figure V-22: Result obtained with 70 cm of the fibre when the transmitted pump is double passed

The efficiency of the laser proved the quality of the doping, and the utility of the double pass configuration.

As can be seen in figure 22, the pump level was just above threshold, unfortunately it was not possible to increase the pump level with this fibre design combined with the MILON source. A larger NA was needed, so different designs have to be tested like the one described in part V.3.4 of this chapter.

For this laser, which was expected to operate in continuous wave regime, the time dependence of the signal was also checked. For this measurement, a detector with a time constant of less than 1 ns was used. It was sufficient to see any Q-switching or relaxation oscillation. No noticeable variations were measured. The spectrum was also stable in the time domain.

IV-5 Conclusion for the 976nm source

This first approach gave very encouraging results, although the output power was not as high as expected. The double passed pump setup proved to be highly efficient. The fibre design seems to provide low threshold and low quenching which results in high efficiency. The laser output is stable, without any self Q-switching or relaxation oscillations. Those results are encouraging in the aim of having, in the near future a multi-Watt output 976 nm fibre source. The next steps in this work will be to write Bragg grating into the fibre, to try a holey structure to increase the inner cladding NA, and finally to try a rectangular inner cladding design with a diode strip to increase the compactness of the source.

V CONCLUSION

The results obtained are in fairly good agreement with the theory, and the setups described in chapters I , II and III have proved their efficiency.
Effectively these compact sources are efficient. To increase the power up to the level which was reached in industry [9], one should increase the number of diodes and the number of couplers, as one coupler cannot withstand very high power, or increase the number of fibres in the multifibre arrangement because it is prohibitively difficult to launch a large amount of light into one fibre. The couplers are introducing losses in the cavity so if one increases the number of couplers the efficiency will decrease-therefore it seems that the multifibre arrangement is better for this type of application. However, as it has been seen, there are still many remaining problems with this fibre source design, since in most cases slope efficiencies of only 50% were measured. Theoretical estimation also shows that the threshold will increase with the number of fibres. In fact it seems that the best solution is a double fibre with multiple pump injection points.
This is still a promising design since a high efficiency was obtained with one of the arrangements and, as it has been seen in chapter III, there are many possible improvements for this fibre arrangement.
Finally, some encouraging first results for the generation of 976 nm were achieved in a double clad Yb-doped fibre. Though the output power is still low due to the low level of pump light launched into the inner cladding, efficiency against launched pump power reached the level of 85.6 % with the quantum limit being 97% in comparison with the absorbed pump power. This difference seems to be mainly due to a non-perfect feedback for

the pump. Hopefully, future work on this type of fibre laser will lead to a compact multi-Watt level source.

REFERENCES

[1] A. Clarkson and D. C. Hanna, "Two-mirror beam-shaping technique for high-power diode bars," Optics Lett., 1996, Vol.21, No.6, pp.375-377

[2] J. A. Alvarez-Chavez, A. B. Grudinin, J. Nilsson, P. W. Turner, W. A. Clarkson, "Mode selection in high power cladding pumped fibre lasers with tapered section," Technical digest, CWE 7, CLEO'99, Baltimore, 1999.

[3] R. Paschotta, J. Nilsson, P. R. Barber, J. E. Caplen, A. C. Tropper, D. C. Hanna, " Lifetime quenching in Yb-doped fibres," Optics Com., 1997, Vol. 136, pp.375-378.

[4] D. C. Hanna, R. M. Percival, I. R. Perry, R. G. Smart, P. J. Suni, J. E. Townsend, A. C. Tropper, "An Ytterbium-doped monomode fibre laser: broadband tunable operation from 1.010 to 1.162 μm and three-level operation at 974 nm," *J. Mod. Opt.*, 1990, Vol. 37, pp. 517-525

[5] J. D. Minelly, L. A. Zenteno, M. J. Dejneka, W. J. Miller, D.V. Kuksenkov, M. K. Davis, S. G. Crigler, M. E. Bardo, "High power diode pumped single-transverse-mode Yb fiber laser operating at 976nm," Postdeadline paper, PD2, OFC 2000, Baltimore, 2000.

[6] A. S. Kurkov, E. M. Dianov, V. M. Paramonov, O. I. Medvedkov, S.A. Vasiliev, A. Yu Laptev, A. A. Umnikov, A. N. Guryanov, "Efficient Yb fiber laser at 980 nm pumped by a high- brightness semi-conductor source," Technical Digest, CtuQ2, CLEO'2001, Baltimore, 2001.

[7] US patent No: US 5,991,314 "Design for a Yb-doped CP fiber laser for operating near EDFA absorption band."

[8] K. Morishita, M. S. Yataki, W. A. Gambling, "In-line optical fibre filters using dispersive materials," Electronics lett., vol.23, pp.319-21, 1987.

[9] Dominic, S. MacCormack, R. Waarts, S. Sanders, S. Bicknese, R. Dohle, E. Wolak, P.S. Yeh, E. Zucker, "110 W fibre laser," Postdeadline paper, CPD 11, CLEO'99, Baltimore, 1999.

[10] P. J. Bennett, T. M. Monro, D. J. Richardson, "Towards practical holey fibre technology: Fabrication, Splicing, Modeling, and Characterization," Optics Letters, 1999, vol. 24, pp.1203-5.

CHAPTER VI: BACKGROUND THEORY: Q-SWITHING

I INTRODUCTION

In contrast to conventional solid state lasers, double clad fibre lasers require long cavities (often several tens of meters) to achieve efficient absorption of pump radiation from high power diode lasers. The reason for this is the small core area, which leads to a large cladding-to-core area ratio and low pump absorption in typical double-clad fibres. The small doped core area with a tight mode confinement also leads to a high gain for relatively small amounts of energy stored in the form of excited Yb-ions. The high gain leads to losses via amplified spontaneous emission (ASE) or even spurious lasing between pulses. This limits the energy that can be stored in the gain medium and thus the pulse energy of a Q-switched fibre laser. Furthermore, a long fibre and small core area exacerbate nonlinear effects like self phase modulation, stimulated Raman scattering, and stimulated Brillouin scattering. These can also be detrimental for Q-switched operation. To increase the energy storage and reduce fibre nonlinearities, it is necessary to increase the core area, which decreases the mode confinement permitting the use of shorter fibres without compromising the absorption efficiency.

In this chapter two main models will be developed to simulate the behaviour of the fibre laser in the Q-switched regime, and emphasise the importance of the mode area. Several rate equation models [5-11] have been developed for the dynamics of solid-state Q-switched lasers [5-8], these were the first ones used for simulations for this work. Many of these models neglect the ASE energy loss mechanism, but for high-energy Q-switched fibre lasers it is essential to include this effect [12,13]. Therefore, a second model still based on rate equations is described as in [11] but including ASE.

II Q-SWITCHING IN LOW ENERGY SYSTEM

In a low gain system one can consider that ASE is negligible. Therefore, the models described in [5-7] which are suitable for bulk lasers can be used. In this case the model is analytical. It gives the energy as a function of the laser repetition rate.
The first step is to give an expression for the energy as a function of the high Q population inversion (lasing) and the low Q population inversion (not lasing) difference ΔN:

$$E = h\nu V\Delta N \ , \tag{1}$$

Where $h\nu$ is the photon energy, V is the gain volume. In this equation, losses were neglected along the fibre (cavity) as with the following expressions except for the threshold.
The next step is to consider the CW regime. When operating in this regime the output power is proportional to the following difference in the population inversion:

$$P_{cw} = h \cdot \nu \cdot V \cdot \frac{(n_\infty - n_{th})}{\tau_{21}}, \tag{2}$$

Where n_∞ is a measure of the pump rate for the given population inversion that would result in the absence of any stimulated emission, n_{th} is the population inversion (ions/m^3) at the laser threshold and τ_{21} is the upper level lifetime of Yb^{3+}. The following equation was used to determine n_{th} [6]:

$$n_{th} = \frac{\ln(\frac{1}{R_1 \cdot R_2}) + n_T \cdot \sigma_{as} \cdot L}{2 \cdot (\sigma_{es} + \sigma_{as}) \cdot L} \tag{3}$$

In this equation $R_{1,2}$ are the coupler reflectivities, L represents the internal losses in the cavity (in dB), σ_{es} and σ_{as} are the emission and absorption cross-section at the emission

wavelength (σ_{es}=2.0×10^{-20} cm^2, σ_{as}=1.4x10^{-23} cm^2, they are typical values at the typical signal wavelength of 1080 nm), n_T is the total number of Yb ions per unit volume.
Then, the difference of population inversion ΔN can be defined, as a function of the frequency of switching (f_r). For this case, it is estimated that the high Q population inversion is negligible, i.e. the pulse extracts most of the stored energy.

$$\Delta N = n_\infty \cdot (1 - \exp(-\frac{1}{\tau_{21} \cdot f_r})) \quad (4)$$

From this one can write a simple equation for the energy as a function of the repetition rate and the output power in the cw regime.

$$E = (P_{cw} \cdot \tau_{21} + n_{th} \cdot h \cdot \nu \cdot V) \cdot (1 - \exp(-\frac{1}{\tau_{21} \cdot f_r})) \quad (5)$$

This model works only for low power. For example if the fibre has a large core (15 μm), which generates less ASE, with a 250 mW average output power. The results are shown in figures 1 and 2, for the average power and the pulse energy.
These results are well correlated with those found in experiments (see Chapter VII).
However, if one considers a standard fibre with the same pump power, the same maximum energy will be obtained, although this is not practically possible; such a fibre would never give more than 60 μJ because of ASE.
So for large pump intensity (or with a small core area), another model, which includes ASE will be needed. This model will be described in next part. It will not include frequency dependence, simply giving the maximum extractable energy. In conclusion this first model has the advantage of easily describing a complete behaviour of the Q-switched laser (energy as a function of the frequency) but only when ASE is negligible. Hence this is a model for low energy (compared to the energy storage capacity at a specific core size) behaviour.

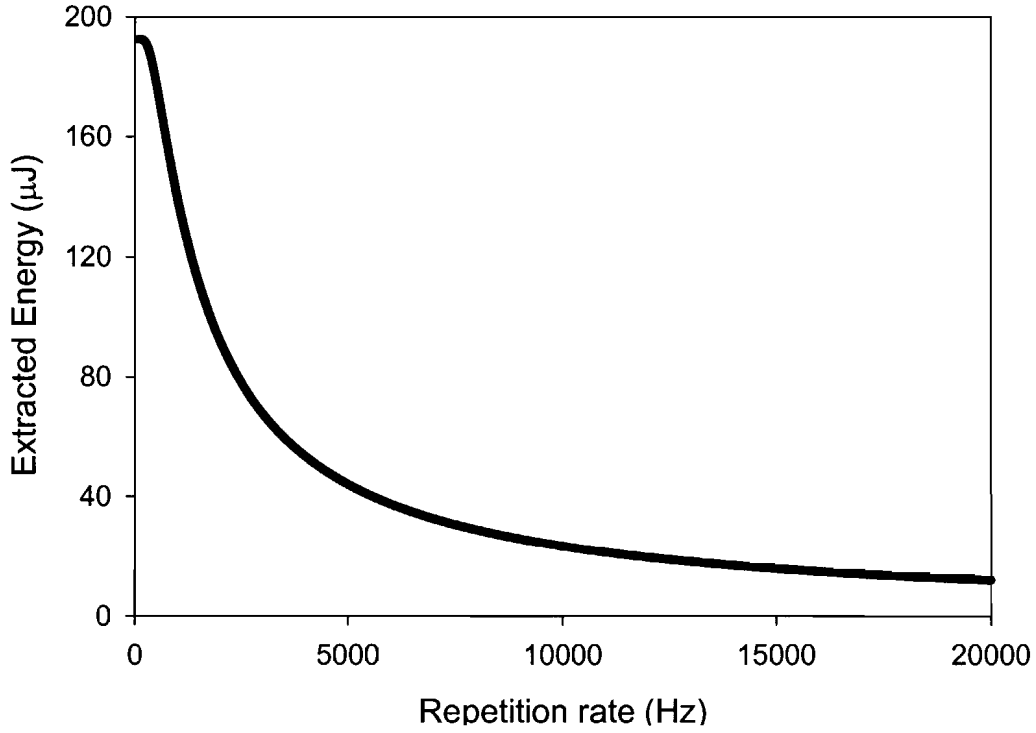

Figure VI-1: Calculation for the extracted energy as a function of the repetition rate

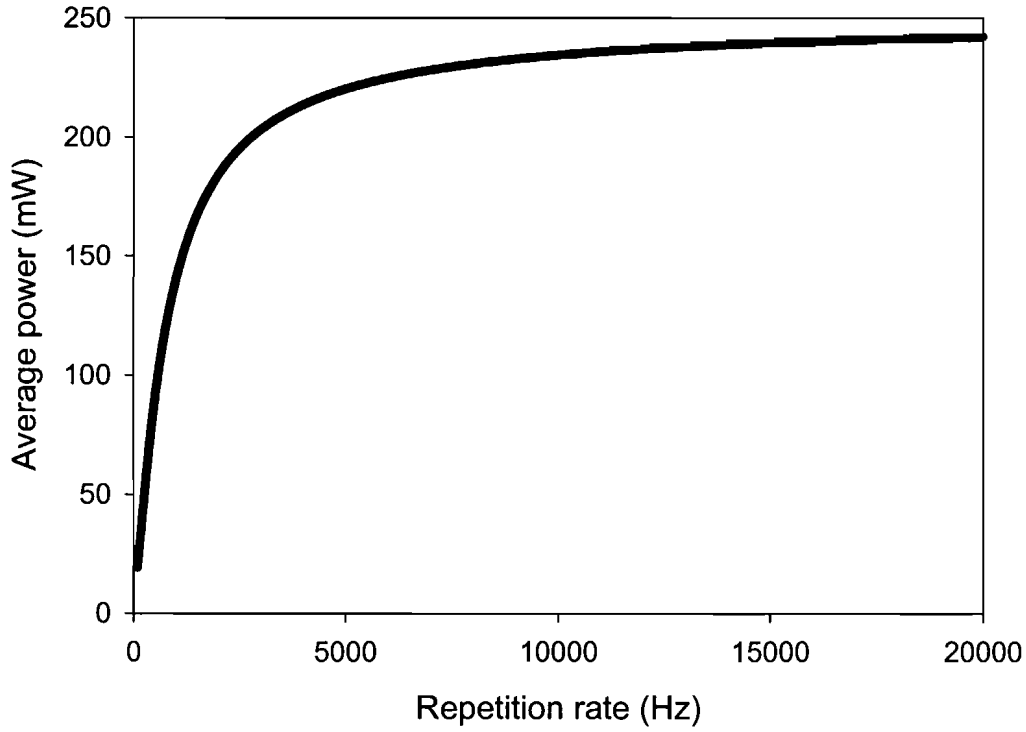

Figure VI-2: Calculation of the average power as a function of the repetition rate

III HIGH ENERGY MODEL, INCLUDING ASE.

Now, strong pumping will be considered, thus strong ASE. Then, the saturation energy E_{sat} is a key parameter for the amount of energy that can be stored in a laser. It is given by:

$$E_{sat} = \frac{h\nu_s A}{(\sigma_{es} + \sigma_{as}) \cdot \Gamma_s} \quad (6)$$

Where $h\nu_s$ is the signal photon energy, σ_{es} and σ_{as} are the emission and absorption cross-sections at the emission wavelength (σ_{es}=2.0×10^{-20} cm^2, σ_{as}=1.4x10^{-23} cm^2, they are typical values at the typical signal wavelength of 1080 nm), A is the doped area, and Γ_s is the signal mode overlap with the active dopant.

To be more precise, this parameter can be linked to the gain, the stored energy (E_{stored}) and the extractable energy (E_{ext}), using the following steps:

$$G = \frac{10}{\ln(10)} \Gamma_s ((\sigma_{es} + \sigma_{as}) \int_0^l n_2(z)dz - \sigma_{as} n_{tot} l) \quad (7)$$

$$E_{stored} = h\nu_s A \int_0^l n_2(z)dz \quad (8)$$

Where n_2 and n_{tot} are the upper and total population densities (ion/m^3). By observing that the energy can only be extracted until the gain is equal to zero, it can be seen that the system needs to store energy until a bleaching level (E_{bleach}) for which G=0 is reached, thus one can determine the relation between the gain, the extractable energy, the saturation energy, and the stored energy.

$$G_{dB} = 4.34 \cdot \left(\frac{E_{stored}}{E_{sat}} - \frac{E_{bleach}}{E_{sat}}\right) \quad (9)$$

$$E_{bleach} = \sigma_{as} n_{tot} \Gamma_s \cdot l \cdot E_{sat} \quad (10)$$

$$E_{ext} = E_{stored} - E_{bleach} = 4.34 \cdot E_{sat} \cdot G_{dB} \quad (11)$$

As a rule of thumb, the extractable energy stored in a fibre (i.e., energy above the bleaching level of the fibre) is limited to around ten times the saturation energy. Above that, any additional pumping power is simply lost as ASE between pulses, without significantly increasing the stored energy. The gain grows by 4.34 dB if the stored energy increases by E_{sat}, with the energy loss to ASE increasing by roughly the same amount, or even more in the presence of spurious feedback. Thus, ASE power losses grow exponentially with the stored energy. Once ASE begins to dominate the overall power losses, further pumping soon

becomes quite inefficient. With σ_{es} and σ_{as} more or less fixed by the dopant ion (but wavelength dependant), the doped area A and the signal overlap Γ_s are the only parameters available for increasing the limit of energy storage via an increased value of E_{sat}. Note however, that for a given core size and a given refractive index geometry, A and Γ_s are not independent. Rather, the signal overlap increases with the doped area, and the ratio A/Γ_s can only be varied over a limited range if the dopant is restricted to the core (with a fixed refractive index geometry). Thus, a larger doped area does not necessarily lead to significantly larger saturation energy. Instead, special geometries such as ring-doping [14] are better for increasing the ratio A/Γ_s and thus E_{sat} within a fixed refractive index geometry. Alternatively, by increasing the mode size using modified refractive index geometry, one can also increase the ratio A/Γ_s, and this was the approach taken for the experimental work to obtain a larger saturation energy (Chapter VII).

Although the saturation energy, given by the simple expression in equation 6, is very closely related to the maximum extractable energy from a fibre laser other, more complex and less transparent, equations are required for precise evaluations of the extractable energy under specific pumping conditions. Here, the most important parameter is the maximum energy that can be stored and extracted at repetition rates low enough for the system to reach a steady state between pulses. A time-independent analysis of the system, including ASE, between pulses is then sufficient. A simple model was used with a single wavelength for the ASE and signal, similar to the one described in [11]:

$$\frac{dP_p(z)}{dz} = -\Gamma_p \sigma_{ap} n_1(z) P_p(z) \tag{12}$$

$$\pm \frac{dP^{\pm}_{ASE}(z)}{dz} = \Gamma_s(\sigma_{es} n_2(z) - \sigma_{as} n_1(z)) P^{\pm}_{ASE}(z) + \Gamma_s n_2(z) \sigma_{es} \cdot 2 n_m h\nu_{ASE} \Delta\nu_{ASE} \tag{13}$$

$$n_2(z) = n_{tot} \cdot \frac{\frac{P_p(z)\sigma_{ap}\Gamma_p}{h\nu_p A} + \frac{P^{tot}_{ASE}(z)\sigma_{as}\Gamma_s}{h\nu_{ASE} A}}{\frac{P_p(z)(\sigma_{ap}+\sigma_{ep})\Gamma_p}{h\nu_p A} + \frac{1}{\tau_2} + \frac{P^{tot}_{ASE}(z)(\sigma_{as}+\sigma_{es})\Gamma_s}{h\nu_{ASE} A}} \tag{14}$$

$$n_1(z) = n_{tot} - n_2(z) \tag{15}$$

$$P_{ASE}^{tot}(z) = P_{ASE}^{+}(z) + P_{ASE}^{-}(z) \quad (16)$$

Here, n_2 and n_1 are the upper and lower level population densities (ion/m^3), P_p is the pump power (the pumping is uni-directional), $P_{ASE}^{\pm}$ is the signal power, co (+) and counter (–) propagating relative to the pump, $\Delta\nu_{ASE}$ is the ASE bandwidth, n_m the number of transverse modes excited in the cavity (excluding polarization degeneracy), τ_2 is the lifetime of the upper laser level, and $\Gamma_{p,s}$ are the pump and signal overlaps with the doped area. The last term in equation 13 represents the spontaneous emission that seeds the ASE, considering the same conditions as in [11] for recoupled spontaneous emission. Rayleigh back-scattering is neglected.

In this model, it was assumed that the pump is evenly distributed throughout the core and inner cladding, in each transverse cross-section of the fibre, despite the fact that the inner cladding is highly multi-moded for the pump. While each mode experiences a different characteristic absorption, a practical, well designed cladding-pumped fibre should exhibit essentially uniform absorption along its length due to a combination of mode scrambling techniques and special geometrical fibre designs. In practice, a single equation (equation 12) is enough to describe the evolution of all pump modes. The signal may also be multi-moded as well, with different gain for different modes. In equation 13, an effective number n_m of signal modes that see essentially the same gain was assumed. The core may support more modes than this, however it was assumed that the gain for those modes is low enough to neglect them. The effective number of transverse modes depends on the overlap between different modes and the gain medium, mode coupling, as well as, how the different modes saturate the gain medium.

The system of equations (12-16) is repeatedly integrated along the fibre until a solution is found that satisfies the boundary conditions for the ASE and pump power. For a fibre with a perpendicular cleave at the pump-launch end (with ~4% reflectivity) and an angle cleave at the other, the boundary conditions, for the pump, are given by the power launched through the perpendicular fibre end. For the signal, they become:

$$P_s^{+}(0) = 0.04P_s^{-}(0) \quad (17)$$

and

$$P_s^-(l) = 0 \tag{18}$$

In equation 18, l is the fibre length. The solution provides the steady-state ASE power evolution and Yb inversion profile along the fibre. The extractable energy is readily evaluated as the difference between the stored energy and the energy required to bleach the Yb signal reabsorption:

$$E_{ext} = h\nu_s A\left\{\int_0^l n_2(z)dz - n_{tot}L\frac{\sigma_{as}}{\sigma_{as}+\sigma_{es}}\right\} \tag{19}$$

Figure 3 shows the extractable energy in the limit of low repetition rates as a function of pump power, calculated using the model above. The fibres had a simple step-index distribution with core diameters of 40 μm and 6 μm (Γ_s=0.75 for both). The fibres were 10 m long. The pump absorption was 3 dB/m for cladding pumping (the Ytterbium concentration was 3000 p.p.m by weight). For both fibres the generated laser beam was assumed to be single-moded, even though the large-core fibre would actually be intrinsically multi-moded. In order to demonstrate the impact of the ASE, the extractable energy was also calculated in the absence of the ASE source term for the same fibres. The two points on the graph represent two experimental results (Chapter VII) obtained at 500 Hz, 1.3 mJ (33 μm core) and 2.3 mJ (40 μm core). This repetition rate was low enough to correspond to the regime described by the model. The two experimental points are 3 dB below the theoretical value. Background losses, which were neglected, and incomplete energy extraction are possible reasons for the discrepancy. Furthermore, the experimental conditions do not correspond exactly to the assumptions used in the simulations. For example, the core size of one fibre is slightly smaller. However, at this level of absorbed pump power (5 W), ASE self-saturation is small for these core dimensions. Without ASE self-saturation, the influence of core size is small, so the results should be comparable. To conclude, the extractable energy calculated with the model gives a fair indication of the resulting pulse energy at low repetition rates.

In figure 3, the calculated energy scales almost proportionally with the core area at high pump powers: for 10 W pump power the calculated extractable energy is 0.11 mJ for the 6 μm core fibre and 4.3 mJ for the large core fibre (with core area approximately 40 times larger). For the 40 μm core fibre, the efficiency with which energy is stored rolls off above 6

W of pump power, at ~4 mJ of extractable energy. For the small core fibre, the energy storage efficiency starts to roll off at 300 mW, and the extractable energy is limited to ~0.1 mJ. Above these pump levels, ASE self-saturation prevents further energy storage, and a larger mode area is required to relax the ASE limit, as previously discussed. The calculations thus confirm that (i) ASE limits energy storage at high pump powers, and (ii) the energy that can be stored at high pump powers is proportional to the mode area with this simple core design.

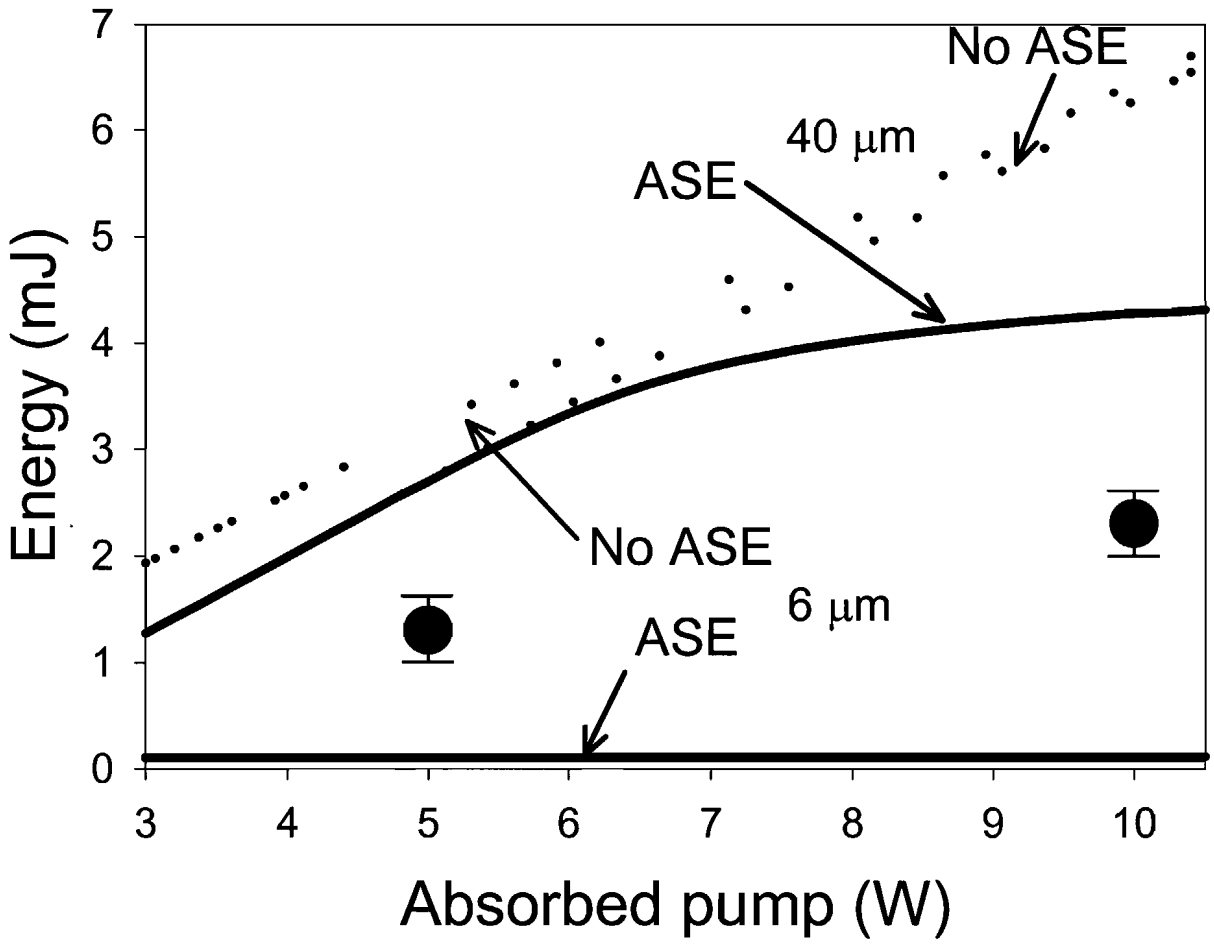

Figure VI-3: Calculated extractable energy versus absorbed pump power for fibres with 6 and 40 μm diameter cores. Solid curves: ASE included in the calculations. Dashed curves: ASE suppressed in the calculations. The dots represent measured pulse energies for a 33 μm core fibre (at 5 W of absorbed pump power) and a 40 μm core fibre (at 10 W of absorbed pump power).

The spontaneous emission that seeds the ASE is proportional to the number of operating modes in equation 13. Therefore, all else being equal, a SM fibre can reach a higher gain, extractable energy, and actual pulse energy than a MM fibre can (note that even a single, typically fundamental, mode can extract all of the extractable energy from the fibre, insofar as the mode interacts with the whole doped region). Consider, for instance, a fibre laser operating on 50 transverse modes. The ASE source term is then 50 times stronger than for a SM fibre. Therefore, the gain can be 50 times (i.e., 17 dB) larger with a single mode than with 50 modes before ASE self-saturation sets in. Since the ASE is strongly seeded by the 4% reflection in one cavity end, the 17 dB is actually a double-passed gain. Thus, the single-pass gain difference between a single-moded and a 50-moded fibre is expected to be ~8.5 dB. This gain corresponds to a stored energy of $2 \times E_{sat}$, or around 20 – 30% of the expected extractable energy. Simulations confirmed this result.

If the NA is kept fixed and the core diameter is increased, the reduction in the energy storage, because of increasing ASE losses to an increasing number of modes, is very much smaller than the growth of energy storage because of a larger core size. Under these premises, the area of a 50-moded core is approximately 50 times larger than that of a single-moded core. The ~20% reduction in energy storage because of the extra ASE losses in a multi-mode core is negligible compared to the 50-fold increase of energy storage from the larger area. Thus, the extractable energy is expected to scale with the mode area even if the fibre becomes multi-moded.

Finally, to estimate the maximum extractable energy, calculations for a 70 μm core with a NA of 0.05 were performed. The fibre length was 10 m and the absorption the same as before. The results are shown in figure 4.

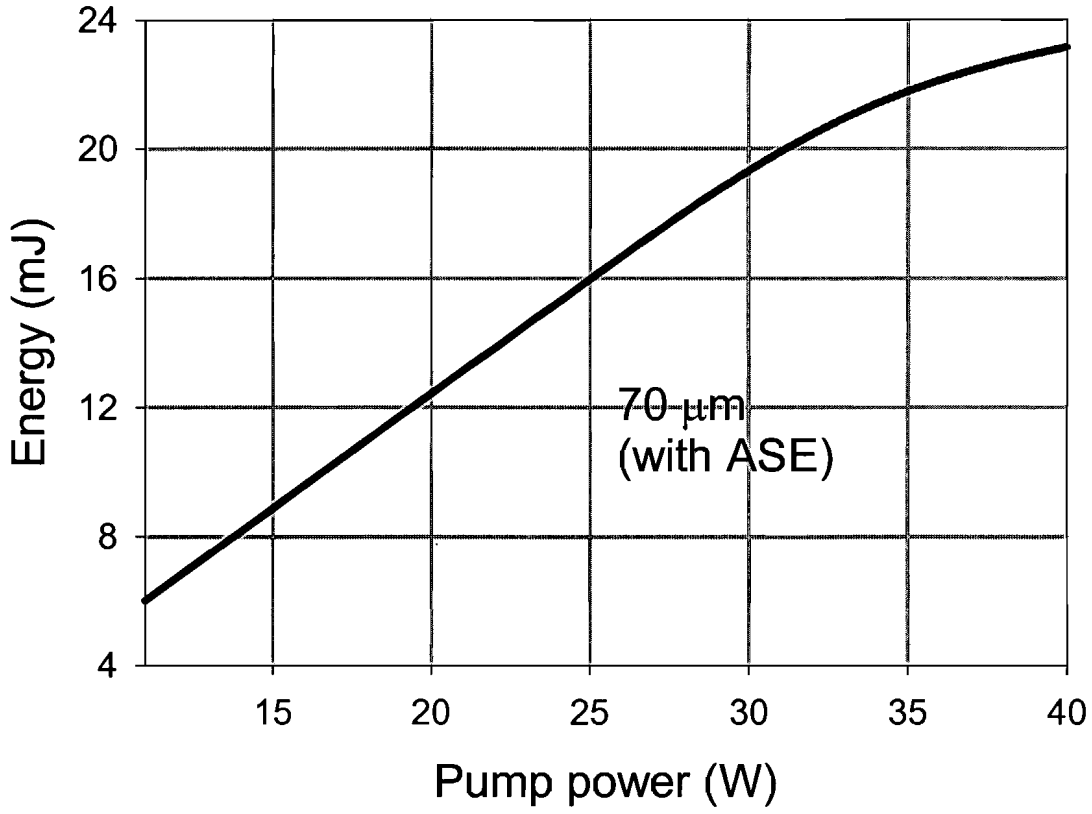

Figure VI-4: Calculation of the extractable energy for a very large core size (70 µm)

With this core size the threshold is much higher and the fibre has to be strongly pumped before producing any energy. This calculation shows that one can reach the order of 10 mJ with a Q-switched fibre laser if the core is large enough and the pump power sufficient.

IV CONCLUSION

The models described in this chapter give an understanding of what could happen in a Q-switched fibre laser. The first described well the temporal behaviour of the laser, although it was only relevant for a low energy system. For a high-energy system, the second model showed how important the core size is for reducing the effect of ASE. It also proved that the number of modes should be kept low enough in order to have high energy.
The calculations show that Q-switched fibre lasers can reach energy outputs as high as 10 mJ. In the following chapter the experimental work will be described.

REFERENCES

[1] H. L. Offerhaus, J. A. Alvarez-Chavez, J. Nilsson, P. W. Turner, W. A. Clarkson, D. J. Richardson, "Multi-mJ, multi-Watt Q-switched fiber laser," Opt. Lett., vol. 25, pp. 37-39, 2000.

[2] C. C. Renaud, R. J. Selvas-Aguilar, J. Nilsson, P. W. Turner and A. B. Grudinin, "Compact, high energy Q-switched cladding pumped fiber laser with a tuning range over 40 nm," IEEE Photon. Technol. Letters, vol. 11, pp. 976-978, 1999.

[3] C. C. Renaud, H. L. Offerhaus, J. A. Alvarez-Chavez, J. Nilsson, P. W. Turner, W. A. Clarkson, D. J. Richardson and A. B. Grudinin, "Designs for efficient high-energy high brightness Q-switched cladding-pumped ytterbium-doped fibre lasers," Technical digest, CMP1, CLEO'2000, San-Francisco (2000)

[4] C. C. Renaud, H. L. Offerhaus, J. A. Alvarez-Chavez, J. Nilsson, W. A. Clarkson, P. W. Turner, D. J. Richardson, and A. B. Grudinin, "Characteristics of Q-switched cladding-pumped ytterbium-doped fiber lasers with different high-energy fiber designs," IEEE J. Quantum Electron., vol. 37, pp. 199-206, 2001.

[5] A. Siegman, *Lasers*. Mill Valley, CA: Univ. Sci. Books, 1986, ch.26.

[6] W. Koechner, *Solid-state laser engineering*. Berlin, Germany: Springer-Verlag, 1996, vol.1, ch.8.

[7] M. J. F. Digonnet, Ed., *Rare Earth Doped Fiber Lasers and Amplifiers*, New York: Marcel Dekker, 1993.

[8] P. Roy, D. Pagnoux, "Analysis and Optimization of a Q-switched Erbium Doped Fiber Laser Working with a Short rise Time Modulator," Optical Fiber Tech. vol. 2, pp. 235-240, 1996

[9] I. Kelson and A. Hardy, "Strongly pumped fiber lasers," IEEE J. Quantum Electron., vol. 34, pp. 1570-1577, 1998

[10] I. Kelson and A. Hardy, "Optimisation of strongly pumped fiber lasers," J. Lightwave Technol., vol. 17, pp. 891-897, 1999

[11] E. Desurvire, *Erbium-doped fiber amplifiers*, New York: Wiley-Interscience,1994, ch. 1.

[12] O. G. Okhotnikov, J.R. Salcedo, "Emission Buildup in Q-switched Fiber Lasers," Opt. Lett., vol. 20, pp. 887-888, 1995

[13] J. Nilsson and B. Jaskorzynska, "Modeling and optimization of low repetition-rate high-energy pulse amplification in cw-pumped erbium-doped fiber amplifiers," Opt. Lett., vol. 18, pp. 2099-2101, 1993.

[14] J. Nilsson, R. Paschotta, J. E. Caplen, and D. C. Hanna, "Yb^{3+}-ring-doped fiber for high energy pulse amplification," Opt. Lett., vol. 22, pp. 1092-1094, 1997.

CHAPTER VII: RESULTS ON Q-SWITCHED FIBRE LASER

I INTRODUCTION

As stated in the previous chapter, to increase the energy storage and reduce fibre nonlinearities, it is necessary to increase the core area, which decreases the mode confinement and permits the use of shorter fibres without compromising the absorption efficiency. However, this route also leads to a multi-moded core and compromised beam quality, unless special fibre designs are used. One possibility is to use a large mode area (LMA) fibre with a complex, low-NA, refractive index profile. LMA fibres are either single- or few-moded with selective Yb-doping that also promotes high beam quality. A Q-switched fibre laser capable of generating 2.3 mJ pulses in a cladding pumped configuration [1] based on LMA fibre has been recently reported. The core area in this case was 1300 μm^2 – more than a factor of 50 greater than that in standard Yb-doped single-mode fibres [2]. CW laser operation of multimode fibres with a tapered section for suppression of higher order modes [3] has also been reported. This is another relatively simple possibility for a fibre laser with high beam quality and a large effective mode area with performance that can be comparable to that of LMA fibres, and is therefore attractive also for Q-switching.

In this chapter, I first compare the performance of Yb-doped Q-switched fibre lasers based on these two fibre types and investigate key design issues for the generation of high-energy Q-switched pulses. Then, a larger core fibre (60 μm) was used to see how much energy one could extract from a fibre laser. Finally, the tunability of the Q-switched fibre laser is studied at a lower power regime to avoid damaging the bulk diffraction grating used for tuning the emission wavelength.

II EXPERIMENTAL SETUP

The typical experimental setup used for the Q-switched fibre lasers is shown in figure 1. The fibres were either end-pumped by a beam-shaped diode bar [4], delivering 35 W of power at 915 nm, or side pumped with two multimode couplers (or a multifibre arrangement) which permitted launching of 2.6 W from two 1.5 W laser diodes emitting at 976 nm. With the first launching system, up to 25 W could be launched into a 200 μm diameter fibre. A dichroic mirror was used to separate the signal and pump at the pump launch end, which also served as the out-coupling end. The fibre was cleaved perpendicularly, and the 4% Fresnel reflection provided the feedback at this end of the cavity. The other fibre end was angle-cleaved to suppress feedback, and an external high-reflecting mirror closed the cavity, or a bulk grating (600 lines/mm blazed at 1 μm, blaze angle: 30 degrees) used to test the tunability of the system. The mirror reflected back the first-order beam from an acousto-optic modulator (AOM) that was on-off modulated to act as a Q-switch. The diffraction efficiency was up to 70%, depending on beam parameters (20% in the compact setup because, no better AOM was available at this time). The switching time was measured to be 130 ns on average. The AOM was switched with 1 μs pulses, for optimum extraction efficiency.

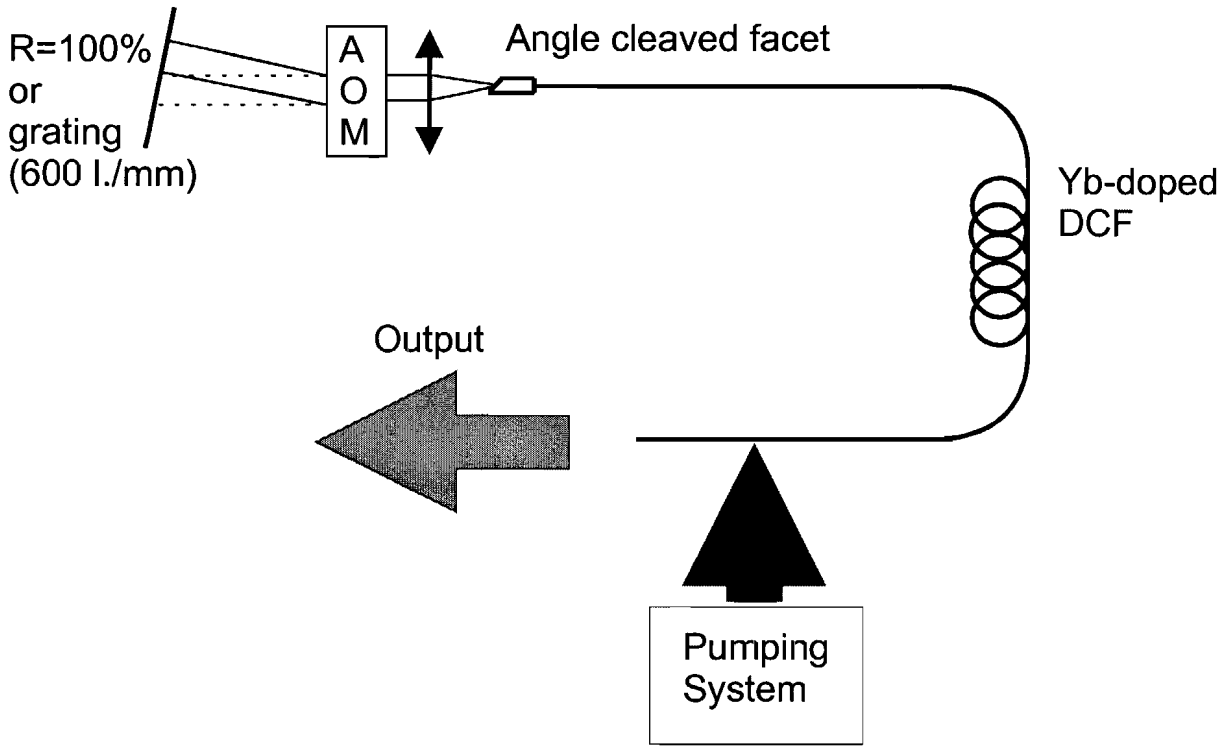

Figure VII-1: Experimental setup

For measuring the pulse energy, a silicon detector with a time constant of ~10 μs was used. The detector integrates the output signal over this time, so for significantly shorter pulses, the peak output signal from the detector is proportional to the pulse energy. At the same time, the integration time is sufficiently short to ensure that the signal level between pulses, generated by ASE, is negligible compared to the peak signal level from the detector (corresponding to the pulse energy). The energy detector was calibrated with the laser operating at a high repetition rate, where ASE between pulses is negligible (verified with an optical spectrum analyzer). The pulse energy is then simply the average power divided by the pulse repetition rate. The pulse energy is thus readily evaluated, and the energy detector can be calibrated accordingly. For measuring pulse shapes, a fast silicon detector with a time constant of less than 10 ns was used. For measuring average power, a thermal power meter was used.

III FIBRES

Three types of fibres were investigated: LMA (Large Mode Area, fibre #1 and #2), Multi-Mode Large Core (MMLC, fibre #3 #4 and #5) and single mode fibre (#6) with a typical core geometry and NA (i.e., not designed for high energy storage). Fibre #4 was the same as fibre

#3, except that the fibre was adiabatically tapered down at the pump end to single mode core dimensions. This tapered section suppressed higher-order modes in the cavity [4]. Previous work has shown that reducing the fibre diameter with a taper significantly improves the beam quality (M^2 value reduced from 2.6 to 1.4) with a low output power penalty (1 dB) [3]. This intensity enhancement is caused by the fibre taper and the resulting selective mode excitation at the pump launch end of the laser cavity. As a rough estimation $(M^2)^2$ can be taken as an upper limit for the effective number of lasing modes. The NA of the taper (surrounded by air) is nominally high enough to guide the pump through the taper without radiation losses, even though the fibre is significantly thinner in the taper. This taper (made with an electric arc) incurred a pump loss of 20%, maybe because of scratches , imperfections on the surface, and maybe the fact it was not perfectly adiabtic.

	fibre #1 LMA	fibre #2 LMA	Fibre #3 MMLC	fibre #4 MMLC	Fibre #5 MMLC	Fibre#6 SM
Core diameter, μm	20	40	33	33	60	7
Dopant [$*10^{25}$ ions/m^3]	4.32	1.83	4.23	4.23	48	1.6
Inner cladding diameter, μm	150	100 x 400	200	200	300	125
NA	0.06	0.06	0.13	0.13	0.05	0.1
M^2	1.3	3.0	7.0	1.8	7	1.2
CW slope efficiency, %	83	83	84	84	79	50
Measured absorption @ 915nm, dB/m (bent)	2.0	2.5	3.0	3.0	6.0	2.0

Table VII-1: Characteristics of the fibers used in the experiments

The fibres were first characterized in cw operation, using a setup similar to the one in Figure 1, but without the AOM and the HR mirror. Instead, the fibres were perpendicularly cleaved at both ends, and the double-ended laser output power was measured. Table 1 lists important characteristics of the fibre lasers. In this chapter, the fibres designed for high-energy storage (1 – 4) will primarily be discussed, while fibre #6 is included for comparison. It is important to notice that fibre #5 was studied to see how far one could go in energy storage.

The fibres were circular, except for fibre #2 which had a rectangular inner cladding. All fibres had a centered core. The slope efficiencies of all fibres except #6 were approximately the same. Fibre #6 suffered from excess pump propagation losses (about 2 dB over the length of the fibre). This reduced its slope efficiency. The dopant concentrations (in the solution used for soaking) are given for information knowing that they will be different in the fibre. The absorption coefficients are hard to correlate with the doping level since the cladding to core ratio is not a good parameter to use for LMA fibre, (the design of LMA includes ring doping) and for centro-symmetric design (Some modes are not crossing the core). In a first approximation, concentration and efficiency are uncorrelated, because of some limiting effect such as quenching, which was not measured.
While the M^2-value of the MMLC fibre #3 is intrinsically larger than that of the LMA fibres, a comparably low value can be obtained with a taper (fibre #4). Besides the core design, the cladding size is another important geometrical characteristic as it influences the pump launch efficiency and therefore the maximum achievable output power.

IV RESULTS AND DISCUSSION

IV-1 Comparison of energy levels and limitations

Figure 2 shows the pulse energy and average output power, including ASE, as a function of the repetition rate when the high-energy fibres (1–4) were Q-switched. The fibres were 10 m long (tightly bent for maximum absorption), which was enough for efficient pump absorption. The pump level was adjusted to generate 3 W of laser output power with the AOM constantly on, with the setup in figure 1. At high repetition rates (over around 15 kHz), the average power is maintained around 3 W, and the pulse energy is simply this power divided by the repetition rate. The pulse energy grows as the repetition rate decreases and exceeds 0.5 mJ at 4 kHz for the high-energy fibres (#1-4). The average power, on the other hand, drops for low repetition rates (below 10 – 15 kHz), as typical for Q-switched lasers.

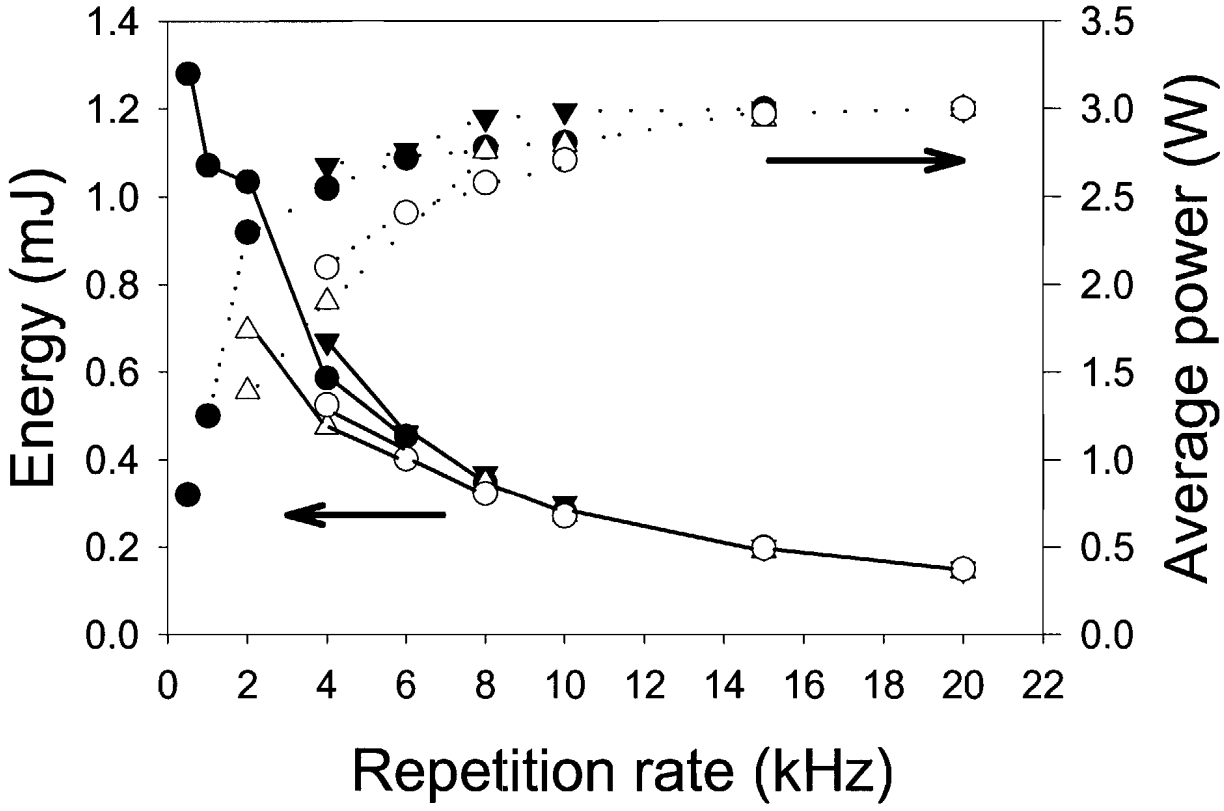

Figure VII-2: Energy and average power versus the repetition rate for fibre #2 (filled triangle), fibre #1 (empty triangle), fibre #3 (filled circle) and fibre #4 (empty circle). All measurements were taken with the same pump rate.

Comparing the behaviour of the different high-energy fibres, one can see that the average power and the pulse energy from fibre #1 are smaller than that of the other fibres at low repetition rate. The reason for this is its smaller core diameter with correspondingly smaller saturation energy. As the repetition rate is reduced, more energy is stored in the fibres between pulses. Especially for fibre #1, this leads to a large gain, which via ASE losses prevents further efficient energy storage. Most of the ASE is emitted in the AOM end of the fibre rather than in the outcoupling end. Therefore, also the average output power, including ASE and measured from the outcoupling end with a thermal power-meter, drops with lower repetition rates. Fibres #2 and #3 have larger cores with larger saturation energies, and are therefore less influenced by this effect. Fibre #4 is the same as fibre #3, except that it includes a mode-selecting taper and emits a nearly diffraction-limited beam, while the beam from fibre laser #3 is highly multi-moded. At high repetition rates, the pulse energy is the same, as a result of the adjustment of the pump power to equal cw output power – the

pumping of fibre #4 is slightly stronger to compensate for the cw signal and pump loss of the taper. However, at low repetition rates, the pulse energy depends only weakly on the pump power, because of the ASE self-saturation. Thus, the stronger pumping of fibre #4 will not compensate the taper signal losses at low repetition rates. Therefore, the pulse energy and average output power become lower with fibre #4 than with #3 at low repetition rates. However, the loss in the taper is small, and the energy penalty is limited to 10 %. Note also that with a better taper, losses would be even smaller. In fact, since fibre #4 operates on fewer modes than fibre #3 (see the M^2-values in Table 1), ASE losses should be smaller, so fibre #4 could even generate higher-energy pulses than fibre #3 in the low repetition rate regime. However, this effect is small and more than offset by signal losses in the taper.

In figure 2, the fibre lasers were studied over repetition rates for which one could obtain reliable Q-switching. Fibre facet damage and spurious lasing for MM fibres limited the repetition rates at low frequency, as the pulses reached peak powers exceeding the damage threshold for too low a repetition rate. This limit varied between 0.5 and 4 kHz from fibre to fibre, depending on core area and pulse duration. At high repetition rates, the pump power was not enough to re-pump the fibre between pulses, leading to missing pulses, and limiting the repetition rate upwards. The upper limit varied from fibre to fibre too, from 10 to 20 kHz, because of differences in energy extraction efficiency as well as laser threshold, pump power, and pump intensity.

Fibre #6 (with a single-mode core of standard geometry) was also tried in this configuration. The standard fibre (#6) was 5 m long with 0.8 W of cw output power with the AOM constantly on. At higher pump levels than that, it was difficult to achieve stable Q-switching. A pulse energy of 70 μJ was reached at 10 kHz repetition rate. For lower repetition rates than this, spurious lasing occurred between pulses. With this fibre laser, a relatively small extractable energy of approximately 70 μJ already generated enough gain for lasing even with the AOM off. Compared to fibre #6, the high-energy fibres are significantly better and all relatively similar to each other, as expected given the core sizes of the different fibres.

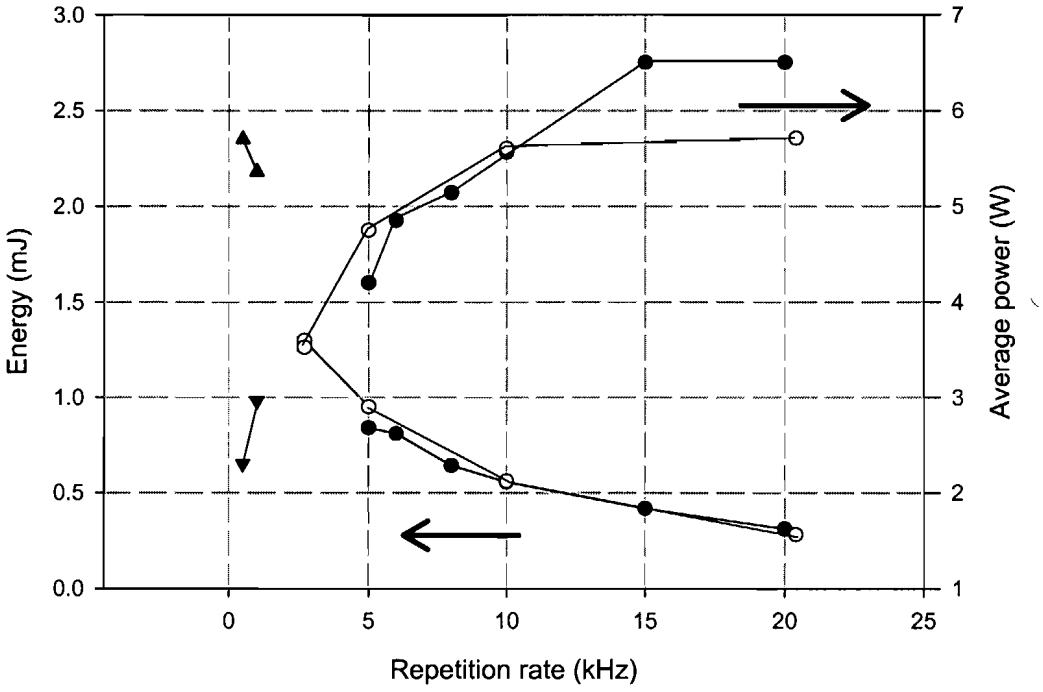

Figure VII-3: Energy and average power versus the repetition rate for fibre #2 (white circle and black triangle) and fibre #3 (black circle) at the maximum pump level.

The fibre lasers were then pumped with maximum pump power available (35 W incident) in order to reach highest possible pulse energies and investigate pulse energy limits in this regime. Figure 3 shows the results obtained during this experiment. Either damage to the facet or the onset of lasing between pulses limited the pulse energy. Damage to the out-coupling facet was observed with all fibres, at peak powers of 10 – 14 kW, for ~100 ns pulses (power densities in the region of 2 GW/cm^2). Onset of lasing between pulses was also observed, but only with the standard NA fibres (#3-4,6). Lasing between pulses is a result of spurious feedback or Rayleigh back-scattering [5]. Both of these effects are more severe in higher-NA fibres. The amount of Rayleigh backscattering is proportional to the NA squared and to the fibre length. So, Rayleigh back-scattering in the MMLC fibres is 5 – 10 dB stronger than in the LMA fibres, creating an effective feedback of around –30 dB. Other sources of feedback, e.g., from an imperfectly angled fibre end, are also larger with a higher

NA, although these are very difficult to estimate without measurements. Figure 3 shows pulse energy and average output power (including ASE) vs. repetition rate for fibre #2 and #3. From 35 W of power from the beam-shaped diode bars, 22 W could be launched into fibre #3 and 20 W into fibre #2. For both fibres, the AOM diffraction efficiency dropped to 50%, which explains the relatively low average power now obtained. The drop in diffraction efficiency may be an effect of a degraded beam quality: At higher pump power, the fibre gain reaches a higher value, so that even higher-order modes can build up to significant energy. This degrades the beam quality, which may lead to a reduced diffraction efficiency. The fibres were used in different lengths and with different setups. For fibre #2, a length of 10 m was used in the setup shown in figure 1 (empty circles in figure 4). This configuration was limited in pulse energy by facet damage. For fibre #3, a length of 10 m was used in the setup of figure 1 (filled circles in figure 3). This configuration, with a higher-NA fibre, was limited in pulse energy by spurious lasing between pulses. A 35 m long piece of fibre #2 was also investigated in a setup that included wavelength selective ASE feedback in the output-coupling end [6] (for all other Q-switched laser measurements, the setup of figure 1 was used). With this arrangement, the highest pulse energy was reached, 2.3 mJ at 500 Hz (filled triangles in figure 3). The NA was sufficiently low to keep back-scattering at acceptable levels even at this fibre length. Moreover, the long fibre produced pulses that were long enough (with low enough peak powers) to prevent fibre facet damage even at the highest pulse energies.

IV-2 Comparison of ASE levels

Because reflections in the out-coupling end seed the ASE propagating towards the AOM, most of the power lost as ASE between pulses is emitted at the AOM end. However, some ASE is also present in the laser output. This ASE typically peaks around 1040 nm, figure 4 shows the fraction of ASE in the laser output power for fibres #2 and #3 as a function of the repetition rate, for 10 m long fibres. The pump power was adjusted to generate 3 W of average power at high repetition rates. The ASE build-up time was about 0.4 ms for both fibres. Therefore, for both fibres, the ASE becomes significant only at pulse repetition rates below 2 kHz. The ASE reaches a level of 20% of the total power at 0.5 kHz. However, this ASE background can be reduced by using wavelength selective output coupling and ASE recycling as in [1].

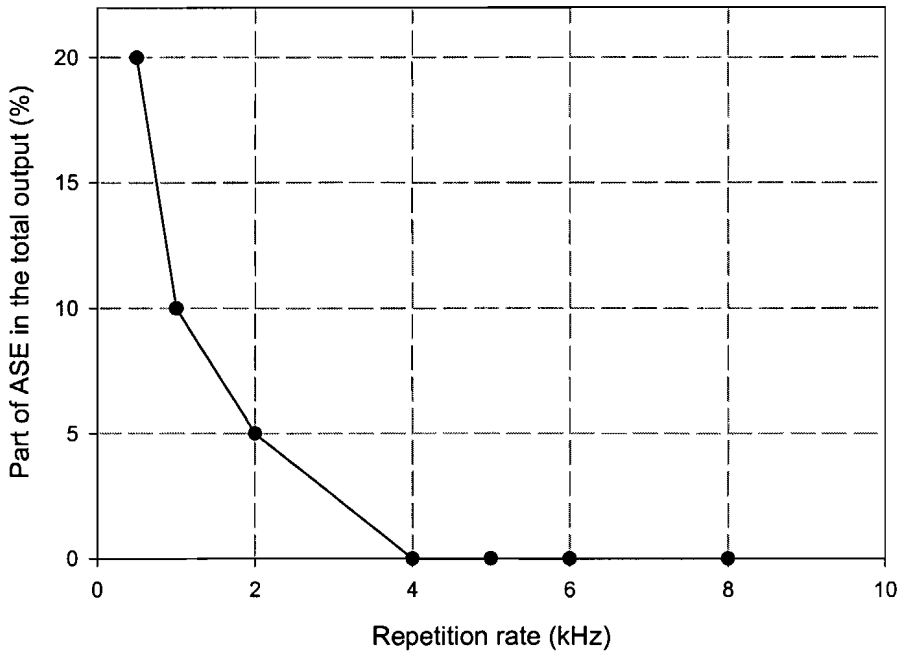

Figure VII-4: ASE share of the total output power versus the repetition rate.

For fibre #1, the ASE build-up time was 0.3 ms, with the pump power adjusted to generate 3 W of average power at high repetition rates. Thus, as expected, the gain builds up more quickly in this smaller core fibre than in fibres #2 and 3. The ASE build-up time was also measured in fibre #6. Even though the pump power was now much smaller (less than 2 W), the ASE still built up in 50 μs. This clearly demonstrates the faster ASE and gain build-up in a smaller-core fibre. Because of the fast build-up of gain in these fibres, spurious inter-pulse lasing occurred for repetition rates below 2 kHz and 10 kHz for fibre #1 and #6, respectively. The relatively high NA with more Rayleigh back-scattering also contributes to the spurious lasing of fibre #6.

IV-3 Comparison for pulse shape and width

The energy of the Q-switched pulses did not depend critically on fibre length, provided that the peak power was low enough to avoid facet damage. The main influence of the length was on the temporal shape of the output pulses, as shown in figure 5. For this measurement, fibre #2 was used with lengths of 5, 10, 15 (not shown) and 35 m at a repetition rate of 2 kHz. The

full-width half-maximum pulse durations were 80 ns, 100 ns, 120 ns and 500 ns for these fibre lengths, respectively. Measurements with 5 and 10 m of fibres #1 and #3 gave similar results.

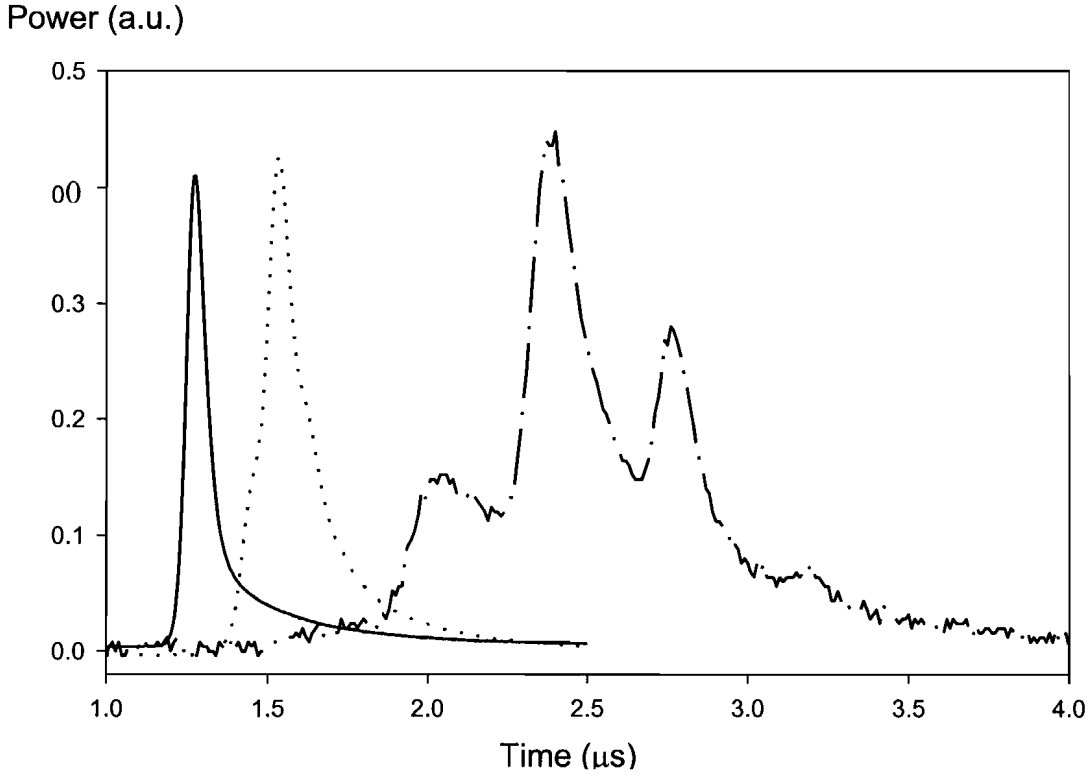

Figure VII-5: Pulse shapes for different fibre lengths. 5m (plain), 10m (dot) and 35m (dash-dot)

For laser cavities so long that the pulse round-trip time exceeded the pulse duration, the pulse split up as can be seen in figure 5 for the 35 m long fibre. Compared to short fibres, the peak intensity is then significantly reduced and the damage limitation on the fibre facet is relaxed so that a higher energy level can be reached. However, in many applications a clean single pulse is required, in which case the maximum fibre length is around 25 – 30 m in this case. The repetition rate influences the pulse duration, too: At higher repetition rates, the pulses become longer as the smaller amount of energy stored between pulses leads to a lower gain and a slower pulse build-up. For instance, at a repetition rate of 20 kHz, the pulse duration was between 400 and 900 ns depending on the fibre length, the pump level and the core size.

IV-4 Very large core fibre

Here, the focus is on maximizing the pulse energy paying less attention to beam quality. The fibre had a 60 μm core (NA 0.05, simple step index design) and a 300 μm inner cladding diameter. The inner cladding was non-circular to improve the pump absorption. The fibre was silicone-coated, giving a nominal NA of 0.4 for the inner cladding. As it has been shown in the previous chapter, the maximum extractable energy (as limited by ASE or spurious lasing) is around ten times the saturation energy, which in this case gives around 20 mJ. With this fibre and a double end pumping, up to 30 W of pump power could be launched into the fibre from two beam shaped 915 nm diode bars. With a free-running fibre laser with feedback from perpendicularly cleaved ends, the double-ended output power reached 17 W. When the AOM was inserted the power dropped to 10.2 W (single-ended) with the AOM always on (with feedback for the first-order beam).

The low core NA and a short fibre length (3.5 m) helped to reduce Rayleigh backscattering. To avoid facet damage, a 3 mm piece of 300 μm core-less fibre (silica rod) was spliced at both fibre ends. The signal beam expanded inside these fibres to larger diameter. This eliminated the damage problem and also reduced the feedback from the fibre ends. These were supposed to increase the spot size up to 300μm, but they were slightly too long to preserve the beam quality.

Then, the laser was Q-switched by on-off modulating the AOM. The pulse energy and average output powers are shown in figure 6. The average power curve includes ASE, which accounted for as much as 30% of the average power at 500 Hz. At that repetition rate, the pulse energy was 7.7 mJ. Neither fibre facet damage nor spurious lasing between pulsing was observed.

Even though the laser operation was below the ASE-limit, the presence of ASE indicates that even higher pulse energy could be obtained if the ASE could be avoided. However, ASE seeding/recirculation as in [1] could not be used to increase the pulse energy since the laser wavelength coincided with the ASE peak at 1037 nm. However, with a longer fibre, the laser should shift to longer wavelengths. This would allow the recirculation of the ASE and the achievement of higher pulse energies.

Because of the short fibre length, clean single pulses of a relatively short duration (250 ns) were observed. Hence, a peak power as high as 30 kW was reached.

The beam propagation parameter (M^2) was measured to be 31. This was much higher than the value measured without the 3 mm core-less fibre termination ($M^2 = 7$). This might be because

the termination was too long. One can expect to be able to improve the beam-quality with a shorter termination (which, however, is difficult to manufacture).

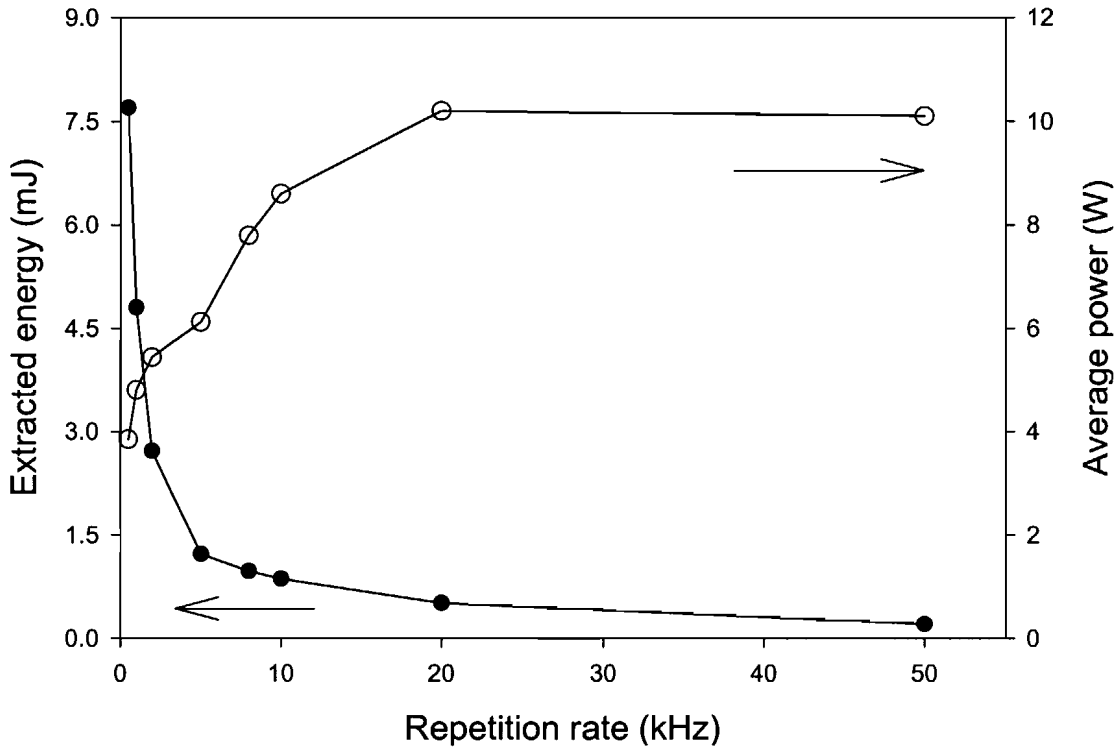

Figure VII-6: Extracted energy (black) and average power (white) against the repetition rate

IV-5 Tunability

In a lower pump power configuration, the grating (600 lines/mm, blazed at 1 μm, blaze angle was 30 degrees) was used to tune the wavelength instead of the high reflectivity mirror. The grating was used in Litrow incidence and rotated to tune the wavelength. The output energy of this system, as a function of the repetition rate, is shown in figure 7 for a lasing wavelength of 1070 nm. The energy reached 150 μJ at a repetition rate of 500 Hz. This low energy was essentially due to the low level of power (20 % of the total output power in cw) in the first order of diffraction of the AOM used in this setup.

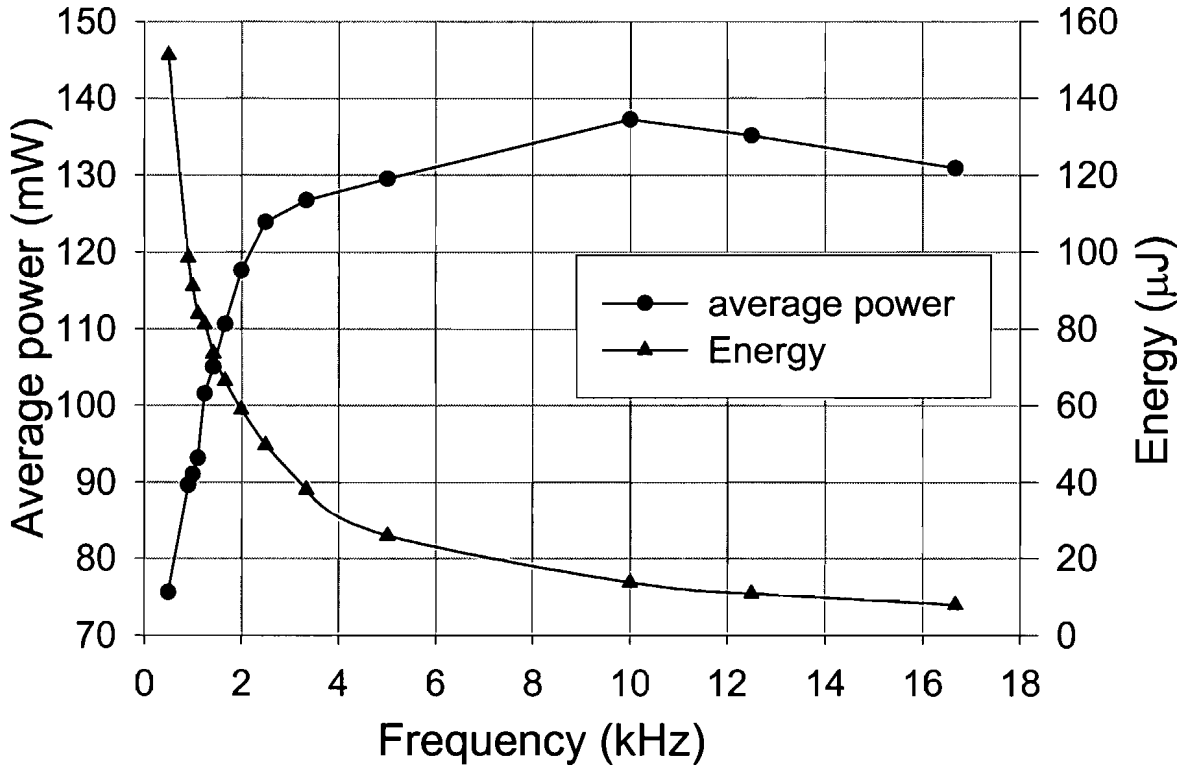

Figure VII-7: Evolution of the energy and the average output power versus the frequency in Q-switched regime of operation. Results obtained with a bulk grating, the lasing wavelength was 1070 nm.

To measure the tuning range, the system was set at a repetition rate of 1 kHz, at this point the energy was above 100 µJ and the pulse width was 80 ns. The results of tunability shown in figure 8, gives a broad tuning range of 40 nm (1060-1100) in which the energy stays above 100 µJ. It is important to note as well that during those measurements the alignment of the system remained the same, and that a slight change in this alignment can improve the output average power (i.e. the energy). However, this improvement in output energy does not consequently change the tuning range.

Figure VII-8: Tuning range of the Q-switched fibre laser. The measurement was done at a repetition rate of 1 kHz.

V CONCLUSION

Q-switched cladding pumped Yb-doped fibre lasers operating at mJ level were theoretically and experimentally studied. Theoretical results show that the energy storage is limited by strong ASE between pulses, because of the high gain in the fibre. Due to the tight modal confinement in fibres, the high gain appears at a relatively low energy. However, the energy storage scales with the core area. Two types of large core fibres were studied: low NA, few moded large mode area fibres as well as standard NA multimode fibres. For similar core sizes and at a fixed repetition rate, the energy extracted from both types of fibre was comparable, and in fair agreement with simulations. Good spatial quality was obtained directly from the LMA fibre and also from a multimode fibre incorporating a mode-selecting tapered section. Experimentally, although strong ASE ultimately limits the pulse energy, it was difficult to reach this limit. Instead, spurious lasing between pulses, or often even fibre facet damage, restricted the pulse energy. Facet damage could be avoided with longer fibres, which produce longer pulses with lower peak powers. Alternatively, it could be avoided with an improved

fibre termination. This was shown in further experiments with a very large core fibre. It gave a record breaking extracted energy of 7.7 mJ, and with quite a short fibre and spliced silica rod at both ends, both facet damage and spurious lasing were suppressed.

Compared to large-core multi-mode fibres, the complex low NA LMA design allows for higher gain before Rayleigh scattering and spurious feedback initiates lasing. It also generates less ASE at a given level of gain. Therefore, somewhat more energy can be stored at low repetition rates. With a long low-NA LMA fibre, both facet damage and spurious lasing were avoided. On the other hand, multimode fibres are easier to manufacture, and the use of a simple fibre taper results in a beam quality comparable to that of the LMA fibre. Although not studied here, tapering can be used for improving the beam quality of LMA fibres, too. For example, calculations show that a fibre with a 70 μm core can reach over 20 mJ of extractable energy for pump powers exceeding 30 W. Realistically, accounting for losses and incomplete energy extraction, such a fibre should be capable of generating 10 mJ pulses. One can expect that a combination of an LMA fibre and a taper would generate a high brightness beam even with a 70 μm core or more. The results obtained with a step index 60 μm core fibre proved that one can build a 10 mJ fibre source with high beam quality [7].

REFERENCES

[1] H. L. Offerhaus, J. A. Alvarez-Chavez, J. Nilsson, P. W. Turner, W. A. Clarkson, and D. J. Richardson, "Multi-mJ, multi-watt Q-switched fiber laser," Opt. Lett., vol. 25, pp. 37-39, 2000.

[2] N. G. R. Broderick, H. L. Offerhaus, D. J. Richardson, R. A. Sammut, J. Caplen, and L. Dong, "Large mode area fibers for high power applications," Opt. Fiber Technol., vol. 5, pp. 185-196, 1999.

[3] J. A. Alvarez-Chavez, A. B. Grudinin, J. Nilsson, P. W. Turner, W. A. Clarkson, "Mode selection in high power cladding pumped fibre lasers with tapered section," Technical digest, CWE 7, CLEO'99, Baltimore, 1999.

[4] W. A. Clarkson, D. C. Hanna, "Two-mirror beam-shaping technique for high-power diode bars," *Optics Lett.,* 1996, Vol.21, No.6, pp.375-377

[5] M. E. Fermann, "Single-mode excitation of multimode fibres with ultrashort pulses," Opt. Lett., v. 23, pp. 52-54, 1998

[6] R. Oron, A. A. Hardy, "Rayleigh backscattering and amplified spontaneous emission in high-power ytterbium fibre amplifiers," J. Opt. Soc. Am. B, v. 16, No.5, pp 695-701, 1999

[7] A. Galvanauskas, Z. Sartania, M. Birschoff, "Millijoule femtosecond fibre CPA system," postdeadline paper, PD3, ASSL 2001, Seattle, 2000

[8] J. Nilsson, R. Paschotta, J. E. Caplen, and D. C. Hanna, "Yb^{3+}-ring-doped fiber for high energy pulse amplification," Opt. Lett., vol. 22, pp. 1092-1094, 1997.

CONCLUSION AND FUTURE WORK

I CONCLUSION

During this work, both the compactness of fibre source and the lasing possibilities of ytterbium-doped fibre were investigated.

At first, different efficient launching schemes based on different pump sources and optical systems were developed. All these schemes gave a good launching efficiency (above 80%) for a high level of compactness, which was the aim of this study. Furthermore, two different ways of having the pump separated from the signal were detailed. Both were via coupling between multimode guides. Both methods provided as efficient laser as a standard end-pumping scheme and allowed coupling of most of the pump light into the doped fibre. The best solution seems to be the multifibre arrangement, since in this case, losses in the core should be avoided. Such a system can also use more than two fibres and allow a high number of pump sources. This can also be associated with polarisation multiplexing of pump sources.

During the investigation of lasing possibilities for ytterbium-doped fibre, continuous wave operation was first tested. This first measurement allowed testing of the different pumping schemes. This proved that the multiple fibre arrangement was as efficient as end pumping the fibre, with the advantage of separating the pump and the signal. Furthermore, 975 nm emission was obtained from an ytterbium doped cladding pumped fibre laser. With a double

passed pump scheme, up to 85% slope efficiency was reached. This kind of fibre source can generate several Watts at 975 nm, if the cladding is well designed and adapted to the pump source. Furthermore, if these fibre lasers contain a fibre Bragg grating a narrow line-width can be achieved. The main challenge, for such a source, is to make the cladding small enough to reduce the threshold and to have a high NA to launch as much pump power as possible. Then, the Q-switched regime was investigated. First, the importance of using a large core area to generate high pulse energy was proved. Secondly, the main limiting factors to obtain an efficient Q-switched fibre laser were determined. It was found that after the core size, the facet damage threshold and the Rayleigh backscattering were the two main problems to tackle. The fibre facet damage threshold was increased by splicing short silica rods at both ends of the fibre. This increased sufficiently the spot diameter to avoid any facet damage. The easiest solution to limit Rayleigh backscattering was to use low core NA, and short fibre (high level of doping, thus short absorption length). By using these methods, up to 7.7 mJ pulse energy was extracted from of an ytterbium doped fibre laser with a core of 60 μm. Note that the launching technique, the coupling technique, and the results for Q-switched fibre laser, could be applied to any other rare-earth doped fibre, with probably the same success.

II FUTURE WORK

As said previously, the compact systems (couplers and multifibre arrangement) could be applied to any type of rare earth doped fibre laser. However, it would be interesting to develop a more accurate theoretical model to describe the behaviour of multifibre arrangement, since the model was just designed to overestimate the losses and included a lot of approximations. This model should be based on beam propagation. This will give a better knowledge of the multifibre arrangements. Furthermore, a "figure of eight fibre" (Chapter V) should be studied to see how it improves the performances: lower losses and better coupling plus asymmetric cladding shape.

Then for Q-switched fibre laser, the use of very large core (>50 μm) and special index profile (low NA) associated with tapering, should allow the achievement of more than 10 mJ with high brightness. The first problem to tackle will be the added ending length. In the experiment they were too long to keep a good beam quality. Therefore, there is still need to investigate some means of having those high-energy pulses with a high beam quality.

The use of an ytterbium doped fibre laser to generate 976 nm seems to be a solution for pumping of EDFAs, and the two important issues will be the brightness of the pump sources and the design of the inner cladding. For the inner cladding the next steps for investigation will be either a thin fibre with low index polymer coating or hole structure around the inner cladding, as well as using cladding design to match the source brightness.
In the longer term, one can think about using the Q-switched source for non-linear effects, or developing pulsed fibre lasers at 976 nm. Finally, if high power at 976 nm was achieved with a narrow line-width (several Watt), it would be an interesting project to study the fourth harmonic generation. This harmonic is exactly 244 nm, it would therefore provide a stable compact source to write fibre Bragg gratings.

APPENDIX A

We will give here some important numbers describing the propagation in a fibre. We will consider that we know a, the core radius, and NA, the core numerical aperture. We know as well the core and cladding indexes (n_{core} and n_{clad}), and the wavelength of propagation (λ). Then we will have the following constant defining the propagation in the fibre

$$\frac{2\pi}{\lambda}\cdot n_{clad} < \beta \leq \frac{2\pi}{\lambda}\cdot n_{core} \qquad \text{(A–1)}$$

$$V = \frac{2\cdot\pi}{\lambda}\cdot a \cdot NA \qquad \text{(A–2)}$$

$$U = a\cdot\sqrt{(\frac{2\pi}{\lambda}\cdot n_{core})^2 - \beta^2} \qquad \text{(A–3)}$$

$$W = \sqrt{V^2 - U^2} \qquad \text{(A–4)}$$

$$\Delta = \frac{NA^2}{2} \qquad \text{(A–5)}$$

APPENDIX B

Details of the equations in Chapter III:

First the Threshold pump power (P_{th}) and the slope efficiency (η) are expressed as:

$$P_{th} = \frac{h \cdot \nu_p \cdot P_s^{cs} \cdot (\alpha \cdot L - \ln(R))}{1 - (G_{max} \cdot R)^{-\delta}} \quad \text{(B-1)}$$

$$\eta = \frac{\eta_q \cdot (1 - R_2) \cdot P_s^{is}}{\tau_{eff} \cdot P_s^{cs}} \cdot (1 - (G_{max} \cdot R)^{-\delta}) \quad \text{(B-2)},$$

where α represents the losses for the signal, L is the cavity length, $R^2=R_1R_2$ and $R_{1,2}$ are the reflectivity of the two outputs of the laser (the signal is taken at R_2). Gmax is the maximum gain, δ is the saturation power ratio, η_q is the quantum efficiency, τ_{eff} is the effective output transmission and P_s^{is}, P_s^{cs} are respectively the intrinsic-saturation power and the cross-saturation power. Those last terms are expressed as following:

$$G_{max} = \exp((\alpha_p / \delta - \alpha) \cdot L) \quad \text{(B-3)}$$

$$\delta = \frac{P_s^{cs}}{P_p^{is}} \quad \text{(B-4)}$$

$$\eta_q = \frac{\lambda_p}{\lambda_s} \quad \text{(B-5)}$$

$$\tau_{eff} = (1 - R_2) + (1 - R_1) \cdot \sqrt{\frac{R_2}{R_1}} \quad \text{(B-6)}$$

$$P_s^{is} = \frac{A_{eff}}{\Gamma_s} \cdot \frac{1}{\tau_{21}} \cdot \frac{1}{\sigma_{21} + \sigma_{12}} \quad \text{(B-7)}$$

$$P_s^{cs} = P_s^{is} \tag{B-8}$$

In those equations α_p is the losses for the pump, λ_p and λ_s are the wavelength of the pump and the signal, A_{eff} is the effective dopant area (core radius squared times Pi), Γs is the overlap integral of the signal with the core , P_p^{is} is the intrinsic-saturation pump power. The spectroscopic data are given in chapter III.

If we consider a Gaussian mode the overlap integral is expressed as:

$$\Gamma_s = 1 - \exp\left(\frac{-2 \cdot r_{co}^{\,2}}{\omega^2}\right) \tag{B-9}$$

In which r_{co} is the core radius and ω is the signal beam waist. Finally the intrinsic-saturation pump power is:

$$P_p^{is} = \frac{A_{eff}}{\Gamma_p} \cdot \frac{1}{\tau_{21}} \cdot \frac{1}{\sigma_{02} + \sigma_{20}} \tag{B-10}$$

Γp is the overlap integral for the pump and has the same expression as for the signal, but instead of the signal beam waist, the pump beam waist has to be used.

APPENDIX C

Journal publications:

1. J. M. Sousa, J. Nilsson, C. C. Renaud, J. A. Alvarez-Chavez, A. B. Grudinin and J. D. Minelly, "Broad-Band Diode-Pumped Ytterbium-Doped Fibre Amplifier with 34 dBm Output Power," IEEE Photonics Tech. Letters, vol. 11, pp. 39-41, 1999.
2. C. C. Renaud, R. J. Selvas-Aguilar, J. Nilsson, P. W. Turner and A. B. Grudinin, "Compact, high energy Q-switched cladding pumped fibre laser with a tuning range over 40 nm," IEEE Photonics Tech. Letters, vol. 11, pp. 976-978, 1999.
3. C. C. Renaud, H. L. Offerhaus, J. A. Alvarez-Chavez, J. Nilsson, W. A. Clarkson, P. W. Turner, D. J. Richardson, A. B. Grudinin, "Characteristics of Q-switched cladding-pumped Ytterbium-doped fibre lasers with different high-energy fibre design," IEEE J. Quantum Electron., vol 37 ,pp, 2001
4. J. K. Sahu, C. C. Renaud, K. Furusawa, R. Selvas, J. A. Alvarez-Chavez, D. J. Richardson, and J. Nilsson, "Jacketed air-clad cladding pumped ytterbium doped fibre laser with wide tuning range," submitted to Electron. Letters June 2001.

Conferences:

1. J. Nilsson, J.A. Alvarez-Chavez, P.W. Turner, W.A. Clarkson, C.C. Renaud, and A.B. Grudinin, "Widely tunable high-power diode-pumped double-clad Yb3+-doped fiber laser," *ASSL 99*, Boston, 1999.
2. A. B. Grudinin J. Nilsson, P. W. Turner, C. C. Renaud, W. A. Clarkson and D. N. Payne, "Single clad coiled optical fibre for high power lasers and amplifiers," Postdeadline papers, CPD 26, CLEO'99, Baltimore, 1999.
3. J. A. Alvarez-Chavez, J. Nilsson, P. W. Turner, W. A. Clarkson, C. C. Renaud, R. Selvas-Aguilar, D. C. Hanna, and A. B. Grudinin, "Single-polarisation narrow-linewidth wavelength-tunable high-power diode-pumped double-clad ytterbium-doped fiber laser," technical digest CLEO Europe, Munich, 1999.
4. C. C. Renaud, H. L. Offerhaus, J. A. Alvarez-Chavez, J. Nilsson, W. A. Clarkson, P. W. Turner and A. B. Grudinin "Designs for efficient high-energy high-brightness Q-switched cladding-pumped ytterbium-doped fibre lasers," Technical digest CLEO'2000, San Fransisco, 2000.
5. C. C. Renaud, J. A. Alvarez-Chavez, J. K. Sahu, J. Nilsson, D. J. Richardson and W. A. Clarkson, "7.7 mJ pulses from a large core Yb-doped cladding-pumped Q-switched fibre laser," Technical digest, CLEO'2001, Baltimore, 2001.
6. J. K. Sahu, C. C. Renaud, J. Nilsson, W. A. Clarkson, S. A. Alam, and A. B. Grudinin, "Single-polarization laser operation in polarization-maintaining single-polarization pumped erbium-doped fiber," Technical digest CLEO'2001, Baltimore, 2001.

APPENDIX D

Fabrication numbers for the fibres described in chapter V and VII

Chapter V:

Fibre #1: HD465-01

Fibre #2: HD514-01

Fibre #3: HD515-01

Fibre #4: HD516-01

Fibre #5: HD551-01

Fibre #6: HD556-01

Fibre #7: HD621-01

Chapter VII:

Fibre #1: HD533-01

Fibre #2: HD533-03

Fibre #3: HD551-02

Fibre #4: HD551-02

Fibre #5: HD614-01

Fibre #6: HD556-03